

## ABSTRACT

YUAN, CHENGZHI. Synthesis of Hybrid/Switched Control Systems and Its Applications. (Under the direction of Dr. Fen Wu.)

Due to the wide presence of digital devices in control applications, a large variety of engineering systems exhibit rather complicated dynamical behaviors that can be typically modelled as hybrid dynamical systems, i.e., systems that combine continuous dynamics with discrete events. This prompts a great demand of developing new techniques for hybrid system analysis and advanced hybrid controller synthesis. As a subclass of hybrid systems, switched systems typically consist of a family of differential/difference equations and a rule that orchestrates the switching among them. In spite of the rich literatures on hybrid dynamical systems analysis, the problem of hybrid output-feedback controller synthesis has not yet been addressed adequately due to the lack of available techniques and convex solution for the associated optimization problem. Thus, the major motivating theme of this dissertation research is developing effective hybrid control algorithms that simultaneously yield optimal controlled performance and tractable computational synthesis conditions for various complex dynamical systems.

We first study the output-feedback control synthesis problem for a class of switched parameter-dependent systems that can be described as a linear fractional transformation (LFT) parameter-dependent model. A novel hybrid gain-scheduling control scheme is proposed, which consists of a standard switching dynamic output-feedback LFT control law and a supervisor that monitors the switching signal and enforces a reset/impulsive rule for the controller states at each switching time instant. It is shown that under the proposed hybrid controller structure, the associated output-feedback control synthesis conditions guaranteeing weighted  $\mathcal{L}_2$  performance can be formulated in terms of finite numbers of linear matrix inequalities (LMIs), which can be solved effectively using semi-definite programming. These results make a significant breakthrough for the theoretical research on gain-scheduling control synthesis of switched LFT systems via convex optimization. Specifically, it significantly simplifies the optimal output-feedback control design

procedure such that the weighted  $\mathcal{H}_\infty$  optimal control solution can be readily obtained by solving a convex constrained optimization problem. Moreover, both full-order and reduced-order output-feedback control synthesis problems can be addressed under a unified framework. This theoretical finding has been successfully applied to high-performance hybrid gain-scheduling missile autopilot design, and its effectiveness and advantages over existing missile control methods have also been demonstrated through nonlinear simulations on a longitudinal missile dynamics over a wide range of operating conditions.

We then investigate a more complicated control design problem, i.e., mixed  $\mathcal{H}_\infty$  and output regulation control for a class of switched linear dynamics subject to effects of persistent switched exosignals. The problem of output regulation specifies the control task of achieving not only the overall closed-loop stability but also the tracking and/or rejection of persistent reference/disturbance generated by an exosystem. This problem is addressed in this dissertation research by developing a new hybrid output regulator structure and a new mathematical technique, namely the multiple coordinate transformation (MCT) technique. We consider both switched controlled plant and the exosystem described by switched linear models. The proposed hybrid output regulator structure is constructed as an impulsive switched linear system, and embraces the exosystem dynamics as the internal model. It is shown that the associated hybrid output regulator synthesis conditions that guarantee overall weighted  $\mathcal{L}_2$  stability and output regulation performance are established as a set of LMIs plus linear matrix equations, which are computationally tractable via convex optimization. Apart from the technical novelty of the new hybrid control architecture and new MCT technique, another important contribution of these results lies in that the exosignals containing the reference to track are generated by a switched system consisting of multiple linear models. This would render more sophisticated descriptions for tracking control comparing to merely utilizing a pure linear or nonlinear exosystem. This work would therefore enhance the control system capability and design flexibility. Usefulness of the proposed approach has been demonstrated by solving the hybrid output regulation problem for a mechanical system.

All the aforementioned results are obtained under the assumption that dynamics/parameters of the controlled plant is precisely known or online measurable for controller design. However, modeling uncertainties are ubiquitous in practical control engineering applications. This motivates us to consider the control synthesis problem for systems with large uncertainties. The control problem under consideration is posed in the two-degree-of-freedom framework, i.e., the control design tasks include feedback stabilization control design and feedforward performance filter design. In this research, we focus on developing a feedforward control scheme with a pre-specified feedback control part for a class of uncertain systems that can be described in a standard LFT form. A min-switching-based switched feedforward controller structure is first proposed for both  $\mathcal{H}_2$  and  $\mathcal{H}_\infty$  robust stabilization problems. Stability and performance analysis conditions are established by using a piecewise Lyapunov function combined with the min-switching control technique. Based on the analysis results, the associated synthesis conditions are finally formulated as a special type of bilinear matrix inequalities (BMIs), which can be solved by means of convex LMI optimization coupled with a line search. This proposed robust switched feedforward control scheme outperforms existing ones based on single quadratic Lyapunov function, and leads to less conservative control designs. Successful application to the tracking control problem of a ship steering system demonstrates the effectiveness and usefulness of the proposed approach.

© Copyright 2016 by Chengzhi Yuan

All Rights Reserved

Synthesis of Hybrid/Switched Control Systems and Its Applications

by  
Chengzhi Yuan

A dissertation submitted to the Graduate Faculty of  
North Carolina State University  
in partial fulfillment of the  
requirements for the Degree of  
Doctor of Philosophy

Mechanical Engineering

Raleigh, North Carolina

2016

APPROVED BY:

---

Dr. Paul I. Ro

---

Dr. Aranya Chakraborty

---

Dr. Stephen L. Campbell

---

Dr. Fen Wu  
Chair of Advisory Committee

## DEDICATION

To my parents *Yincheng Yuan* and *Lizhuan Yuan*.

To my dear sister *Xiaoqiong Yuan* and my wife *Xiao Song*.

## BIOGRAPHY

Chengzhi Yuan received the Bachelor of Science degree in Control Science and Engineering and the Master of Science degree in Control Theory and Application both from the College of Automation Science and Engineering at South China University of Technology (P.R. China) in 2009 and 2012, respectively. He enrolled in Dept. of Mechanical & Aerospace Engineering at NCSU in the fall of 2012. He has been a teaching fellow of the Preparing the Professoriate (PTP) program in the Graduate School of NCSU, from 2015 to 2016.

## ACKNOWLEDGEMENTS

First and foremost, I would like to thank sincerely my adviser, Dr. Fen Wu, who gave me the great opportunity to come to NC State and guided my research. It is my fortune to have such a great adviser, not only for providing consistent advice and guidance to my research, but also for being a very good friend of mine. I really have been benefited a lot from the insightful discussions and suggestions he provided to both of my research and career life.

I am also grateful to my thesis committee members, Dr. Paul I. Ro, Dr. Aranya Chakraborty and Dr. Stephen Campbell for their constructive comments on my research work and presentation. I have been fortunate enough to also learn from them in the classroom.

I acknowledge the National Science Foundation for their financial support under the grant CMMI-1200242 through Dr. Fen Wu.

I feel indebted to the love and support from my parents and my sister who always encourage and believe me. Their everlasting and unconditional love and emotional support gave me confidence to stick to my decision, and courage to chase my dream. I can not thank my wife enough for her accompanying and caring.

Finally, I would like to thank other colleagues and friends for the enjoyable memories we shared in both scientific and personal life.

# TABLE OF CONTENTS

<b>LIST OF TABLES</b> . . . . .	<b>vii</b>
<b>LIST OF FIGURES</b> . . . . .	<b>viii</b>
<b>LIST OF NOTATIONS</b> . . . . .	<b>ix</b>
<b>Chapter 1 Introduction</b> . . . . .	<b>1</b>
1.1 Motivations and Objectives . . . . .	1
1.2 Preliminaries . . . . .	6
1.2.1 Stability definition of switched linear systems . . . . .	7
1.2.2 $\mathcal{L}_2$ ( $\ell_2$ ) performance under min-switching . . . . .	7
1.2.3 Weighted $\mathcal{L}_2$ ( $\ell_2$ ) performance under (average) dwell-time switching . . . . .	9
1.3 Dissertation Outline . . . . .	11
<b>Chapter 2 Hybrid Gain-Scheduling Control</b> . . . . .	<b>13</b>
2.1 Introduction . . . . .	14
2.2 Hybrid Gain-Scheduling Control of Switched LFT Systems . . . . .	17
2.2.1 Full-Order Case . . . . .	21
2.2.2 Reduced-Order Case . . . . .	26
2.3 Missile Modeling and Autopilot Design . . . . .	33
2.3.1 Switched LFT Modeling of Missile . . . . .	34
2.3.2 Control Problem Setup . . . . .	39
2.3.3 Control Synthesis and Simulation Results . . . . .	42
2.4 Summary . . . . .	48
<b>Chapter 3 Almost Output Regulation of Switched Linear Dynamics with Switched Exosignals</b> . . . . .	<b>50</b>
3.1 Introduction . . . . .	51
3.2 Preliminaries . . . . .	54
3.2.1 Weighted $\mathcal{L}_2$ ( $\ell_2$ ) Analysis for Switched Linear Systems with ADT . . . . .	54
3.2.2 Dilated LMI Representations of the BRL . . . . .	56
3.3 Main Results . . . . .	56
3.4 Application to A Mechanical System . . . . .	69
3.5 Summary . . . . .	76
<b>Chapter 4 Robust Switched Feedforward Control of Uncertain LFT Systems</b> . . . . .	<b>78</b>
4.1 Introduction . . . . .	78
4.2 Problem Statement . . . . .	81
4.3 Robust $\mathcal{H}_2$ Control . . . . .	84
4.3.1 Robust $\mathcal{H}_2$ Analysis . . . . .	84
4.3.2 Robust $\mathcal{H}_2$ Controller Synthesis . . . . .	88
4.4 Robust $\mathcal{H}_\infty$ Control . . . . .	92

4.4.1	Robust $\mathcal{H}_\infty$ Analysis . . . . .	92
4.4.2	Robust $\mathcal{H}_\infty$ Controller Synthesis . . . . .	94
4.5	Examples . . . . .	96
4.5.1	A Numerical Example . . . . .	97
4.5.2	Application to A Ship Steering Problem . . . . .	99
4.6	Summary . . . . .	102
<b>Chapter 5 Conclusion . . . . .</b>		<b>104</b>
5.1	Dissertation Contributions and Concluding Remarks . . . . .	104
5.2	Future Work . . . . .	107
<b>References . . . . .</b>		<b>111</b>

## LIST OF TABLES

Table 2.1	Effects of the partitioning of $\mathcal{P}$ on optimized weighted $\mathcal{L}_2$ performance (with fixed $(\lambda_0, \mu) = (0.1, 1.2)$ ). . . . .	43
Table 2.2	Effects of the dwell-time parameters $(\lambda_0, \mu)$ on optimized weighted $\mathcal{L}_2$ performance (with fixed partition of $\mathcal{P}$ as in Case III). . . . .	45
Table 4.1	Optimized robust $\mathcal{H}_2$ norms (Example 1). . . . .	98
Table 4.2	Optimized robust $\mathcal{H}_\infty$ norms (Example 2). . . . .	101

## LIST OF FIGURES

Figure 2.1	The proposed hybrid control scheme. . . . .	19
Figure 2.2	Weighted open-loop interconnection of missile plant. . . . .	39
Figure 2.3	Partition the scheduling parameter space $\mathcal{P}$ . . . . .	44
Figure 2.4	Missile dynamic response to a sequence of step acceleration commands. . . . .	48
Figure 2.5	Perturbed response to a sequence of step acceleration commands. . . . .	49
Figure 3.1	Diagram of a mechanical system with switched dynamics [90]. . . . .	69
Figure 3.2	Relations between $(\lambda_0, \mu)$ and optimized $\gamma$ as well as $\tau_a^*$ . . . . .	72
Figure 3.3	Exosystem states and switching signal. . . . .	75
Figure 3.4	Simulation results for the hybrid output regulation of the mechanical system (3.28). . . . .	77
Figure 4.1	Tracking performance comparison (Example 1). . . . .	98
Figure 4.2	Control diagram for the ship steering problem (Example 2). . . . .	100
Figure 4.3	Time-domain simulation of robust feed-forward control (Example 2). . . . .	102

## LIST OF NOTATIONS

$\mathbf{I}[k_1, k_2]$	for two integers $k_1, k_2, k_1 < k_2, \mathbf{I}[k_1, k_2] := \{k_1, k_1 + 1, \dots, k_2\}$
$\mathcal{D}$	a differentiator for continuous-time systems and a difference operator for discrete-time systems
$\ x\ $	$= (x^T x)^{\frac{1}{2}}$ for vector $x$
$\mathcal{M}$	the class of Metzler matrices consists of all matrices $\Pi \in \mathbb{R}^{N \times N}$ with elements $\pi_{ij}$ , such that $\pi_{ij} \geq 0$ for all $j \neq i \in \mathbf{I}[1, N]$ and $\sum_{i=1}^N \pi_{ij} = 0$ for all $j \in \mathbf{I}[1, N]$
$\tilde{\mathcal{M}}$	the class of Metzler matrices consists of all matrices $\tilde{\Pi} \in \mathbb{R}^{N \times N}$ with elements $\tilde{\pi}_{ji}$ , such that $\tilde{\pi}_{ji} \geq 0$ and $\sum_{j=1}^N \tilde{\pi}_{ji} = 1$ for all $i \in \mathbf{I}[1, N]$
$\mathbb{N}$	set of natural numbers
$\mathbb{R}$	set of real numbers
$\mathbb{R}_+$	set of non-negative real numbers
$\mathbb{R}^n$	set of $n$ -dimensional real vectors
$\mathbb{R}^{m \times n}$	set of real $m \times n$ matrices
$\mathbb{R}^{m \times n}$	set of real $m \times n$ matrices
$\mathbb{S}^n$	set of symmetric matrices in $\mathbb{R}^{n \times n}$
$\mathbb{S}_+^n$	set of positive definite matrices in $\mathbb{R}^{n \times n}$
$\mathcal{L}_2$	space of square integrable functions, that is, for any $x \in \mathcal{L}_2$ , $\ x\ _2 := (\int_0^\infty x^T(t)x(t)dt)^{\frac{1}{2}} < \infty$ .
$\ell_2$	space of square summable functions, that is, for any $x \in \ell_2$ , $\ x\ _2 := (\sum_{k=0}^\infty x^T(k)x(k))^{\frac{1}{2}} < \infty$ .
$M^T$	the transpose of the matrix $M$
$M^{-1}$	the inverse of the invertible matrix $M$
$M > 0$ ( $M \geq 0$ )	the matrix $M$ is positive definite (positive semi-definite)

$M < 0$ ( $M \leq 0$ )	the matrix $M$ is negative definite (negative semi-definite)
$X > Y$ ( $X \geq Y$ )	the matrix $X - Y$ is positive definite (positive semi-definite)
$X < Y$ ( $X \leq Y$ )	the matrix $X - Y$ is negative definite (negative semi-definite)
$\text{diag}\{a_1, a_2, \dots, a_n\}$	the $n$ by $n$ diagonal matrix with $a_1, a_2, \dots, a_n$ as the diagonal elements
$He\{\cdot\}$	the hermitian operator, $He\{M\} = M + M^T$
$\star$	induced by symmetry in large symmetric matrix expressions

# Chapter 1

## Introduction

### 1.1 Motivations and Objectives

Recent years have witnessed the rapid development of hybrid systems for both theoretical and practical reasons (see, e.g., [48, 10, 23, 26, 31, 33, 95, 105, 91] and the references therein). Typically, hybrid dynamical systems represent a large class of dynamic systems that combine continuous dynamics with discrete events. Such type of systems are intensively studied in control community, not only because they can be used effectively to model highly complex systems and/or systems with large uncertainties, but also because some limitations of traditional control designs can be relaxed or even avoided by introducing hybrid components into the control structures, leading to improved control performance and design flexibility. For example, the wide presence of digital devices in modern control applications results in a large variety of engineering systems exhibiting rather complicated dynamical behaviors, such as abrupt parameter variations in electronics, digital communication networks, and smart power grid systems; and sudden changes of system configurations in automobile transmission systems, power split powertrain systems of hybrid electric vehicles, automated traffic control, and cyber-physical networks. All of these complex physical systems can be typically modelled as hybrid dynamical systems. On the other hand, modern computer-based engineering control systems are prompting an

urgent demand of advanced control strategies to meet stringent performance requirements, which however usually goes beyond the capability of classical linear/nonlinear control design techniques. Hybrid control techniques provide a new perspective for high-performance control designs. Typical examples of applying hybrid control techniques to overcome limitations of classical linear/nonlinear control schemes include: reset control systems [63, 95, 96], switching control systems [48, 105, 58], impulsive control systems [102, 23, 38], and discrete-event control systems [33], etc.

As a special class of hybrid systems, switched systems consist of a family of subsystems (continuous time or discrete time) and a logical rule that orchestrates the switching between them. The defining feature of a switched control system is that in addition to the control laws, the switching logic serves as another important mechanism determining the hybrid nature of the system dynamics. Widespread applications of switched control systems have been seen over a broad range of areas, such as aerospace autopilot designs, multi aerial/groud vehicle corporation systems, robotic manipulators, electric circuits, industrial manufacturing process control systems, energy power systems, and mobile networked control systems. This justifies the extensive research efforts over the past decades on both analysis and design of switched control systems, see, e.g., [48, 82, 54, 67, 10]. Despite of many powerful tools for linear and nonlinear analysis, the problems of stability and stabilization of switched systems are of great challenge due to the involvement of the switching logic. For example, even the switching control of multiple linear time-invariant (LTI) plants has been considered to be a non-trivial problem since it is possible to cause instability by switching among multiple LTI systems that are all individually asymptotically stable, or stabilize multiple unstable systems through a properly-designed switching logic [48]. For stability analysis of switched control systems, under different switching scenarios, two problems are raised and studied in the field:

1. *Stability of autonomous switched system:* Under arbitrary switching signals, what are the conditions that guarantee asymptotic stability of a switched system?
2. *Stability of controlled switched system:* For a given switching signal, what are the con-

ditions that guarantee asymptotic stability of a switched system? How to specify these switching signals?

For autonomous/arbitrary switching, the stabilization problem can be regarded as a robust design problem, and the existence of a common Lyapunov function (CLF) provides a sufficient and necessary condition to guarantee the robust stability against arbitrary switching [48]. Research along the line of using CLF technique for analysis and design of switched control systems mainly focuses on: developing effective mechanisms to construct different type of common Lyapunov functions; and devising advanced switching control strategies to pursue better controlled performance. In particular the existence of a switching compensator which stabilizes the plant under arbitrary switching is discussed in [61]; and an advanced hybrid controller structure for robust stabilization of switched linear systems with arbitrary switching signals were developed in [94] by using a min-of-quadratic piecewise Lyapunov function. However, requiring all the subsystems of a switched system sharing a common Lyapunov function could be very restrictive, and such a CLF may not exist or very hard to find for some switched systems. Moreover, the CLF-based stability condition might become too conservative especially when a particular switching logic is concerned. Therefore, in the context of switched systems with controlled switching, it is reasonable to constitute the switching logic in the system design and find a suitable one such that stabilization as well as performance improvement can be achieved. To this end, the multiple Lyapunov function (MLF) technique [67, 10, 91, 98] serves as an effective alternative approach to the CLF-based technique. The key idea of multiple Lyapunov function is that instead of sharing a common Lyapunov function, it is allowed for each individual subsystem to possess its own Lyapunov or Lyapunov-like function, which thus forms the so-called multiple Lyapunov functions for the associated switched system. This basic idea was originally presented in [10]. Subsequent research along this line is focusing on devising different types of switching logics such that overall stability can be guaranteed under the MLF framework. Two typical switching logics prevailing the current switching control literature are worth to be mentioned. The first one is the state-dependent “min-switching logic” as proposed in [29, 28].

Under the min-switching logic, stability of switched systems is achieved by requiring a decreasing sequence to be formed and comparing the values of multiple Lyapunov functions at each switching time instants. This switching logic ensures that the switching behavior can only occur when the value of Lyapunov function with respect to the currently active subsystem is not minimal, and another subsystem associated with a minimal Lyapunov function value will be switched to at the time instant. The second one is the time-driven “dwell-time (DT) switching logic” [37]. Different from the min-switching logic, the concept of DT switching is defined for a switched system with all individual subsystems asymptotically stable. It is well-known that a switched system is stable if all individual subsystems are stable and the switching is sufficiently slow such that the transient effects can dissipate after each switch. The DT switching logic therefore provides a simple way to quantitatively specify this slow switching. Specifically, it restricts the class of admissible switching signals to be signals with the property that each pair of consecutive switching times is separated with a fix minimal amount of time, namely the “dwell time”. Under the DT switching logic, stability conditions of switched systems are established with the MLFs technique, i.e., in order to guarantee stability, the Lyapunov function is allowed to exhibit bounded increase at each switching time instant while required to decrease with a sufficiently fast converging rate when no switching occurs. This DT switching strategy was later on extended to an average sense, namely the average dwell-time (ADT) switching logic [37]. The ADT switching logic relaxes the DT one in the sense that it allows the possibility of switching fast when necessary and then compensating for it by switching sufficiently slowly later. This relaxation significantly widens the application of ADT switching in solving various practical engineering problems, such as [58, 62, 52].

It should be noted that in spite of the rich literature on stability and/or performance analysis of switched control systems, the synthesis problem for switched control systems has not yet been addressed adequately. For state-feedback control of switched systems, the MLF technique with quadratic Lyapunov-like functions have been successful because the derived conditions can usually be formulated as linear matrix inequalities (LMIs) and convex optimization problems

[8], and globally optimal solutions can be obtained for most performance objectives by using efficient numerical algorithms [8]. However, the output-feedback switching control synthesis problem is non-trivial. As opposed to the LTI systems, the separation principle is in general not valid for switched systems. So the switching output feedback control problem cannot be addressed by designing a state-feedback controller and an observer separately. In addition, the boundary condition that is used to guarantee overall switching stability by constraining the difference between two adjacent Lyapunov functions usually leads to undesirable results under different switching frameworks. For state-dependent switching control [29], a special structure has to be imposed on the MLFs, which inevitably introduces certain degree of conservatism; for time-driven switching control [57], the boundary condition could result in non-convex synthesis conditions (in the form of bilinear matrix inequalities (BMIs)), which are difficult to solve. Such a problem has not been addressed adequately in most of the current work, and there is still a lack of an effective way to tackle the BMI problem involved. When specified to ADT switching control, two methods typically used for dealing with this problem can be found in the literature (see, e.g., [84] and [58]). In particular, [84] separated the design procedure into two sequential steps: firstly design a  $\mathcal{H}_\infty$  controller for each plant subsystem individually, and then evaluate the ADT as well as the weighted  $\mathcal{L}_2$ -gain performance based on the boundary condition. This approach excludes the boundary condition from the controller synthesis, but might result in an unacceptable disturbance attenuation level and/or an unreasonably large dwell time. As opposed to [84], [58] incorporated the boundary condition into the controller synthesis, and the associated BMI problem was circumvented by using a controller state reset technique. However, the resulting control scheme in [58] is essentially state-feedback, since the plant states are required to be available at each switching instant for controller state reset. As such, developing an effective design scheme for switching output-feedback control synthesis under the MLF framework is highly desirable but remains as a challenging problem.

Motivated from the discussions above, in this dissertation research, our objective is to solve the challenging switching output-feedback control synthesis problem under the MLF frame-

work by developing a systematic and unified framework that is capable of rendering stringent performance and computational efficacy simultaneously. Instead of focusing on devising new computational algorithms to solve the aforementioned NP-hard BMI conditions, we are seeking to develop new switching output-feedback controller structures that would lead to computationally tractable synthesis conditions such that the optimal control solution can be readily obtained via convex optimization. Furthermore, in addition to the stabilization objective for switched linear systems, we will consider different switched control problems with various performance objectives, such that the developed results can be applied readily to solve practical engineering control problems. Specifically, we aim to

1. Develop new switching linear parameter-varying (LPV) control schemes for high-performance gain-scheduling linear fractional transformation (LFT) systems. The control objectives include both asymptotic stabilization and  $\mathcal{H}_\infty$  disturbance attenuation performance.
2. Develop new switching output-feedback control schemes for hybrid output regulator synthesis of a class of switched linear systems affected by switched exosignals, such that mixed  $\mathcal{H}_\infty$  performance and almost asymptotic output regulation can be achieved.
3. Develop advanced robust  $\mathcal{H}_2$  and  $\mathcal{H}_\infty$  switching disturbance feedforward control schemes for systems subject to time-varying LFT uncertainties.

## 1.2 Preliminaries

In this section, some preliminary results on switched linear systems will be first recalled, which will be useful for the development of the subsequent chapters.

A typical switched linear system subject to exogenous disturbance can be described as

$$\begin{bmatrix} \mathcal{D}x \\ e \end{bmatrix} = \begin{bmatrix} A_\sigma & B_\sigma \\ C_\sigma & D_\sigma \end{bmatrix} \begin{bmatrix} x \\ d \end{bmatrix} \quad (1.1)$$

where  $x \in \mathbb{R}^n$  is the state with initial condition  $x(0) = x_0$ ,  $e \in \mathbb{R}^{n_e}$  is the error/performance output and  $d \in \mathbb{R}^{n_d}$  is the external disturbance.  $\sigma(t) \in \mathbf{I}[1, N]$  is the switching rule that selects a particular sequence of subsystems among  $N$  available ones defined by  $\{A_i, B_i, C_i, D_i\}, i \in \mathbf{I}[1, N]$ . For two integers  $k_1, k_2, k_1 < k_2$ , we denote  $\mathbf{I}[k_1, k_2] = \{k_1, k_1 + 1, \dots, k_2\}$ . The symbol  $\mathcal{D}$  denotes a differentiator for continuous-time systems and a difference operator for discrete-time systems.

### 1.2.1 Stability definition of switched linear systems

The stability definitions for continuous-time and discrete-time switched linear systems are given as follows.

**Definition 1** ([48]). *The continuous-time switched linear system (1.1) with  $d \equiv 0$  is globally uniformly exponentially stable (GUES) under certain switching signal if there exist constants  $c > 0, \lambda > 0$  such that the solution of the system satisfies  $\|x(t)\| \leq ce^{-\lambda t}\|x(0)\|, \forall t \geq 0$ .*

**Definition 2** ([48]). *The discrete-time switched linear system (1.1) with  $d \equiv 0$  is globally uniformly exponentially stable (GUES) under certain switching signal if there exist a class  $\mathcal{KL}$  function  $\beta$  such that for all initial conditions  $x_0$ , the solution of the system satisfies  $\|x_k\| \leq \beta(\|x_0\|, k), \forall k \geq 0$ .*

### 1.2.2 $\mathcal{L}_2$ ( $\ell_2$ ) performance under min-switching

In the context of min-switching control, the following will first recall an important concept of Lyapunov-Metzler inequality. The class of Metzler matrices for continuous-time systems denoted by  $\mathcal{M}$  consist of all matrices  $\Pi \in \mathbb{R}^{N \times N}$  with elements  $\pi_{ij}$ , such that  $\pi_{ii} \leq 0$  for all  $i \in \mathbf{I}[1, N]$  and  $\sum_{i=1}^N \pi_{ij} = 0$  for all  $j \in \mathbf{I}[1, N]$ . Another class of Metzler matrices for discrete-time systems denoted by  $\tilde{\mathcal{M}}$  consists of all matrices  $\tilde{\Pi} \in \mathbb{R}^{N \times N}$  with elements  $\tilde{\pi}_{ji}$ , such that  $\tilde{\pi}_{ji} \geq 0$  and  $\sum_{j=1}^N \tilde{\pi}_{ji} = 1$  for all  $i \in \mathbf{I}[1, N]$ .

The following definitions pertain to the  $\mathcal{L}_2$  and  $\ell_2$  disturbance attenuation performance for continuous-time and discrete-time systems, respectively.

**Definition 3** ([48]). *Given certain switching signal  $\sigma$ , the continuous-time switched linear system (1.1) is said to achieve an  $\mathcal{L}_2$  disturbance attenuation level  $\gamma$  from  $d$  to  $e$ , if under zero initial conditions, the system (1.1) is GUES and satisfies  $\int_0^\infty \|e(t)\|^2 dt < \gamma^2 \int_0^\infty \|d(t)\|^2 dt$  for any  $d \in \mathcal{L}_2$ .*

**Definition 4** ([48]). *Given certain switching signal  $\sigma$ , the discrete-time switched linear system (1.1) is said to achieve an  $\ell_2$  disturbance attenuation level  $\gamma$  from  $d$  to  $e$ , if under zero initial conditions, the system (1.1) is GUES and satisfies  $\sum_{k=0}^\infty \|e(k)\|^2 < \gamma^2 \sum_{k=0}^\infty \|d(k)\|^2$  for any  $d \in \ell_2$ .*

Adopting the piecewise quadratic Lyapunov function to the switched linear system (1.1),

$$V(x) = \min_{1 \leq j \leq N} x^T P_j x \quad (1.2)$$

where  $P_j > 0$ ,  $\forall j \in \mathbf{I}[1, N]$ , it will be shown in the next theorem that if these positive definite matrices satisfy some well-defined conditions, then the min-switching strategy

$$\sigma = \arg \min_{1 \leq j \leq N} x^T P_j x \quad (1.3)$$

stabilizes the switched systems with a guaranteed  $\mathcal{L}_2$  ( $\ell_2$ ) disturbance attenuation level for continuous-time (discrete-time) settings. At the point  $x$  where minimum in (1.2) is not unique, the function  $V(x)$  is not differentiable and the switching rule  $\sigma$  can be switched to any subsystem achieving minimal Lyapunov function value, the chattering (if it occurs) is always stable as discussed in [28].

**Theorem 1** ([28, 14]). *The min-switching strategy (1.3) is globally stabilizing the switched linear system (1.1) with guaranteed  $\mathcal{L}_2$  ( $\ell_2$ ) performance if:*

1. *In continuous-time case: there exist symmetric positive definite matrices  $P_i$  and a Metzler*

matrix  $\Pi \in \mathcal{M}$  satisfying

$$\begin{bmatrix} A_i^T P_i + P_i A_i + \sum_{j=1}^N \pi_{ji} P_j & \star & \star \\ B_i^T P_i & -\gamma I & \star \\ C_i & D_i & -\gamma I \end{bmatrix} < 0, \quad \forall i \in \mathbf{I}[1, N]. \quad (1.4)$$

2. In discrete-time case: there exist symmetric positive definite matrices  $P_i$  and a Metzler matrix  $\tilde{\Pi} \in \tilde{\mathcal{M}}$  satisfying

$$\begin{bmatrix} -\left(\sum_{j=1}^N \tilde{\pi}_{ji} P_j\right)^{-1} & \star & \star & \star \\ A_i^T & -P_i & \star & \star \\ B_i & 0 & -\gamma I & \star \\ 0 & C_i & D_i & -\gamma I \end{bmatrix} < 0, \quad \forall i \in \mathbf{I}[1, N]. \quad (1.5)$$

Detailed proof of the above theorem has been well-established in [28, 14].

### 1.2.3 Weighted $\mathcal{L}_2$ ( $\ell_2$ ) performance under (average) dwell-time switching

The following first recall the definitions of dwell-time and average dwell-time switching logics.

**Definition 5** ([48]). A switching signal  $\sigma$  is said to have a dwell time (DT)  $\tau_D$  if

1. In continuous-time case:  $t_{k+1} - t_k \geq \tau_D$ ,  $\forall k \in \mathbb{N}$  where  $t_k, t_{k+1}$  denotes the switching instants.
2. In discrete-time case:  $k_{l+1} - k_l \geq \tau_D$ ,  $\forall l \in \mathbb{N}$  where  $k_l, k_{l+1}$  denotes the switching instants.

**Remark 1.** For discrete-time case, since  $k_l$  and  $k_{l+1}$  are integers that denotes the number of samples, the dwell-time  $\tau_D$  is also an integer number denoting the number of samples.

When all subsystems are asymptotically stable, the switched linear system (1.1) is asymptotically stable if the dwell time  $\tau_D$  is sufficiently large [48]. This concept is relaxed to average

dwell-time in [37] to allow fast switching when necessary and compensate it by switching sufficiently slowly later.

**Definition 6** ([48]). *Let  $N_\sigma(t, T) < \infty$  denote the number of discontinuities of a switching signal  $\sigma$  on the interval  $(t, T)$ . We say that  $\sigma$  has an average dwell-time  $\tau_a$  if there exist two positive numbers  $N_0$  and  $\tau_a$  such that*

$$N_\sigma(t, T) \leq N_0 + \frac{T - t}{\tau_a}, \quad \forall T \geq t \geq 0. \quad (1.6)$$

$N_0$  is called the chattering bound. In general, if we discard the first  $N_0$  switches (more, precisely, the smallest integer greater than  $N_0$ ), then the average dwell time between consecutive switches is at least  $\tau_a$ .

**Remark 2.** *The concept of ADT switching has been extensively used in the literature for stability analysis and stabilization of switched systems (e.g., [37, 108, 103]). The ADT constraint (1.6) essentially provides an upper bound on the frequency of switchings occurred during a finite interval  $(s, t]$ . The special case of  $N_0 = 1$  reduces to a dwell time condition in which any two consecutive switches must be separated by at least  $\tau_a$  units of time. Also, as an extreme case,  $\tau_a \rightarrow 0$  implies that the constraint on the switches is almost disappear and arbitrary fast switching is allowed. Therefore, the ADT constraint under consideration is more general and flexible by covering the dwell-time switching and arbitrary switching as special cases.*

**Definition 7** ([108]). *The switched system (1.1) with ADT switching is said to be GUES with a weighted  $\mathcal{L}_2$  ( $\ell_2$ ) gain  $\gamma$  from  $d$  to  $e$ , if under zero initial conditions, the system (1.1) is GUES and satisfies*

- for the continuous-time case,

$$\int_0^\infty e^{-\lambda t} \|e(t)\|^2 dt \leq \gamma^2 \int_0^\infty \|d(t)\|^2 dt \quad (1.7)$$

for some  $\lambda > 0$  and any  $d \in \mathcal{L}_2$ .

- for the discrete-time case,

$$\sum_{t=0}^{\infty} \lambda^t \|e(t)\|^2 \leq \gamma^2 \sum_{t=0}^{\infty} \|d(t)\|^2 \quad (1.8)$$

for some  $0 < \lambda < 1$  and any  $d \in \ell_2$ .

### 1.3 Dissertation Outline

The detailed outline of this dissertation is as follows:

Chapter 1 overviews the research on switched systems and emphasizes on the literature that motivates the research in this dissertation. The objectives of the research are discussed and some preliminaries are presented.

Chapter 2 presents a novel hybrid gain-scheduling output-feedback control scheme for high-performance missile autopilot design. The nonlinear dynamics of a pitch-axis missile model is considered, and reformulated as a switched linear fractional transformation (LFT) systems. Based on this, robust stability with guaranteed weighted  $\mathcal{L}_2$  disturbance attenuation property is analyzed using the average dwell time switching and multiple Lyapunov function techniques. The proposed hybrid control scheme is shown to be systematic yet simple for both full-order and reduced-order missile autopilot designs. The novelty can be reflected from three important aspects: (1) The synthesis conditions of the hybrid missile autopilot are formulated in terms of a finite number of LMIs, which can be solved effectively via convex optimization without parameter-space gridding; (2) Stringent controlled performance can be obtained without requiring parameter variation bound information for both controller synthesis and implementation; (3) Reduced controller state order can be always achieved regardless the settings of performance weighting functions employed. Comprehensive numerical simulations are provided to support the technical results.

Chapter 3 explores a more complicated switched tracking control problem, i.e., the switching output regulation problem. The output regulation problem specifies the control task of achieving

not only the overall closed-loop stability, but also the tracking and/or rejection of persistent references/disturbances generated by an exosystem. In this research, we consider both controlled plant and the exosystem as switched linear systems. A new hybrid output regulator structure and a new multiple coordinate transformation technique are proposed to establish switching output regulation and weighted  $\mathcal{H}_\infty$  controlled performance. Under the average dwell time switching control framework, the hybrid output regulator synthesis conditions are formulated in terms of a set of linear matrix inequalities (LMIs) plus linear matrix equations, which can be solved effectively using existing convex optimization algorithms. A mechanical system example is used to demonstrate the effectiveness of the proposed approach.

Chapter 4 considers the robust feedforward stabilization problem under the switching control framework for a class of uncertain systems described in a standard linear fractional transformation form. It is assumed that a switching feedback controller has been designed for the uncertain system. A new min-switching-type dynamic feedforward control scheme is proposed for both robust  $\mathcal{H}_2$  and  $\mathcal{H}_\infty$  control designs. Switching stability is established using the piecewise Lyapunov function technique, while the control synthesis conditions are formulated as a special type of bilinear matrix inequalities (BMIs), which can be solved via LMI optimization plus a line search. Advantages of the proposed design methods over existing ones based on using single quadratic Lyapunov function are demonstrated through an application to ship steering control.

Chapter 5 summarizes the contributions of this dissertation and discusses some future research directions.

## Chapter 2

# Hybrid Gain-Scheduling Control

This chapter presents a new hybrid gain-scheduling control method for switched parameter-dependent systems via dynamic output feedback. For controller design purpose, the switched parameter-dependent model is first converted to a switched linear fractional transformation (LFT) system. Then, the new hybrid gain-scheduling autopilot is designed, which consists of a switching dynamic output-feedback LFT controller and a supervisor enforcing a controller state reset at each switching time instant. The proposed hybrid control scheme is shown to provide a systematic yet simple framework for both full-order and reduced-order autopilot designs. Specifically, the associated control synthesis conditions that guarantee weighted  $\mathcal{L}_2$  stability performance are formulated in terms of a finite number of linear matrix inequalities (LMIs), which can be solved effectively via convex optimization without parameter-space gridding. Furthermore, stringent controlled performance and strong robustness against parameter perturbations are achieved using this new control approach, while no parameter variation information is required for both controller synthesis and implementation. Another important novelty of the proposed reduced-order controller lies in that its state order is equal to that of the plant state regardless the settings of performance weighting functions employed. The advantages of the proposed design approach over existing methods will be applied to a nonlinear missile control problem and shown through nonlinear simulations for the missile autopilot design over a wide

range of operating conditions.

## 2.1 Introduction

The autopilot design for modern missiles is a well-known challenging problem not only because the missile itself is a highly complex nonlinear system that involves non-minimum phase dynamics and has wide parameter variations during the missile operation, but also because it is required to be capable of providing stringent controlled performance across the entire flight envelope.

Gain-scheduling, as one of the most popular nonlinear control design techniques, has been demonstrated to be successful for missile autopilot design [45, 72, 80]. In traditional gain scheduling, a fundamental guideline for missile autopilot design is to gain schedule local robust controllers that are designed for several linearized missile models at their respective equilibrium points, so as to yield a global controller. Satisfactory performance could be achieved by using such traditional gain-scheduling controllers. However, due to the local nature of traditional gain-scheduling design, the stability of such controllers remains questionable for the entire flight envelope, especially during the rapid transitions in the missile endgame. With the development of linear parameter-varying (LPV) control theory, LPV-based gain-scheduling techniques have been proposed to pursue high-performance missile autopilots with guaranteed reliability (see, e.g., [3, 7, 64, 71, 78, 81, 87, 68, 52] and the references therein). In particular, [3] used LPV control theory to design gain-scheduling controllers based on a simplified missile model. In [81], the original missile dynamics were equivalently written in a quasi-LPV form via a state transformation, and a robust gain-scheduling controller possessing an inner/outer-loop structure was designed using  $\mu$  synthesis. Later on, based on a second-order quasi-LPV model, a systematic gain-scheduling approach for missile autopilot design was proposed in [87] following the methodology of LPV control from [88], and large improvement in controlled performance was achieved by incorporating scheduling parameter variation information. [68] designed a missile autopilot under multiple performance objectives by using the method from [4]. A switched LPV technique

was further proposed in [52] for both modeling and  $\mathcal{H}_\infty$  control design of missile autopilots.

Current research of missile LPV control mainly focuses on constructing different types of Lyapunov functions. Two types of Lyapunov functions frequently adopted in the field include constant Lyapunov functions (CLFs) [66, 2, 76, 68] and parameter-dependent Lyapunov functions (PDLFs) [1, 6, 88, 83, 52, 86], which leads to two respective synthesis frameworks, i.e., the scaled small-gain framework and the dissipative systems framework. With the CLF-based scheme, the underlying missile LPV system is specified as a linear fractional transformation (LFT) form, and the LFT gain-scheduling controller is fully characterized by a finite number of LMIs [68]. When compared to the CLF-based scheme, the PDLF-based scheme provides a more general and flexible framework for missile control synthesis though, there are several problems associated with this scheme, which could largely limit its applicability in practice. The most critical problem is that the synthesis conditions are often formulated as parameter-dependent LMIs involving infinite dimensional LMIs, which are generally difficult to solve. A standard approach to tackle this difficulty is to apply the gridding technique for the entire value set of the gain-scheduling variables (in this case the angle of attack  $\alpha$  and the Mach number  $M$  for missile problem), and then solve the resulting finite-dimensional optimization problem to obtain an approximate solution of the original synthesis problem. This approximate solution could be risky for stabilizing missile control, and typically requires extensive post-analysis to verify its validity [85]. Moreover, due to the lack of a systematic way of constructing the PDLFs, finding a proper PDLF could be quite involved and time-consuming. For the missile problem, it came with extensive simulation and complicated design procedure. Another significant problem encountered by the PDLF-based scheme is the requirement of parameter variation information for controller synthesis and implementation. This is generally prohibitive, since parameter derivatives either are not available or are difficult to estimate during system operation, especially for missile systems with fast and wide parameter variations. As such, from a practical consideration, the CLF-based scheme might be more suitable for missile autopilots design. However, one drawback of this approach is that using a single constant Lyapunov function might be too

conservative, and the resulting controller might not be able to meet the performance requirement especially when a large parameter variation range is considered. In order to overcome the deficiencies mentioned above, this chapter will propose a new hybrid missile autopilot design approach based on a switching LFT control technique. With this technique, the entire parameter region is partitioned into several small subregions such that a family of LFT controllers can be designed for multiple parameter subregions, and better controlled performance can be achieved by switching among these controllers instead of simply using a single controller derived from the CLF-based scheme. More importantly, compared to the PDLF-based scheme, the proposed hybrid control scheme will not only significantly reduce computational complexity in controller synthesis by avoiding parameter-space gridding, but also facilitate controller implementation since no derivative information of the scheduling parameters is required.

The methodology of incorporating switching techniques into LPV/LFT control design, which defines the switching LPV/LFT control technique, was firstly presented in [50], which is further extended in [51] by introducing average dwell time switching logic [37]. Further investigations along this line can be seen in [58, 103]. It has been demonstrated that the switching LPV/LFT control technique is effective in improving the performance of LPV control systems. However, there are several problems yet to be addressed adequately in most of current work, such as eliminating bilinear matrix inequality (BMI) constraints in controller synthesis and enhancing the implementability of LPV/LFT controllers [58, 103].

In this chapter, we present a new hybrid gain-scheduling control method for missile autopilot design by using the switching LFT control technique with the average dwell time logic. For controller design purpose, the nonlinear missile dynamics will be first modeled as a switched LFT system by partitioning the entire operating region of the scheduling variables (the angle of attack  $\alpha$  and the Mach number  $M$ ) into several subregions. Then, based on this setup, the new hybrid gain-scheduling autopilot design scheme is proposed, which consists of a switching dynamic output-feedback LFT controller and a supervisor that monitors the switching signal and enforces a reset rule for the controller states at each switching time instant. The pro-

posed hybrid control scheme provides a systematic yet simple framework for both full-order and reduced-order high performance missile autopilot designs. It is advantageous over existing missile control methods in three important ways. First, the associated control synthesis conditions that guarantee weighted  $\mathcal{L}_2$  stability performance are formulated in terms of a finite number of LMIs. As a result, the controller coefficient matrices can be readily solved through a convex optimization problem without taking the gridding and post-analysis procedures that are typically required in most existing LPV design techniques (see, [58, 52, 85]). Second, stringent controlled performance over a wide range of operating conditions, and strong robustness against perturbed system parameters are achieved without utilizing scheduling parameter variations in both controller synthesis and implementation. Another important novelty of the proposed hybrid controller lies in its reduced-order form, i.e., the controller state order is equal to that of the plant state regardless what type and how many performance weighting functions are employed. This would largely facilitates the missile autopilot implementation in practice, especially when more complicated weighting functions are employed for more stringent performance goals.

The rest of this chapter is organized as follows. Section 2.2 presents both full-order and reduced-order hybrid gain-scheduling controllers for a class of switched LFT systems with average dwell time. The controller synthesis conditions are also given in this section. Section 2.3 then applies the proposed approach to the missile benchmark problem. This includes a derivation of a switched LFT model, the control problem setup, and the discussion on controller synthesis results and nonlinear simulations. Finally, Section 2.4 summarizes the chapter.

## 2.2 Hybrid Gain-Scheduling Control of Switched LFT Systems

In this section, a hybrid gain-scheduling control scheme will be proposed for ADT switched LFT systems. Both full-order and reduced-order controllers will be presented. It will be shown that with this proposed hybrid control scheme, the associated controller synthesis problems are formulated as LMI optimization problems, which can be solved efficiently.

Consider an open-loop switched LFT parameter-dependent system described by:

$$\begin{bmatrix} \dot{x}_p \\ q_p \\ e \\ y \end{bmatrix} = \begin{bmatrix} A_{p,i} & B_{p0,i} & B_{p1,i} & B_{p2,i} \\ C_{p0,i} & D_{p00,i} & D_{p01,i} & D_{p02,i} \\ C_{p1,i} & D_{p10,i} & D_{p11,i} & D_{p12,i} \\ C_{p2,i} & D_{p20,i} & D_{p21,i} & D_{p22,i} \end{bmatrix} \begin{bmatrix} x_p \\ p_p \\ d \\ u \end{bmatrix} \quad (2.1)$$

$$p_p = \Theta_i q_p$$

where  $i \in \mathbf{I}[1, N_p]$ ,  $N_p > 1$  is the number of subsystems,  $x_p \in \mathbb{R}^n$  is the plant state,  $u \in \mathbb{R}^{n_u}$  is the control input,  $e \in \mathbb{R}^{n_e}$  is the controlled/performance output,  $d \in \mathbb{R}^{n_d}$  is the disturbance,  $y \in \mathbb{R}^{n_y}$  is the measurement output, and  $p_p, q_p \in \mathbb{R}^{n_p}$  are the pseudo-input and output. It is assumed that the LFT representation (2.1) for all  $i \in \mathbf{I}[1, N_p]$  is well-posed, i.e.,  $(I_{n_p} - D_{p00,i}\Theta_i)$  is invertible for any allowable parameter values. Furthermore, the time-varying parameter  $\Theta_i$  satisfies  $\|\Theta_i\| \leq 1, \forall i \in \mathbf{I}[1, N_p]$ , and obeys the following structure:

$$\Theta_i = \{diag\{\theta_{1,i}I_{r_{1,i}}, \theta_{2,i}I_{r_{2,i}}, \dots, \theta_{s,i}I_{r_{s,i}}\} : |\theta_{j,i}| \leq 1, j \in \mathbf{I}[1, s]; i \in \mathbf{I}[1, N_p]\} \quad (2.2)$$

where  $\sum_{j=1}^s r_{j,i} = n_p$  represents the order of the corresponding LFT for all  $i \in \mathbf{I}[1, N_p]$ . The time-varying parameter  $\Theta_i$  is assumed to be available in real-time for gain-scheduling control use. All of the state-space data are real and assumed to be known for control design. Two assumptions concerning the switched LFT plant (2.1) are also given:

**(A1)** The triple  $(A_{p,i}, [B_{p0,i} \ B_{p2,i}], \begin{bmatrix} C_{p0,i} \\ C_{p2,i} \end{bmatrix})$  is stabilizable and detectable for all  $\Theta_i$  satisfying (2.2) and  $i \in \mathbf{I}[1, N_p]$ ;

**(A2)**  $D_{p22,i} = 0$  for all  $i \in \mathbf{I}[1, N_p]$ .

Note that these two assumptions are quite standard in the context of LPV control, assumption (A1) guarantees the existence of a stabilizing gain-scheduling output-feedback controller for each subsystem in (2.1), while assumption (A2) considerably simplifies the derivation. These

technical assumptions can be relaxed with more complicated formulae, see [85] for more details.

The proposed hybrid gain-scheduling control scheme (as shown in Fig. 2.1) consists of a standard switching dynamic output-feedback controller  $\mathcal{C}_\sigma$  and a supervisor enforcing a reset rule to the controller state at each switching time instant.  $\sigma$  is the signal governing the switching between the subsystems, which is defined as a piecewise constant function with the value chosen from the set  $\mathbf{I}[1, N_p]$ . It is assumed that  $\sigma$  is continuous from the right everywhere. For missile control problem, the value of switching signal  $\sigma$  depends on the time-varying parameter  $\Theta_\sigma$  (which will be clarified in Section 2.3), and thus governs the dynamic behavior of the closed-loop system. As such, the switching signal  $\sigma$  will be incorporated with the hybrid controller for missile autopilot design to achieve overall stability and desired controlled performance. The switching gain-scheduling controller  $\mathcal{C}_\sigma$  has one-to-one correspondence with the switched LFT plant  $\mathcal{G}_\sigma$ . Specifically, during the flowing time intervals, the switched LFT plant  $\mathcal{G}_\sigma$  will be controlled using the switching gain-scheduling controller  $\mathcal{C}_\sigma$ . Once switching occurs, the controller state will undergo a reset/jump action at the switching time instant. The introduction of a reset mechanism into the switching controller structure is motivated from [103], interested readers are referred to this reference for more details.

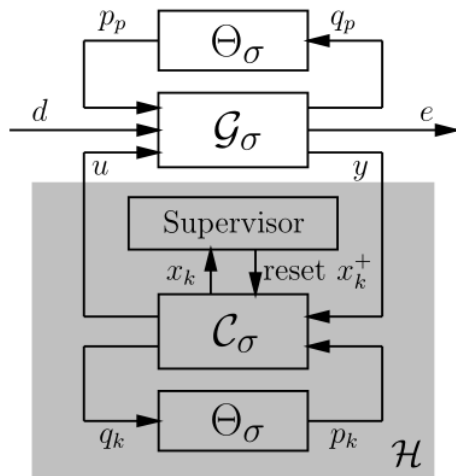


Figure 2.1: The proposed hybrid control scheme.

A switched Lyapunov function consisting of multiple quadratic Lyapunov functions (MQLFs) [10], together with an average dwell time (ADT) logic [37], will be used for stability analysis and control design. The switched Lyapunov function can be defined as

$$V_\sigma(x) = x^T P_\sigma x \quad (2.3)$$

where  $P_\sigma$  is a positive definite matrix with  $\sigma \in \mathbf{I}[1, N_p]$ . Each Lyapunov function  $V_i(x)$  ( $\forall i \in \mathbf{I}[1, N_p]$ ) corresponds to one particular subsystem.

Different from traditional Lyapunov-based analysis, to guarantee stability of a switched control system under the ADT switching logic (see Definition 6), the value of the discontinuous Lyapunov function  $V_\sigma$  is not necessarily decreasing along the entire system trajectory, but is allowed to increase with a bounded amount at each switching time instant. The possible increases of the Lyapunov function will be compensated by its decreasing during the dwell-time interval by limiting the average switching frequency over a given time interval no greater than  $\frac{1}{\tau_a}$ . The constraint on Lyapunov functions at each switching instant, which is the so-called boundary condition, is formulated as

$$\frac{1}{\mu} V_j \leq V_i \leq \mu V_j, \quad \forall i, j \in \mathbf{I}[1, N_p], \quad (2.4)$$

where  $\mu > 1$  is a pre-specified scalar.

In most previous studies of dwell-time switching output-feedback control, the controller synthesis conditions usually turn out to be non-convex due to the existence of the boundary condition (2.4). In this chapter, this problem will be resolved by following the methodology from [103] to embed a reset loop into the switching control structure (as shown in Fig. 2.1).

In the following development, we will first present the design of a full-order hybrid gain-scheduling controller for the switched LFT plant (2.1), and then extended to the scheme of reduced-order case by assuming that partial plant states are available for feedback use.

### 2.2.1 Full-Order Case

The full-order hybrid gain-scheduled controller with one-to-one correspondence to the LFT plant (2.1) is constructed in the form of

$$\begin{aligned} \begin{bmatrix} \dot{x}_k \\ q_k \\ u \end{bmatrix} &= \begin{bmatrix} A_{k,i} & B_{k0,i} & B_{k1,i} \\ C_{k0,i} & D_{k00,i} & D_{k01,i} \\ C_{k1,i} & D_{k10,i} & D_{k11,i} \end{bmatrix} \begin{bmatrix} x_k \\ p_k \\ y \end{bmatrix} \\ p_k &= \Theta_i q_k \\ x_k^+ &= \Delta_{ij} x_k, \quad \text{when switching occurs} \end{aligned} \tag{2.5}$$

where the controller state  $x_k \in \mathbb{R}^n$  has the same dimension of the plant state, the two subscripts of the reset matrix  $\Delta_{ij}$ ,  $i, j \in \mathbf{I}[1, N_p]$  with  $i \neq j$ , are used to denote respectively the indices of the pre-switching subsystem  $i$  and the post-switching subsystem  $j$ .  $p_k, q_k \in \mathbb{R}^{n_p}$  are the pseudo-input and output of the controller, sharing the same dimension of the counterparts in system (2.1). The controller gain matrices ( $A_{k,i}, B_{k0,i}, B_{k1,i}, C_{k0,i}, C_{k1,i}, D_{k00,i}, D_{k01,i}, D_{k10,i}, D_{k11,i}$ ) and the reset matrices  $\Delta_{ij}$  of compatible dimensions are subject to design, while the gain-scheduling matrices  $\Theta_i, \forall i \in \mathbf{I}[1, N_p]$  are given by the open-loop system (2.1).

With the open-loop LFT plant (2.1) and the hybrid controller (2.5), the resulting hybrid closed-loop system can be deduced as

$$\begin{aligned} \begin{bmatrix} \dot{x}_{cl} \\ q_{cl} \\ z \end{bmatrix} &= \begin{bmatrix} A_{cl,\sigma} & B_{cl0,\sigma} & B_{cl1,\sigma} \\ C_{cl0,\sigma} & D_{cl00,\sigma} & D_{cl01,\sigma} \\ C_{cl1,\sigma} & D_{cl10,\sigma} & D_{cl11,\sigma} \end{bmatrix} \begin{bmatrix} x_{cl} \\ p_{cl} \\ d \end{bmatrix} \\ p_{cl} &= \Theta_{cl,\sigma} q_{cl} \\ x_{cl}^+ &= A_{r,ij} x_{cl}, \quad \text{when switching occurs} \end{aligned} \tag{2.6}$$

where  $x_{cl} = [x_p^T \ x_k^T]^T$ ,  $p_{cl} = [p_p^T \ p_k^T]^T$ ,  $q_{cl} = [q_p^T \ q_k^T]^T$ , and

$$\begin{aligned} \begin{bmatrix} A_{cl,\sigma} & B_{cl0,\sigma} & B_{cl1,\sigma} \\ C_{cl0,\sigma} & D_{cl00,\sigma} & D_{cl01,\sigma} \\ C_{cl1,\sigma} & D_{cl10,\sigma} & D_{cl11,\sigma} \end{bmatrix} &= \begin{bmatrix} A_{p,\sigma} & 0 & B_{p0,\sigma} & 0 & B_{p1,\sigma} \\ 0 & 0 & 0 & 0 & 0 \\ \hline C_{p0,\sigma} & 0 & D_{p00,\sigma} & 0 & D_{p01,\sigma} \\ 0 & 0 & 0 & 0 & 0 \\ \hline C_{p1,\sigma} & 0 & D_{p10,\sigma} & 0 & D_{p11,\sigma} \end{bmatrix} + \begin{bmatrix} 0 & B_{p2,\sigma} & 0 \\ I & 0 & 0 \\ \hline 0 & D_{p02,\sigma} & 0 \\ 0 & 0 & I \\ \hline 0 & D_{p12,\sigma} & 0 \end{bmatrix} \\ &\times \begin{bmatrix} A_{k,\sigma} & B_{k1,\sigma} & B_{k0,\sigma} \\ C_{k1,\sigma} & D_{k11,\sigma} & D_{k10,\sigma} \\ C_{k0,\sigma} & D_{k01,\sigma} & D_{k00,\sigma} \end{bmatrix} \begin{bmatrix} 0 & I & 0 & 0 & 0 \\ C_{p2,\sigma} & 0 & D_{p20,\sigma} & 0 & D_{p21,\sigma} \\ 0 & 0 & 0 & I & 0 \end{bmatrix}, \\ \Theta_{cl,\sigma} &= \begin{bmatrix} \Theta_\sigma & 0 \\ 0 & \Theta_\sigma \end{bmatrix}, \quad A_{r,ij} = \begin{bmatrix} I & 0 \\ 0 & \Delta_{ij} \end{bmatrix}. \end{aligned}$$

$\sigma \in \mathbf{I}[1, N_p]$  is the switching signal. Based on the above definitions of the two subscripts of  $A_{r,ij}$ , we have  $i = \sigma$  and  $j = \sigma^+$ . The superscript “+” stands for the time instant immediately after the switching, since a switching occurs instantaneously. Note that the plant state will not be altered during the switching.

Using the ADT technique with multiple quadratic Lyapunov functions, the following theorem presents the synthesis conditions for the full-order hybrid controller (2.5) in terms of LMIs, together with an algorithm for the controller construction.

**Theorem 2.** *Consider the open-loop switched LFT system (2.1). Given two positive scalars  $\lambda_0 \in \mathbb{R}_+$  and  $\mu > 1$ , if there exist positive definite matrices  $R_i, S_i \in \mathbb{S}^{n \times n}$ , and  $L_i, J_i \in \mathbb{S}^{n_p \times n_p}$ , rectangular matrices  $\hat{A}_{k,i} \in \mathbb{R}^{n \times n}$ ,  $\begin{bmatrix} \hat{B}_{k0,i} & \hat{B}_{k1,i} \end{bmatrix} \in \mathbb{R}^{n \times (n_p + n_y)}$ ,  $\hat{C}_{k0,i} \in \mathbb{R}^{n_p \times n}$ ,  $\hat{C}_{k1,i} \in \mathbb{R}^{n_u \times n}$ ,  $\begin{bmatrix} \hat{D}_{k00,i} & \hat{D}_{k01,i} \end{bmatrix} \in \mathbb{R}^{n_p \times (n_p + n_y)}$ ,  $\begin{bmatrix} \hat{D}_{k10,i} & \hat{D}_{k11,i} \end{bmatrix} \in \mathbb{R}^{n_u \times (n_p + n_y)}$ ,  $\hat{\Delta}_{ij} \in \mathbb{R}^{n \times n}$ , and a positive*

scalar  $\gamma \in \mathbb{R}_+$ , such that the following conditions hold for all  $i, j \in \mathbf{I}[1, N_p]$  with  $i \neq j$ ,

$$\begin{bmatrix}
He\{A_{p,i}R_i + B_{p2,i}\hat{C}_{k1,i}\} + \lambda_0R_i & \star & \star \\
\hat{A}_{k,i} + A_{p,i}^T + C_{p2,i}^T\hat{D}_{k11,i}^TB_{p2,i}^T + \lambda_0I & He\{S_iA_{p,i} + \hat{B}_{k1,i}C_{p2,i}\} + \lambda_0S_i & \star \\
L_iB_{p0,i}^T + \hat{D}_{k10,i}^TB_{p2,i}^T & \hat{B}_{k0,i}^T & -L_i \\
B_{p0,i}^T + D_{p20,i}^T\hat{D}_{k11,i}^TB_{p2,i}^T & B_{p0,i}^TS_i + D_{p20,i}^T\hat{B}_{k1,i}^T & -I \\
B_{p1,i}^T + D_{p21,i}^T\hat{D}_{k11,i}^TB_{p2,i}^T & B_{p1,i}^TS_i + D_{p21,i}^T\hat{B}_{k1,i}^T & 0 \\
C_{p0,i}R_i + D_{p02,i}\hat{C}_{k1,i} & C_{p0,i} + D_{p02,i}\hat{D}_{k11,i}C_{p2,i} & D_{p00,i}L_i + D_{p02,i}\hat{D}_{k10,i} \\
\hat{C}_{k0,i} & J_iC_{p0,i} + \hat{D}_{k01,i}C_{p2,i} & \hat{D}_{k00,i} \\
C_{p1,i}R_i + D_{p12,i}\hat{C}_{k1,i} & C_{p1,i} + D_{p12,i}\hat{D}_{k11,i}C_{p2,i} & D_{p10,i}L_i + D_{p12,i}\hat{D}_{k10,i} \\
\star & \star & \star & \star & \star \\
\star & \star & \star & \star & \star \\
\star & \star & \star & \star & \star \\
-J_i & \star & \star & \star & \star \\
0 & -\gamma I & \star & \star & \star \\
D_{p00,i} + D_{p02,i}\hat{D}_{k11,i}D_{p20,i} & D_{p01,i} + D_{p02,i}\hat{D}_{k11,i}D_{p21,i} & -L_i & \star & \star \\
J_iD_{p00,i} + \hat{D}_{k01,i}D_{p20,i} & J_iD_{p01,i} + \hat{D}_{k01,i}D_{p21,i} & -I & -J_i & \star \\
D_{p10,i} + D_{p12,i}\hat{D}_{k11,i}D_{p20,i} & D_{p11,i} + D_{p12,i}\hat{D}_{k11,i}D_{p21,i} & 0 & 0 & -\gamma I
\end{bmatrix} < 0 \quad (2.7)$$

$$\begin{bmatrix}
\mu R_i & \star & \star & \star \\
\mu I_n & \mu S_i & \star & \star \\
R_i & I_n & R_j & \star \\
\hat{\Delta}_{ij} & S_j & I_n & S_j
\end{bmatrix} \geq 0 \quad \begin{bmatrix}
R_i & \star \\
I_n & S_i
\end{bmatrix} > 0 \quad (2.8)$$

$$\begin{bmatrix}
L_i & \star \\
I_{n_q} & J_i
\end{bmatrix} > 0 \quad (2.9)$$

where  $L_i\Theta_i = \Theta_iL_i$  and  $J_i\Theta_i = \Theta_iJ_i$ . Then, the hybrid closed-loop system (2.6) is exponentially stabilized by the full-order hybrid controller (2.5) for every switching signal  $\sigma$  with average dwell

time

$$\tau_a \geq \frac{\ln(\mu)}{\lambda_0}, \quad (2.10)$$

and the weighted  $\mathcal{L}_2$  gain from the disturbance  $d$  to the controlled output  $z$  is less than  $\gamma$ .

Moreover, the controller matrices are readily obtained with the following algorithm:

- Solve  $N_i, M_i$  and  $U_i, W_i$  for all  $i \in \mathbf{I}[1, N_p]$  from the factorization problem  $I - R_i S_i = M_i N_i^T$ , and  $I - L_i J_i = U_i W_i^T$ .
- Compute the controller matrices  $A_{k,i}, B_{k0,i}, B_{k1,i}, C_{k0,i}, C_{k1,i}, D_{k00,i}, D_{k01,i}, D_{k10,i}, D_{k11,i}$  and  $\Delta_{ij}$  for all  $i, j \in \mathbf{I}[1, N_p]$  and  $i \neq j$  with

$$\begin{aligned} \begin{bmatrix} A_{k,i} & B_{k0,i} & B_{k1,i} \\ C_{k0,i} & D_{k00,i} & D_{k01,i} \\ C_{k1,i} & D_{k10,i} & D_{k11,i} \end{bmatrix} &= \begin{bmatrix} N_i & 0 & S_i B_{p2,i} \\ 0 & W_i & J_i D_{p02,i} \\ 0 & 0 & I \end{bmatrix}^{-1} \\ &\times \begin{bmatrix} \hat{A}_{k,i} - S_i A_{p,i} R_i & \hat{B}_{k0,i} - S_i B_{p0,i} L_i & \hat{B}_{k1,i} \\ \hat{C}_{k0,i} - J_i C_{p0,i} R_i & \hat{D}_{k00,i} - J_i D_{p00,i} L_i & \hat{D}_{k01,i} \\ \hat{C}_{k1,i} & \hat{D}_{k10,i} & \hat{D}_{k11,i} \end{bmatrix} \begin{bmatrix} M_i^T & 0 & 0 \\ 0 & U_i^T & 0 \\ C_{p2,i} R_i & D_{p20,i} L_i & I \end{bmatrix}^{-1} \\ \Delta_{ij} &= N_j^{-T} (\hat{\Delta}_{ij} - S_j R_i) M_i^{-T}. \end{aligned} \quad (2.11)$$

*Proof.* The proof is based on the Scaled Bounded Real Lemma and the congruence transformation theory [110]. For the closed-loop system (2.6), we define the multiple quadratic Lyapunov functions as  $V_i(x_{cl}) = x_{cl}^T P_i x_{cl}$ ,  $\forall i \in \mathbf{I}[1, N_p]$ , and partition the Lyapunov function matrices  $P_i$  and the associated scaling matrices denoted by  $\Lambda_i$  according to the dimensions of the plant and controller state as

$$P_i = \begin{bmatrix} S_i & N_i \\ N_i^T & X_i^{-1} \end{bmatrix}, \quad \Lambda_i = \begin{bmatrix} J_i & W_i \\ W_i^T & Y_i^{-1} \end{bmatrix}.$$

Furthermore, we specify

$$\begin{aligned} Z_{1,i} &= \begin{bmatrix} R_i & I \\ M_i^T & 0 \end{bmatrix}, & Z_{2,i} &= \begin{bmatrix} I & S_i \\ 0 & N_i^T \end{bmatrix} \\ T_{1,i} &= \begin{bmatrix} L_i & I \\ U_i^T & 0 \end{bmatrix}, & T_{2,i} &= \begin{bmatrix} I & J_i \\ 0 & W_i^T \end{bmatrix} \end{aligned}$$

such that  $P_i Z_{1,i} = Z_{2,i}$  and  $\Lambda_i T_{1,i} = T_{2,i}$ . Then, we have  $X_i^{-1} = -N_i^T R_i M_i^{-T}$  and  $Y_i^{-1} = -W_i^T L_i U_i^{-T}$ . Based on conditions (2.8) and (2.9), it can be verified that  $P_i > 0$  and  $\Lambda_i > 0$ . According to [110] and [108], to establish switching stability and weighted  $\mathcal{L}_2$ -gain performance for the closed-loop system (2.6), we need to further prove the following Lyapunov conditions:

$$\begin{aligned} \dot{V}_i + q_{cl}^T \Lambda_i q_{cl} - p_{cl}^T \Lambda_i p_{cl} + \frac{1}{\gamma} z^T z - \gamma d^T d &< 0 \\ V_j - \mu V_i &\leq 0 \end{aligned}$$

for all  $i, j \in \mathbf{I}[1, N_p]$  and  $i \neq j$ . These two conditions can be further converted into matrix inequalities by using the Scaled Bounded Real Lemma and Schur complement [110], i.e.,

$$\begin{aligned} &\begin{bmatrix} He\{A_{cl,i}^T P_i\} + \lambda_0 P_i & \star & \star & \star & \star \\ B_{cl0,i}^T P_i & -\Lambda_i & \star & \star & \star \\ B_{cl1,i}^T P_i & 0 & -\gamma I & \star & \star \\ C_{cl0,i} & D_{cl00,i} & D_{cl01,i} & -\Lambda_i^{-1} & \star \\ C_{cl1,i} & D_{cl10,i} & D_{cl11,i} & 0 & -\gamma I \end{bmatrix} < 0, \\ &\begin{bmatrix} \mu P_i & \star \\ P_j A_{r,ij} & P_j \end{bmatrix} \geq 0. \end{aligned}$$

Consequently, performing congruence transformations on the above two inequalities with matrices  $diag\{Z_{1,i}, T_{1,i}, I, T_{2,i}, I\}$  and  $diag\{Z_{1,i}, Z_{1,j}\}$ , respectively, and after some tedious matrix calculation, conditions (2.7) through (2.9) and the controller formulae (2.11) can be deduced.  $\square$

Theorem 2 provides an upper bound on the weighted  $\mathcal{L}_2$  gain for the hybrid closed-loop system (2.6). In order to determine the optimal weighted  $\mathcal{L}_2$  gain performance under a pre-given pair of dwell-time parameters  $(\lambda_0, \mu)$ , one can solve the following LMI optimization problem:

$$\begin{aligned} & \min_{R_i, S_i, L_i, J_i, \hat{A}_{k,i}, \hat{B}_{k0,i}, \hat{B}_{k1,i}, \hat{C}_{k0,i}, \hat{C}_{k1,i}, \hat{D}_{k00,i}, \hat{D}_{k01,i}, \hat{D}_{k10,i}, \hat{D}_{k11,i}, \hat{\Delta}_{ij}} \gamma, \\ & \text{subject to} \quad (2.7), (2.8) \text{ and } (2.9). \end{aligned} \quad (2.12)$$

**Remark 3.** Observe that the reset matrices  $\Delta_{ij}$  (for all  $i, j \in \mathbf{I}[1, N_p]$  with  $i \neq j$ ) of the hybrid gain-scheduled controller (2.5) depend on both indices of the pre- and post-switching subsystems. As a result, there exist  $N_p^2 - N_p$  such reset matrices. Furthermore, as opposed to the method of [58], with the proposed hybrid control scheme, the controller state is reset to a map of the controller state itself, but without resorting to any information of the plant state, which significantly enhances the controller's applicability in practice.

### 2.2.2 Reduced-Order Case

Now, we are in the position to consider the control synthesis problem for the switched LFT system (2.1) using reduced-order output-feedback controllers. The reduced-order control laws are preferable for easy control implementation when the number of plant states becomes large. In particular, for missile control problem, we will show in Section 2.3 that with the proposed hybrid control scheme, the order of the missile autopilot can be largely reduced by directly utilizing the state information of the weighting functions. Based on the switched LFT plant (2.1), we assume without losing any generality that  $x_p = [x_{p1}^T \ x_{p2}^T]^T$  with  $x_{p1} \in \mathbb{R}^{n_1}$ ,  $x_{p2} \in \mathbb{R}^{n_2}$  and  $n_1 + n_2 = n$  being exactly measurable in real time without noise. In such a case, we can partition the measurement output  $y$  of (2.1) as  $y := [y_1^T \ y_2^T]^T$  with  $y_1 \in \mathbb{R}^{n_{y1}}$  and  $y_2 \in \mathbb{R}^{n_2}$  and  $n_{y1} + n_2 = n_y$ , such that  $y_2 = x_{p2}$ . Accordingly, the output matrices  $(C_{p2,i}, D_{p20,i}, D_{p21,i})$  can

be rewritten as follows for all  $i \in \mathbf{I}[1, N_p]$ ,

$$\begin{bmatrix} C_{p2,i} & D_{p20,i} & D_{p21,i} \end{bmatrix} = \left[ \begin{array}{c|c|c} \bar{C}_{p2,i} & \bar{D}_{p20,i} & \bar{D}_{p21,i} \\ \hline 0 & I_{n_2} & 0 \end{array} \right]. \quad (2.13)$$

For the reduced-order control design, in addition to the measurement output  $y_1$ , part of the plant states, i.e.,  $x_{p2}$ , is also treated as a measurable output (denoted as  $y_2$ ) for control use. Then, based on the hybrid control scheme as shown in Fig. 2.1, we will construct the following reduced-order hybrid gain-scheduling controller for the switched LFT plant (2.1).

$$\begin{bmatrix} \dot{x}_k \\ q_k \\ u \end{bmatrix} = \begin{bmatrix} A_{k,i} & B_{k0,i} & B_{k1,i} & B_{k2,i} \\ C_{k0,i} & D_{k00,i} & D_{k01,i} & D_{k02,i} \\ C_{k1,i} & D_{k10,i} & D_{k11,i} & D_{k12,i} \end{bmatrix} \begin{bmatrix} x_k \\ p_k \\ y_1 \\ y_2 \end{bmatrix} \quad (2.14)$$

$$p_k = \Theta_i q_k$$

$$x_k^+ = \begin{bmatrix} \Delta_{1,ij} & \Delta_{2,ij} \end{bmatrix} \begin{bmatrix} y_2 \\ x_k \end{bmatrix}, \quad \text{when switching occurs}$$

where  $i, j \in \mathbf{I}[1, N_p]$  with  $i \neq j$ ,  $x_k \in \mathbb{R}^{n_1}$  is the controller state.  $\Delta_{1,ij} \in \mathbb{R}^{n_1 \times n_2}$  and  $\Delta_{2,ij} \in \mathbb{R}^{n_1 \times n_1}$  are the reset matrices. The two subscripts of the reset matrices with  $i \neq j$ , are used to denote respectively the indices of the pre-switching subsystem  $i$  and the post-switching subsystem  $j$ .  $p_k, q_k \in \mathbb{R}^{n_p}$  are the pseudo-input and output of the controller. The controller gain matrices ( $A_{k,i}, B_{k0,i}, B_{k1,i}, B_{k2,i}, C_{k0,i}, C_{k1,i}, D_{k00,i}, D_{k01,i}, D_{k02,i}, D_{k10,i}, D_{k11,i}, D_{k12,i}$ ) of compatible dimensions and the reset matrices  $\Delta_{1,ij}, \Delta_{2,ij}$  are subject to design, while the gain-scheduled matrices  $\Theta_i, \forall i \in \mathbf{I}[1, N_p]$  are copied from the open-loop plant (2.1).

With the open-loop LFT plant (2.1) and the hybrid controller (2.14), the resulting hybrid closed-loop system can be deduced in the form of (2.6) with  $x_{cl} = [x_{p1}^T \ x_{p2}^T \ x_k^T]^T$ ,  $p_{cl} = [p_p^T \ p_k^T]^T$ ,

$q_{cl} = [q_p^T \ q_k^T]^T$ , and

$$\begin{aligned}
\begin{bmatrix} A_{cl,\sigma} & B_{cl0,\sigma} & B_{cl1,\sigma} \\ C_{cl0,\sigma} & D_{cl00,\sigma} & D_{cl01,\sigma} \\ C_{cl1,\sigma} & D_{cl10,\sigma} & D_{cl11,\sigma} \end{bmatrix} &= \begin{bmatrix} A_{p,\sigma} & 0 & B_{p0,\sigma} & 0 & B_{p1,\sigma} \\ 0 & 0 & 0 & 0 & 0 \\ C_{p0,\sigma} & 0 & D_{p00,\sigma} & 0 & D_{p01,\sigma} \\ 0 & 0 & 0 & 0 & 0 \\ C_{p1,\sigma} & 0 & D_{p10,\sigma} & 0 & D_{p11,\sigma} \end{bmatrix} + \begin{bmatrix} 0 & B_{p2,\sigma} & 0 \\ I_{n_1} & 0 & 0 \\ 0 & D_{p02,\sigma} & 0 \\ 0 & 0 & I_{n_p} \\ 0 & D_{p12,\sigma} & 0 \end{bmatrix} \\
&\times \begin{bmatrix} A_{k,\sigma} & \begin{bmatrix} B_{k1,\sigma} & B_{k2,\sigma} \end{bmatrix} & B_{k0,\sigma} \\ C_{k1,\sigma} & \begin{bmatrix} D_{k11,\sigma} & D_{k12,\sigma} \end{bmatrix} & D_{k10,\sigma} \\ C_{k0,\sigma} & \begin{bmatrix} D_{k01,\sigma} & D_{k02,\sigma} \end{bmatrix} & D_{k00,\sigma} \end{bmatrix} \begin{bmatrix} 0 & I_{n_1} \\ \begin{bmatrix} \bar{C}_{p2,i} \\ 0 \quad I_{n_2} \end{bmatrix} & 0 \\ 0 & 0 \end{bmatrix} \begin{bmatrix} 0 & 0 \\ \bar{D}_{p20,\sigma} & 0 \\ 0 & I_{n_p} \end{bmatrix} \begin{bmatrix} 0 \\ \bar{D}_{p21,\sigma} \\ 0 \end{bmatrix} \\
\Theta_{cl,\sigma} = \begin{bmatrix} \Theta_\sigma & 0 \\ 0 & \Theta_\sigma \end{bmatrix}, \quad A_{r,ij} = \begin{bmatrix} I_{n_1} & 0 & 0 \\ 0 & I_{n_2} & 0 \\ 0 & \Delta_{1,ij} & \Delta_{2,ij} \end{bmatrix}.
\end{aligned} \tag{2.15}$$

The synthesis conditions for the reduced-order hybrid controller (2.14) are summarized in the following theorem.

**Theorem 3.** *Consider the open-loop switched LFT system (2.1). Given two positive scalars  $\lambda_0 \in \mathbb{R}_+$  and  $\mu > 1$ , if there exist positive definite matrices  $R_i \in \mathbb{S}_+^n$ ,  $S_{1,i} \in \mathbb{S}_+^{n_1}$  and  $L_i, J_i \in \mathbb{S}_+^{n_p}$ , rectangular matrices  $S_{2,i} \in \mathbb{R}^{n_1 \times n_2}$ ,  $\hat{A}_{k,i} \in \mathbb{R}^{n_1 \times n_2}$ ,  $\begin{bmatrix} \hat{B}_{k0,i} & \hat{B}_{k1,i} & \hat{B}_{k2,i} \end{bmatrix} \in \mathbb{R}^{n_1 \times (n_p + n_{y_1} + n_1)}$ ,  $\hat{C}_{k0,i} \in \mathbb{R}^{n_p \times n_2}$ ,  $\hat{C}_{k1,i} \in \mathbb{R}^{n_u \times n_2}$ ,  $\begin{bmatrix} \hat{D}_{k00,i} & \hat{D}_{k01,i} & \hat{D}_{k02,i} \end{bmatrix} \in \mathbb{R}^{n_p \times (n_p + n_{y_1} + n_1)}$ ,  $\begin{bmatrix} \hat{D}_{k10,i} & \hat{D}_{k11,i} & \hat{D}_{k12,i} \end{bmatrix} \in \mathbb{R}^{n_u \times (n_p + n_{y_1} + n_1)}$ ,  $\begin{bmatrix} \hat{\Delta}_{1,ij} & \hat{\Delta}_{2,ij} \end{bmatrix} \in \mathbb{R}^{n_1 \times (n_1 + n_2)}$ , and a positive scalar  $\gamma \in \mathbb{R}_+$ , such that the fol-*

lowing conditions hold for all  $i, j \in \mathbf{I}[1, N_p]$  with  $i \neq j$ ,

$$\begin{aligned}
& \left[ \begin{array}{l}
\text{He}\{A_{p,i}R_i + B_{p2,i} \left[ \hat{D}_{k12,i} \quad \hat{C}_{k1,i} \right]\} + \lambda_0 R_i \quad \star \\
\left\{ \begin{array}{l} \left[ I_{n_1} \quad 0 \right] \left( A_{p,i}^T + \bar{C}_{p2,i}^T \hat{D}_{k11,i}^T B_{p2,i}^T \right) \\ + \left[ \hat{B}_{k2,i} \quad \hat{A}_{k,i} \right] + \lambda_0 \left[ I_{n_1} \quad 0 \right] \end{array} \right\} \text{He} \left\{ \left( \left[ S_{1,i} \quad S_{2,i} \right] A_{p,i} + \hat{B}_{k1,i} \bar{C}_{p2,i} \right) \left[ \begin{array}{l} I_{n_1} \\ 0 \end{array} \right] \right\} + \lambda_0 S_{1,i} \\
L_i B_{p0,i}^T + \hat{D}_{k10,i}^T B_{p2,i}^T \quad \hat{B}_{k0,i}^T \\
B_{p0,i}^T + \bar{D}_{p20,i}^T \hat{D}_{k11,i}^T B_{p2,i}^T \quad B_{p0,i}^T \left[ S_{1,i} \quad S_{2,i} \right]^T + \bar{D}_{p20,i}^T \hat{B}_{k1,i}^T \\
B_{p1,i}^T + \bar{D}_{p21,i}^T \hat{D}_{k11,i}^T B_{p2,i}^T \quad B_{p1,i}^T \left[ S_{1,i} \quad S_{2,i} \right]^T + \bar{D}_{p21,i}^T \hat{B}_{k1,i}^T \\
C_{p0,i} R_i + D_{p02,i} \left[ \hat{D}_{12,i} \quad \hat{C}_{k1,i} \right] \quad \left( C_{p0,i} + D_{p02,i} \hat{D}_{k11,i} \bar{C}_{p2,i} \right) \left[ \begin{array}{l} I_{n_1} \quad 0 \end{array} \right]^T \\
\left[ \hat{D}_{k02,i} \quad \hat{C}_{k0,i} \right] \quad \left( J_i C_{p0,i} + \hat{D}_{k01,i} \bar{C}_{p2,i} \right) \left[ \begin{array}{l} I_{n_1} \quad 0 \end{array} \right]^T \\
C_{p1,i} R_i + D_{p12,i} \left[ \hat{D}_{k12,i} \quad \hat{C}_{k1,i} \right] \quad \left( C_{p1,i} + D_{p12,i} \hat{D}_{k11,i} \bar{C}_{p2,i} \right) \left[ \begin{array}{l} I_{n_1} \quad 0 \end{array} \right]^T \\
\star \quad \star \quad \star \quad \star \quad \star \quad \star \\
\star \quad \star \quad \star \quad \star \quad \star \quad \star \\
-L_i \quad \star \quad \star \quad \star \quad \star \quad \star \\
-I_{n_p} \quad -J_i \quad \star \quad \star \quad \star \quad \star \\
0 \quad 0 \quad -\gamma I_{n_d} \quad \star \quad \star \quad \star \\
\left\{ \begin{array}{l} D_{p00,i} L_i + \\ D_{p02,i} \hat{D}_{k10,i} \end{array} \right\} \quad \left\{ \begin{array}{l} D_{p00,i} + \\ D_{p02,i} \hat{D}_{k11,i} \bar{D}_{p20,i} \end{array} \right\} \quad \left\{ \begin{array}{l} D_{p01,i} + \\ D_{p02,i} \hat{D}_{k11,i} \bar{D}_{p21,i} \end{array} \right\} \quad -L_i \quad \star \quad \star \\
\hat{D}_{k00,i} \quad \left\{ \begin{array}{l} J_i D_{p00,i} + \\ \hat{D}_{k01,i} \bar{D}_{p20,i} \end{array} \right\} \quad \left\{ \begin{array}{l} J_i D_{p01,i} + \\ \hat{D}_{k01,i} \bar{D}_{p21,i} \end{array} \right\} \quad -I_{n_p} \quad -J_i \quad \star \\
\left\{ \begin{array}{l} D_{p10,i} L_i + \\ D_{p12,i} \hat{D}_{k10,i} \end{array} \right\} \quad \left\{ \begin{array}{l} D_{p10,i} + \\ D_{p12,i} \hat{D}_{k11,i} \bar{D}_{p20,i} \end{array} \right\} \quad \left\{ \begin{array}{l} D_{p11,i} + \\ D_{p12,i} \hat{D}_{k11,i} \bar{D}_{p21,i} \end{array} \right\} \quad 0 \quad 0 \quad -\gamma I_{n_e}
\end{array} \right] < 0
\end{aligned}
\tag{2.16}$$

$$\begin{bmatrix}
\mu R_i & \star & \star & \star \\
\mu \begin{bmatrix} I_{n_1} & 0 \end{bmatrix} & \mu S_{1,i} & \star & \star \\
R_i & \begin{bmatrix} I_{n_1} & 0 \end{bmatrix}^T & R_j & \star \\
\begin{bmatrix} \hat{\Delta}_{1,ij} & \hat{\Delta}_{2,ij} \end{bmatrix} & S_{1,j} & \begin{bmatrix} I_{n_1} & 0 \end{bmatrix} & S_{1,j}
\end{bmatrix} \geq 0 \quad \begin{bmatrix} R_i & \star \\ \begin{bmatrix} I_{n_1} & 0 \end{bmatrix} & S_{1,i} \end{bmatrix} > 0 \quad (2.17)$$

$$\begin{bmatrix} L_i & \star \\ I_{n_p} & J_i \end{bmatrix} > 0 \quad (2.18)$$

where  $L_i, J_i, i \in \mathbf{I}[1, N_p]$  are block-diagonal matrices commutable with  $\Theta_i$ . Then, the hybrid closed-loop system (2.6) is exponentially stabilized by the reduced-order ( $n_1$ th-order) hybrid controller (2.14) for every switching signal  $\sigma$  with average dwell time  $\tau_a \geq \tau_a^* := \frac{\ln(\mu)}{\lambda_0}$  and the weighted  $\mathcal{L}_2$  gain from the disturbance  $d$  to the controlled output  $e$  is less than  $\gamma$ . Moreover, the controller matrices are obtained through the following algorithm:

- Partition matrices  $R_i = \begin{bmatrix} R_{1,i} & R_{2,i} \\ R_{2,i}^T & R_{3,i} \end{bmatrix}$ ,  $R_i^{-1} = \begin{bmatrix} \dot{R}_{1,i} & \dot{R}_{2,i} \\ \dot{R}_{2,i}^T & \dot{R}_{3,i} \end{bmatrix}$  with  $R_{1,i}, \dot{R}_{1,i} \in \mathbb{S}_+^{n_1}$ ,  $R_{2,i}, \dot{R}_{2,i} \in \mathbb{R}^{n_1 \times n_2}$ ,  $R_{3,i}, \dot{R}_{3,i} \in \mathbb{S}_+^{n_2}$  and let

$$S_{3,i} = \dot{R}_{3,i} + (\dot{R}_{2,i} - S_{2,i})^T (S_{1,i} - \dot{R}_{1,i})^{-1} (\dot{R}_{2,i} - S_{2,i})$$

for all  $i \in \mathbf{I}[1, N_p]$ . Then, we have  $S_i := \begin{bmatrix} S_{1,i} & S_{2,i} \\ S_{2,i}^T & S_{3,i} \end{bmatrix} > 0$ . Note that the matrix  $S_{1,i} - \dot{R}_{1,i}$  is invertible [103].

- Solve  $N_i \in \mathbb{R}^{n \times n_1}$ ,  $U_i, W_i \in \mathbb{R}^{n_p \times n_p}$  for all  $i \in \mathbf{I}[1, N_p]$  through the following factorizations, respectively.

$$S_i - R_i^{-1} = N_i X_i N_i^T$$

$$I_{n_p} - L_i J_i = U_i W_i^T$$

where  $X_i \in \mathbb{R}^{n_1 \times n_1}$ , and define  $M_i := -R_i N_i X_i$  so that  $M_i, N_i$  satisfy the identity  $S_i R_i + N_i M_i^T = I_n$ . Furthermore, we partition  $M_i, N_i$  as

$$M_i = \begin{bmatrix} M_{1,i} \\ M_{2,i} \end{bmatrix}, \quad N_i = \begin{bmatrix} N_{1,i} \\ N_{2,i} \end{bmatrix}$$

so that  $M_{1,i}, N_{1,i} \in \mathbb{R}^{n_1 \times n_1}$  are invertible and  $M_{2,i}, N_{2,i} \in \mathbb{R}^{n_2 \times n_1}$ .

- Compute the controller matrices  $A_{k,i}, B_{k0,i}, B_{k1,i}, B_{k2,i}, C_{k0,i}, C_{k1,i}, D_{k00,i}, D_{k01,i}, D_{k02,i}, D_{k10,i}, D_{k11,i}, D_{k12,i}$  and  $\Delta_{1,ij}, \Delta_{2,ij}$  for all  $i, j \in \mathbf{I}[1, N_p]$  and  $i \neq j$  as

$$\begin{aligned} D_{k11,i} &= \hat{D}_{k11,i}, \quad D_{k10,i} = \left( \hat{D}_{k10,i} - D_{k11,i} \bar{D}_{p20,i} L_i \right) U_i^{-T} \\ \begin{bmatrix} D_{k12,i} & C_{k1,i} \end{bmatrix} &= \left\{ \begin{bmatrix} \hat{D}_{k12,i} & \hat{C}_{k1,i} \end{bmatrix} - D_{k11,i} \bar{C}_{p2,i} R_i \right\} \Omega_i^{-1} \\ B_{k1,i} &= N_{1,i}^{-1} \left\{ \hat{B}_{k1,i} - \begin{bmatrix} S_{1,i} & S_{2,i} \end{bmatrix} B_{p2,i} D_{k11,i} \right\} \\ \begin{bmatrix} B_{k2,i} & A_{k,i} \end{bmatrix} &= N_{1,i}^{-1} \left\{ \begin{bmatrix} \hat{B}_{k2,i} & \hat{A}_{k,i} \end{bmatrix} - \begin{bmatrix} S_{1,i} & S_{2,i} \end{bmatrix} \left( A_{p,i} R_i + B_{p2,i} D_{k11,i} \bar{C}_{p2,i} R_i \right. \right. \\ &\quad \left. \left. + B_{p2,i} \begin{bmatrix} D_{k12,i} & C_{k1,i} \end{bmatrix} \Omega_i \right) - N_{1,i} B_{k1,i} \bar{C}_{p2,i} R_i \right\} \Omega_i^{-1} \\ D_{k01,i} &= W_i^{-1} \left( \hat{D}_{k01,i} - J_i D_{p02,i} D_{k11,i} \right) \\ D_{k00,i} &= W_i^{-1} \left\{ \hat{D}_{k00,i} - J_i \left( D_{p00,i} L_i + D_{p02,i} D_{k10,i} U_i^T \right) \right. \\ &\quad \left. - \left( J_i D_{p02,i} D_{k11,i} + W_i D_{k01,i} \right) \bar{D}_{p20,i} L_i \right\} U_i^{-T} \\ B_{k0,i} &= N_{1,i}^{-1} \left\{ \hat{B}_{k0,i} - \begin{bmatrix} S_{1,i} & S_{2,i} \end{bmatrix} \left( B_{p0,i} L_i + B_{p2,i} D_{k11,i} \bar{D}_{p20,i} L_i \right. \right. \\ &\quad \left. \left. + B_{p2,i} D_{k10,i} U_i^T \right) - N_{1,i} B_{k1,i} \bar{D}_{p20,i} L_i \right\} U_i^{-T} \\ \begin{bmatrix} D_{k02,i} & C_{k0,i} \end{bmatrix} &= \left\{ W_i^{-1} \left( \begin{bmatrix} \hat{D}_{k02,i} & \hat{C}_{k0,i} \end{bmatrix} - J_i C_{p0,i} R_i - J_i D_{p02,i} \begin{bmatrix} \hat{D}_{k12,i} & \hat{C}_{k1,i} \end{bmatrix} \right) \right. \\ &\quad \left. - D_{k01,i} \bar{C}_{p2,i} R_i \right\} \Omega_i^{-1} \\ \begin{bmatrix} \Delta_{1,ij} & \Delta_{2,ij} \end{bmatrix} &= N_{1,j}^{-1} \left\{ \begin{bmatrix} \hat{\Delta}_{1,ij} & \hat{\Delta}_{2,ij} \end{bmatrix} - \begin{bmatrix} S_{1,j} & S_{2,j} \end{bmatrix} R_i \right\} \Omega_i^{-1} \end{aligned} \tag{2.19}$$

$$\text{where } \Omega_i := \begin{bmatrix} R_{2,i}^T & R_{3,i} \\ M_{1,i}^T & M_{2,i}^T \end{bmatrix}.$$

*Proof.* The proof is quite similar to that of Theorem 2. For the closed-loop system (2.6) with (2.15), we still define the multiple quadratic Lyapunov functions as  $V_i(x_{cl}) = x_{cl}^T P_i x_{cl}$ ,  $\forall i \in \mathbf{I}[1, N_p]$ , and partition the Lyapunov function matrices  $P_i$  and the scaling matrices  $\Lambda_i$  according to the dimensions of the plant and controller states as follows.

$$P_i = \begin{bmatrix} S_i & N_i \\ N_i^T & X_i^{-1} \end{bmatrix} := \left[ \begin{array}{cc|c} S_{1,i} & S_{2,i} & N_{1,i} \\ S_{2,i}^T & S_{3,i} & N_{2,i} \\ \hline N_{1,i}^T & N_{2,i}^T & X_i^{-1} \end{array} \right], \quad \Lambda_i = \begin{bmatrix} J_i & W_i \\ W_i^T & Y_i^{-1} \end{bmatrix}.$$

We specify

$$Z_{1,i} = \begin{bmatrix} R_i & \begin{bmatrix} I \\ 0 \end{bmatrix} \\ \begin{bmatrix} M_{1,i}^T & M_{2,i}^T \end{bmatrix} & 0 \end{bmatrix}, \quad Z_{2,i} = \begin{bmatrix} I & \begin{bmatrix} S_{1,i} \\ S_{2,i}^T \end{bmatrix} \\ 0 & N_i^T \end{bmatrix}$$

$$T_{1,i} = \begin{bmatrix} L_i & I \\ U_i^T & 0 \end{bmatrix}, \quad T_{2,i} = \begin{bmatrix} I & J_i \\ 0 & W_i^T \end{bmatrix}$$

such that  $P_i Z_{1,i} = Z_{2,i}$  and  $\Lambda_i T_{1,i} = T_{2,i}$ . Then, we have  $X_i^{-1} = -N_i^T R_i M_i^{-T}$  and  $Y_i^{-1} = -W_i^T L_i U_i^{-T}$ , where  $M_i^T := [M_{1,i}^T \ M_{2,i}^T]$ . Conditions (2.17) and (2.18) confirm that  $P_i > 0$  and  $\Lambda_i > 0$ . The rest of the proof can be completed using a similar idea from [103], details are omitted here.  $\square$

Based on the synthesis conditions given in Theorem 3, the following LMI optimization problem aiming to minimize the weighted  $\mathcal{L}_2$  gain performance with a specified pair of dwell-

time parameters  $(\lambda_0, \mu)$  immediately follows:

$$\begin{aligned} & \min_{R_i, S_{1,i}, S_{2,i}, L_i, J_i, \hat{A}_{k,i}, \hat{B}_{k0,i}, \hat{B}_{k1,i}, \hat{B}_{k2,i}, \hat{C}_{k0,i}, \hat{C}_{k1,i}, \hat{D}_{k00,i}, \hat{D}_{k01,i}, \hat{D}_{k02,i}, \hat{D}_{k10,i}, \hat{D}_{k11,i}, \hat{D}_{k12,i}, \hat{\Delta}_{1,ij}, \hat{\Delta}_{2,ij}} \gamma, \\ & \text{subject to} \quad (2.16), (2.17) \text{ and } (2.18). \end{aligned} \quad (2.20)$$

**Remark 4.** *From the above discussion, we note that the  $D_{p22,i}$  ( $i \in \mathbf{I}[1, 2]$ ) matrices of the associated weighted open-loop switched LFT plant are non-zero, which violates the assumption **(A2)**. Nevertheless, this problem can be overcome by transforming the measurement output  $y$  to  $\tilde{y}$  with  $\tilde{y} = y - D_{p22,i}u$ , so that the resulting system with a new measurement output  $\tilde{y}$  for synthesis will satisfy the assumption **(A2)**. Accordingly, for controller implementation, the control input  $u$  can be computed by using  $u = (I + D_{k11,i}D_{p22,i})^{-1}(C_{k1,i}x_k + D_{k10,i}p_k + D_{k11,i}y_1 + D_{k12,i}y_2)$ . The invertibility of  $I + D_{k11,i}D_{p22,i}$  is deducible from the control synthesis.*

### 2.3 Missile Modeling and Autopilot Design

In this section, we will present the design procedure for missile pitch-axis autopilots by using the proposed hybrid gain-scheduling control scheme. In order to fit the missile dynamics (which is originally given in a quasi-LPV form [85]) into the switched LFT design framework, we will first convert the nonlinear missile model to a switched LFT system in the form of (2.1). Then, a hybrid missile autopilot will be designed to meet the stability and performance specifications by solving the LMI optimization problems (2.12) for full-order controller and (2.20) for reduced-order controller.

### 2.3.1 Switched LFT Modeling of Missile

The pitch-axis missile model taken from [85] is described in the following quasi-LPV form

$$\begin{aligned} \begin{bmatrix} \dot{\alpha} \\ \dot{q} \end{bmatrix} &= \begin{bmatrix} f_1 & 1 \\ f_2 & 0 \end{bmatrix} \begin{bmatrix} \alpha \\ q \end{bmatrix} + \begin{bmatrix} f_3 \\ f_4 \end{bmatrix} \delta, \\ \begin{bmatrix} \eta \\ q \end{bmatrix} &= \begin{bmatrix} f_5 & 0 \\ 0 & 1 \end{bmatrix} \begin{bmatrix} \alpha \\ q \end{bmatrix} + \begin{bmatrix} f_6 \\ 0 \end{bmatrix} \delta, \end{aligned} \quad (2.21)$$

with the nonlinear functions given by

$$\begin{aligned} f_1 &= K_\alpha M \left[ a_n \alpha^2 + b_n |\alpha| + c_n \left( 2 - \frac{M}{3} \right) \right] \cos(\alpha), \\ f_2 &= K_q M^2 \left[ a_m \alpha^2 + b_m |\alpha| + c_m \left( -7 + \frac{8M}{3} \right) \right], \\ f_3 &= K_\alpha M d_n \cos(\alpha), \\ f_4 &= K_q M^2 d_m, \\ f_5 &= K_z M^2 \left[ a_n \alpha^2 + b_n |\alpha| + c_n \left( 2 - \frac{M}{3} \right) \right], \\ f_6 &= K_z M^2 d_n. \end{aligned} \quad (2.22)$$

The physical meaning of different plant variables are listed below:

- $\alpha(t)$  Angle of attack in degrees,
- $q(t)$  Pitch rate in degrees per second,
- $M(t)$  Mach number,
- $\delta_c(t)$  Commanded tail deflection angle in degrees,
- $\delta(t)$  Actual tail deflection angle in degrees,
- $\eta_c(t)$  Commanded normal acceleration in g's,
- $\eta(t)$  Actual normal acceleration in g's.

The variables  $\eta(t)$  and  $q(t)$  are measured, thus available for feedback use. Angle of attack  $\alpha(t)$ , Mach number  $M(t)$  are variables to be used for scheduling purpose. The input to the missile is commanded tail deflection  $\delta_c(t)$ .

Also, the numerical values of various constants in the plant model are

$$\begin{aligned}
K_\alpha &= 1.18587, & K_q &= 70.586, & K_z &= 0.6661697 \\
a_n &= 0.000103 \text{deg}^{-3}, & b_n &= -0.00945 \text{deg}^{-2} \\
c_n &= -0.1696 \text{deg}^{-1}, & d_n &= -0.034 \text{deg}^{-1} \\
a_m &= 0.000215 \text{deg}^{-3}, & b_m &= -0.0195 \text{deg}^{-2} \\
c_m &= 0.051 \text{deg}^{-1}, & d_m &= -0.206 \text{deg}^{-1}
\end{aligned}$$

These coefficients are valid for the missile traveling between Mach number 2 and 4 at an altitude of 20000ft. The operating range of the missile specified by  $(\alpha, M)$  is such that  $-\frac{\pi}{6} \leq \alpha \leq \frac{\pi}{6}$  and  $2 \leq M \leq 4$ .

To convert the nonlinear missile model (2.21) into a switched LFT form, we need to partition the gain-scheduling parameter set denoted by  $\mathcal{P} := [-\frac{\pi}{6}, \frac{\pi}{6}] \times [2, 4]$  into a finite number of closed subsets  $\{\mathcal{P}_i\}_{i \in \mathbf{I}[1, N_p]}$  by means of a family of switching surfaces  $S_{ij}$  ( $i, j \in \mathbf{I}[1, N_p]$ ), so that in each parameter subset, the dynamic behavior of the missile is governed by an associated LFT system. To derive the LFT model with respect to each subregion  $\mathcal{P}_i$  for all  $i \in \mathbf{I}[1, N_p]$ , we first approximate  $\cos(\alpha)$  using a second-order polynomial  $1 - \alpha^2/2$  with a maximum error of 0.36% over the range of  $|\alpha| \leq \frac{\pi}{6}$  rad. The resulting LPV missile model is therefore expressed in terms of polynomial functions of the gain-scheduling parameters  $\alpha(t)$  and  $M(t)$ , which can be readily converted into an LFT form. The state-space LFT model with respect to the parameter

subregion  $\mathcal{P}_i$  can be described as:

$$\begin{bmatrix} \dot{x}_M \\ q_p \\ \eta \end{bmatrix} = \begin{bmatrix} A_{M,i} & B_{M0,i} & B_{M2,i} \\ C_{M0,i} & D_{M00,i} & D_{M02,i} \\ C_{M2,i} & D_{M20,i} & D_{M22,i} \end{bmatrix} \begin{bmatrix} x_M \\ p_p \\ \delta \end{bmatrix}, \quad (2.23)$$

$$p_p = \Theta_i q_p, \quad i \in \mathbf{I}[1, N_p]$$

where  $x_M := [\alpha \ q]^T$ , and  $\Theta_i := \begin{bmatrix} \theta_{1,i} I_4 & 0 \\ 0 & \theta_{2,i} I_5 \end{bmatrix}$  (for all  $i \in \mathbf{I}[1, N_p]$ ) satisfy (2.2) with a block dimension of 9.  $\theta_{\ell,i}$  for  $\ell = 1, 2$  and  $i \in \mathbf{I}[1, N_p]$  are the normalized scheduling parameters satisfying  $\alpha_i = \frac{\bar{\alpha}_i + \alpha_i}{2} + \frac{\bar{\alpha}_i - \alpha_i}{2} \theta_{1,i}$  and  $M_i = \frac{\bar{M}_i + M_i}{2} + \frac{\bar{M}_i - M_i}{2} \theta_{2,i}$  with  $(\alpha_i, M_i) \in \mathcal{P}_i = [\underline{\alpha}_i, \bar{\alpha}_i] \times [\underline{M}_i, \bar{M}_i]$ . The other system matrices for the missile LFT model (2.23) with respect to the

parameter subregion  $\mathcal{P}_i$  for any  $i \in \mathbf{I}[1, N_p]$  are given by

$$\begin{aligned}
A_{M,i} &= \begin{bmatrix} \left(1 - \frac{\bar{\alpha}_i^2}{2}\right) K_\alpha \bar{M}_i \Upsilon_{n,i} & 1 \\ K_q \bar{M}_i^2 \Upsilon_{m,i} & 0 \end{bmatrix}, \quad B_{M2,i} = \begin{bmatrix} \left(1 - \frac{\bar{\alpha}_i^2}{2}\right) K_\alpha d_n \bar{M}_i \\ K_q d_m \bar{M}_i^2 \end{bmatrix}, \\
B_{M0,i} &= \begin{bmatrix} -K_\alpha & -K_\alpha \bar{\alpha}_i & \left(1 - \frac{\bar{\alpha}_i^2}{2}\right) K_\alpha a_n \bar{M}_i & \left(1 - \frac{\bar{\alpha}_i^2}{2}\right) K_\alpha \bar{M}_i (a_n \bar{\alpha}_i + b_n \text{Sign}(\alpha_i)) \\ 0 & 0 & K_q a_m \bar{M}_i^2 & K_q \bar{M}_i^2 (a_m \bar{\alpha}_i + b_m \text{Sign}(\alpha_i)) \\ & & \left(1 - \frac{\bar{\alpha}_i^2}{2}\right) K_\alpha & -\frac{1}{3} \left(1 - \frac{\bar{\alpha}_i^2}{2}\right) K_\alpha c_n \bar{M}_i & 0 & 0 & 0 \\ & & 0 & \frac{8}{3} K_q c_m \bar{M}_i^2 & K_q & K_q \bar{M}_i & 0 \end{bmatrix}, \\
C_{M0,i} &= \begin{bmatrix} \frac{1}{2} \underline{\alpha}_i \bar{\alpha}_i \bar{M}_i \Upsilon_{n,i} & 0 \\ \frac{1}{2} \underline{\alpha}_i \bar{M}_i \Upsilon_{n,i} & 0 \\ \underline{\alpha}_i \bar{\alpha}_i & 0 \\ \underline{\alpha}_i & 0 \\ \underline{M}_i \Upsilon_{n,i} & 0 \\ \underline{M}_i & 0 \\ \underline{M}_i \bar{M}_i \Upsilon_{m,i} & 0 \\ \underline{M}_i \Upsilon_{m,i} & 0 \\ \underline{M}_i \bar{M}_i \Upsilon_{n,i} & 0 \end{bmatrix}, \quad D_{M02,i} = \begin{bmatrix} \frac{1}{2} d_n \underline{\alpha}_i \bar{\alpha}_i \bar{M}_i \\ \frac{1}{2} d_n \underline{\alpha}_i \bar{M}_i \\ 0 \\ 0 \\ d_n \underline{M}_i \\ 0 \\ d_m \underline{M}_i \bar{M}_i \\ d_m \underline{M}_i \\ d_n \underline{M}_i \bar{M}_i \end{bmatrix},
\end{aligned}$$

$$\begin{aligned}
D_{M00,i} &= \begin{bmatrix} 0 & \underline{\alpha}_i & \frac{a_n \underline{\alpha}_i \overline{M}_i}{2} & \frac{\underline{\alpha}_i \overline{M}_i (a_n \overline{\alpha}_i + b_n \text{Sign}(\alpha_i))}{2} & \frac{\underline{\alpha}_i \overline{\alpha}_i}{2} & -\frac{c_n \underline{\alpha}_i \overline{M}_i}{6} & 0 & 0 & 0 \\ 0 & 0 & \frac{a_n \underline{\alpha}_i \overline{M}_i}{2} & \frac{\underline{\alpha}_i \overline{M}_i (a_n \overline{\alpha}_i + b_n \text{Sign}(\alpha_i))}{2} & \frac{\underline{\alpha}_i}{2} & -\frac{c_n \underline{\alpha}_i \overline{M}_i}{6} & 0 & 0 & 0 \\ 0 & 0 & 0 & \underline{\alpha}_i & 0 & 0 & 0 & 0 & 0 \\ 0 & 0 & 0 & 0 & 0 & 0 & 0 & 0 & 0 \\ 0 & 0 & a_n \underline{M}_i & \underline{M}_i (a_n \overline{\alpha}_i + b_n \text{Sign}(\alpha_i)) & 0 & -\frac{c_n \underline{M}_i}{3} & 0 & 0 & 0 \\ 0 & 0 & 0 & 0 & 0 & 0 & 0 & 0 & 0 \\ 0 & 0 & a_m \underline{M}_i \overline{M}_i & \underline{M}_i \overline{M}_i (a_m \overline{\alpha}_i + b_m \text{Sign}(\alpha_i)) & 0 & \frac{8c_m \underline{M}_i \overline{M}_i}{3} & 0 & \underline{M}_i & 0 \\ 0 & 0 & a_m \underline{M}_i & \underline{M}_i (a_m \overline{\alpha}_i + b_m \text{Sign}(\alpha_i)) & 0 & \frac{8c_m \underline{M}_i}{3} & 0 & 0 & 0 \\ 0 & 0 & a_n \underline{M}_i \overline{M}_i & \underline{M}_i \overline{M}_i (a_n \overline{\alpha}_i + b_n \text{Sign}(\alpha_i)) & \underline{M}_i & -\frac{c_n \underline{M}_i \overline{M}_i}{3} & 0 & 0 & 0 \end{bmatrix}, \\
C_{M2,i} &= \begin{bmatrix} K_z \overline{M}_i^2 \Upsilon_{n,i} & 0 \end{bmatrix}, \quad D_{M22,i} = K_z d_n \overline{M}_i^2 \\
D_{M20,i} &= \begin{bmatrix} 0 & 0 & K_z a_n \overline{M}_i^2 & K_z \overline{M}_i^2 (a_n \overline{\alpha}_i + b_n \text{Sign}(\alpha_i)) & K_z \overline{M}_i & -\frac{K_z c_n \overline{M}_i^2}{3} & 0 & 0 & K_z \end{bmatrix},
\end{aligned}$$

where

$$\begin{aligned}
\Upsilon_{n,i} &= 2c_n - \frac{1}{3}c_n \overline{M}_i + b_n \overline{\alpha}_i \text{Sign}(\alpha_i) + a_n \overline{\alpha}_i^2, \\
\Upsilon_{m,i} &= -7c_m + \frac{8c_m \overline{M}_i}{3} + b_m \overline{\alpha}_i \text{Sign}(\alpha_i) + a_m \overline{\alpha}_i^2.
\end{aligned}$$

Therefore, the resulting switched LFT model for the LPV missile plant (2.21) consists of  $N_p$  number of subsystems in the form of (2.23). The associated switching signal  $\sigma$  depends on the scheduling parameters  $(\alpha, M)$ , and follows the switching rule of

$$\sigma = i, \quad \text{if } (\alpha, M) \in \mathcal{P}_i. \quad (2.24)$$

Based on this switched LFT model, we will be able to design a hybrid gain-scheduling autopilot for the missile plant (2.21) by using the technique proposed in Section 2.2.

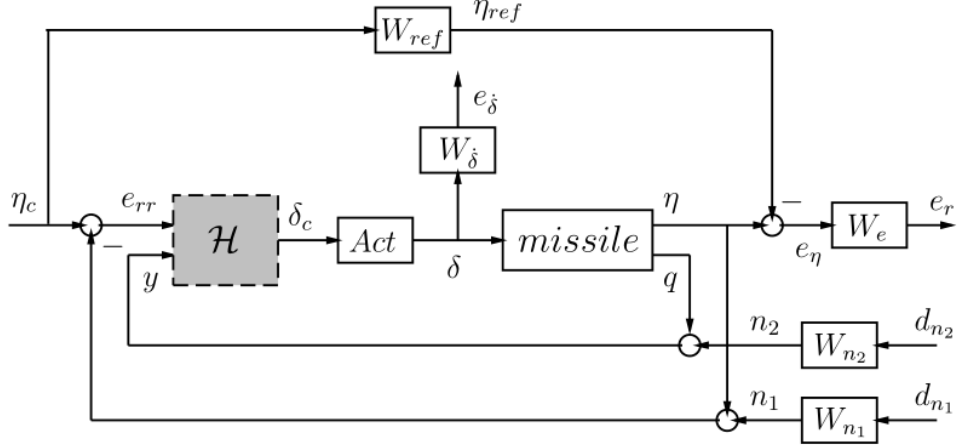


Figure 2.2: Weighted open-loop interconnection of missile plant.

### 2.3.2 Control Problem Setup

The control objective of the missile autopilot is to track step commands of the normal acceleration  $\eta(t)$ , and meet the desired controlled performance for the overall closed-loop system for all  $\alpha(t), M(t) \in \mathcal{P}$ . Specifically, the performance goals for the closed-loop system are: (i) track step commands in  $\eta_c(t)$  with time constant no greater than 0.35 sec, maximum overshoot no greater than 10%, and steady-state error no greater than 1%; (ii) maximum tail deflection rate for 1 g step command in  $\eta_c(t)$  does not exceed 25 deg/sec.

To characterize these overall closed-loop performance specifications, we will augment the missile plant with rational weighting functions. The resulting open-loop interconnection for synthesis is shown in Fig. 2.2, where the grey dashed block  $\mathcal{H}$  corresponds to the hybrid gain-scheduling controller to be designed, and the weighting functions are defined by:

$$\begin{aligned}
 W_{ref}(s) &= \frac{144(-0.05s + 1)}{s^2 + 2 \times 0.8 \times 12s + 144} \\
 W_e(s) &= \frac{0.5s + 17.321}{s + 0.0577} \\
 W_{\dot{\delta}}(s) &= \frac{s}{25(0.005s + 1)} \\
 W_{n_1}(s) &= W_{n_2}(s) = 0.001
 \end{aligned} \tag{2.25}$$

The weighting functions  $W_{ref}$  and  $W_e$  concern about the tracking performance of the actual normal acceleration  $\eta(t)$  to its reference  $\eta_{ref}(t)$  with small steady state error, while a larger error at high frequency range is allowed to avoid dynamic overload.  $W_{\dot{\delta}}$  is used for penalizing the control effort such that reasonable tail deflection profile is achieved during the control process.  $W_{n_1}, W_{n_2}$  are applied to attenuate the effects of sensor noises  $d_{n_1}, d_{n_2}$ .  $Act$  represents the actuator dynamics describing the tail deflection mechanism  $\delta(t)$ , which has been chosen to be 1 for simplicity. Realize the weighting transfer functions (2.25) in state-space representation, we have:

$$W_{ref}(s) : \begin{aligned} \begin{bmatrix} \dot{x}_1 \\ \dot{x}_2 \end{bmatrix} &= A_{ref} \begin{bmatrix} x_1 \\ x_2 \end{bmatrix} + B_{ref} \eta_c = \begin{bmatrix} 0 & 1 \\ -144 & -19.2 \end{bmatrix} \begin{bmatrix} x_1 \\ x_2 \end{bmatrix} + \begin{bmatrix} 0 \\ 1 \end{bmatrix} \eta_c, \\ \eta_{ref} &= C_{ref} \begin{bmatrix} x_1 \\ x_2 \end{bmatrix} = \begin{bmatrix} 144 & -7.2 \end{bmatrix} \begin{bmatrix} x_1 \\ x_2 \end{bmatrix}. \end{aligned}$$

$$W_e(s) : \quad \dot{x}_3 = A_e x_3 + B_e e_\eta = -0.0577x_3 + 17.29215e_\eta,$$

$$e_r = C_e x_3 + D_e e_\eta = x_3 + 0.5e_\eta.$$

$$W_{\dot{\delta}}(s) : \quad \dot{x}_4 = A_{\dot{\delta}} x_4 + B_{\dot{\delta}} \delta = -200x_4 - 1600\delta,$$

$$e_{\dot{\delta}} = C_{\dot{\delta}} x_4 + D_{\dot{\delta}} \delta = x_4 + 8\delta.$$

Combining the above weighting functions with the switched LFT missile model derived in Section 2.3.1, one can obtain the weighted open-loop switched LFT system in the form of (2.1) for controller synthesis. This resulting switched LFT system contains 6 states in which 2 of them are from the missile plant, and remaining 4 states from weighting functions. The system has 4 inputs with 1 control input, 1 command input and 2 disturbance inputs. There are 4 system outputs including 2 measurement outputs and 2 error/performance outputs. Specifically, the

signals of the weighted switched LFT missile model are defined by

$$\begin{aligned}
x_p &:= \begin{bmatrix} \alpha & q & x_1 & x_2 & x_3 & x_4 \end{bmatrix}^T, \\
e &:= \begin{bmatrix} e_r & e_{\dot{\delta}} \end{bmatrix}^T, \\
y_1 &:= \begin{bmatrix} y & e_{rr} \end{bmatrix}^T, \\
d &:= \begin{bmatrix} d_{n_1} & d_{n_2} & \eta_c \end{bmatrix}^T, \\
u &:= \delta_c = \delta.
\end{aligned}$$

The associated pseudo signals  $(p_p, q_p)$ , time-varying parameters  $\Theta_i$  ( $i \in \mathbf{I}[1, N_p]$ ) and switching logic  $\sigma$  have the same definitions as for system (2.23). The weighted open-loop system matrices for controller synthesis are given as follows for all  $i \in \mathbf{I}[1, N_p]$ .

$$\begin{aligned}
A_{p,i} &= \begin{bmatrix} A_{M,i} & 0 & 0 & 0 \\ 0 & A_{ref} & 0 & 0 \\ B_e C_{M2,i} & -B_e C_{ref} & A_e & 0 \\ 0 & 0 & 0 & A_{\dot{\delta}} \end{bmatrix}, \quad B_{p0,i} = \begin{bmatrix} B_{M0,i} \\ 0 \\ B_e D_{M20,i} \\ 0 \end{bmatrix}, \quad B_{p1,i} = \begin{bmatrix} 0 & 0 & 0 \\ 0 & 0 & B_{ref} \\ 0 & 0 & 0 \\ 0 & 0 & 0 \end{bmatrix}, \\
B_{p2,i} &= \begin{bmatrix} B_{M2,i} \\ 0 \\ B_e D_{M22,i} \\ B_{\dot{\delta}} \end{bmatrix}, \quad \begin{bmatrix} C_{p0,i} \\ C_{p1,i} \\ C_{p2,i} \end{bmatrix} = \begin{bmatrix} C_{M0,i} & 0 & 0 & 0 \\ \hline D_e C_{M2,i} & -D_e C_{ref} & C_e & 0 \\ 0 & 0 & 0 & C_{\dot{\delta}} \\ \hline \begin{bmatrix} 0 & 1 \end{bmatrix} & 0 & 0 & 0 \\ -C_{M2,i} & 0 & 0 & 0 \end{bmatrix},
\end{aligned}$$

$$\begin{bmatrix} D_{p00,i} & D_{p01,i} & D_{p02,i} \\ D_{p10,i} & D_{p11,i} & D_{p12,i} \\ D_{p20,i} & D_{p21,i} & D_{p22,i} \end{bmatrix} = \left[ \begin{array}{ccc|ccc} D_{M00,i} & 0 & 0 & 0 & D_{M02,i} \\ \hline D_e D_{M20,i} & 0 & 0 & 0 & D_e D_{M22,i} \\ 0 & 0 & 0 & 0 & D_{\dot{\delta}} \\ \hline 0 & 0 & 0.001 & 0 & 0 \\ -D_{M20,i} & -0.001 & 0 & 1 & -D_{M22,i} \end{array} \right].$$

For reduced-order controller design, since four states from the weighting functions, i.e.,  $x_1, x_2, x_3$  and  $x_4$ , could be readily computed online for feedback control use, the weighted open-loop switched LFT system can be further partitioned to be with (2.13) accordingly. In such a case, we have the associated signals as follows:

$$\begin{aligned} x_{p1} &:= \begin{bmatrix} \alpha & q \end{bmatrix}^T, & x_{p2} &:= \begin{bmatrix} x_1 & x_2 & x_3 & x_4 \end{bmatrix}^T, \\ y_1 &:= \begin{bmatrix} y & e_{rr} \end{bmatrix}^T, & y_2 &:= \begin{bmatrix} x_1 & x_2 & x_3 & x_4 \end{bmatrix}^T. \end{aligned}$$

By further utilizing this portion of state information, the state number of the missile autopilot will be reduced to 2. In fact, it is clear that from the reduced-order control technique, the state number of the missile autopilot will not be greater than that of the missile plant regardless the configurations of the employed weighting functions. This will largely ease the controller implementation and enhance design flexibility, especially when more complicated weighting functions are employed for more stringent performance specifications.

### 2.3.3 Control Synthesis and Simulation Results

Based on the weighted open-loop switched LFT model, two hybrid gain-scheduling controllers corresponding to the full-order and reduced-order cases will be designed using the proposed synthesis conditions in Theorems 2 and 3. The associated controller matrices can be obtained by solving the LMI optimization problems (2.12) and (2.20), respectively.

For switched gain-scheduling control with ADT, since the scheduling parameter space par-

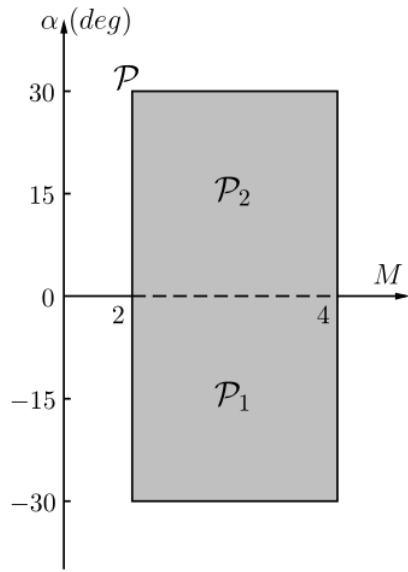
titioning on  $\mathcal{P}$  and the dwell-time parameters  $(\lambda_0, \mu)$  are both involved in the synthesis process, we would like to study their influence on the optimized performance, i.e., the weighted  $\mathcal{L}_2$  gain  $\gamma$ . Tables 2.1 and 2.2 present the optimized  $\gamma$  values associated with different partitions of  $\mathcal{P}$  and specifications of  $(\lambda_0, \mu)$  by solving the problems (2.12) for full-order control and (2.20) for reduced-order control. Table 2.1 compares four different scenarios with different partitions of  $\mathcal{P}$ . As seen from Fig. 2.3, the four scenarios correspond to the cases where  $\mathcal{P}$  is partitioned evenly into 2, 4, 8 and 12 subregions, respectively. The synthesis results under fixed dwell time parameters  $(\lambda_0, \mu) = (0.1, 1.2)$  in Table 2.1 show that better weighted  $\mathcal{L}_2$  gains will be obtained as the parameter space  $\mathcal{P}$  is partitioned to more subregions. However, this will also lead to increased optimization variables, in turn, demanding more computational efforts<sup>1</sup>. Comparing between the full-order control case and the reduced-order control case, it is obvious that the latter one provides a more effective and efficient scheme for missile autopilot design with relatively better performance and significantly less computational cost. More importantly, from the controller implementation point of view, the reduced-order controller is advantageous over the full-order one in the sense of smaller controller state order (4 smaller in this example).

Table 2.1: Effects of the partitioning of  $\mathcal{P}$  on optimized weighted  $\mathcal{L}_2$  performance (with fixed  $(\lambda_0, \mu) = (0.1, 1.2)$ ).

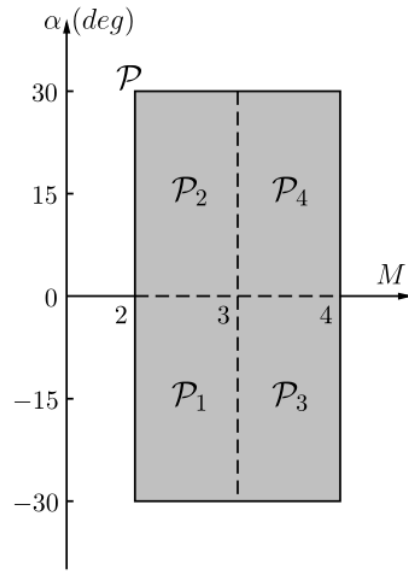
Partitioning of $\mathcal{P}$	Full-Order			Reduced-Order		
	$\gamma$	# of variables	CPU time (sec)	$\gamma$	# of variables	CPU time (sec)
Case I	5.0927	713	12.376	5.0882	517	6.833
Case II	3.3966	1569	100.714	3.3963	1081	34.494
Case III	2.6817	3281	975.918	2.6814	2209	283.039
Case IV	2.4295	4993	3660.272	2.4280	3337	920.649

On the other hand, the synthesis results in Table 2.2 are obtained under a fixed partition of

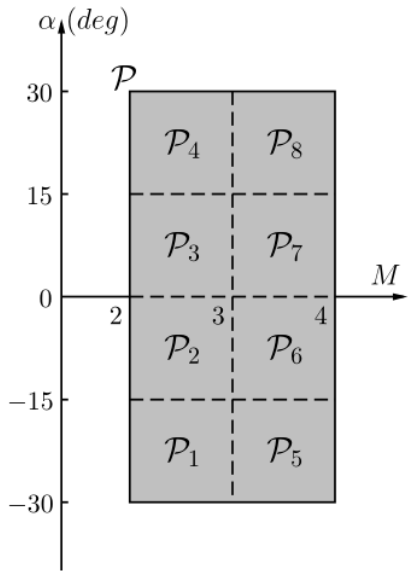
<sup>1</sup>All computations were performed on an Intel 4 Core i7 1.8 GHz PC.



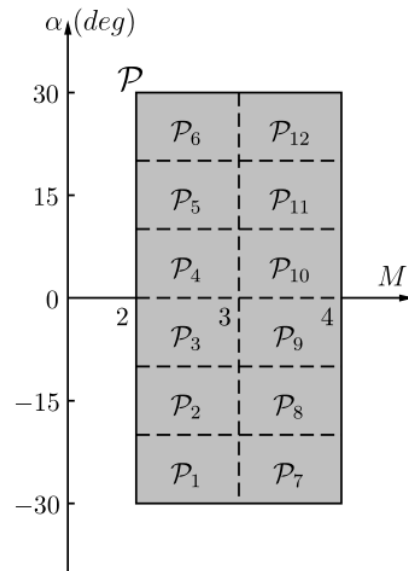
(a) Case I: two subregions



(b) Case II: four subregions



(c) Case III: eight subregions



(d) Case IV: twelve subregions

Figure 2.3: Partition the scheduling parameter space  $\mathcal{P}$ .

$\mathcal{P}$  as in Case III of Fig. 2.3. It is observed that changes caused by either parameter  $\lambda_0$  or  $\mu$  would affect the ADT constraint  $\tau_a^*$  as well as the optimized weighted  $\mathcal{L}_2$  gain  $\gamma$ . Specifically, if  $\lambda_0$  is fixed at 0.1, while  $\mu$  varies from 1.2 to 1.8,  $\tau_a^*$  increases with improved  $\gamma$ . On the other hand, when  $\lambda_0$  increases with fixed  $\mu$ ,  $\tau_a^*$  decreases while  $\gamma$  becomes larger. This experimental data reflects that larger  $\mu$  would result in improved disturbance attenuation level with tighter constraints on the average dwell time. In contrast, variations of  $\lambda_0$  would produce opposite effects on  $\tau_a^*$  and  $\gamma$  as those of  $\mu$ . This phenomenon can be explained by the fact that increasing  $\lambda_0$  is essentially imposing more restrictive (faster) convergency rate on the closed-loop system, while larger  $\mu$  would provide more freedom in synthesizing the multiple Lyapunov functions. Furthermore, comparing the values of  $\gamma$  between the full-order and reduced-order cases (see the fourth and fifth columns in Table 2.2), we observe that the reduced-order control scheme performs slightly better than the full-order control scheme over the range from  $(\lambda_0, \mu) = (0.1, 1.2)$  to  $(\lambda_0, \mu) = (0.1, 1.8)$ , while the advantage becomes more obvious as  $\lambda_0$  increases. In particular, with fixed  $\mu = 1.8$ , when  $\lambda_0$  reaches 0.12, the resulting optimization problem for the case of full-order control is infeasible, while the associated one for the reduced-order case is still capable of providing acceptable performance even  $\lambda_0$  keeps increasing to 0.2. This indicates that the reduced-order control scheme possesses better scalability in optimizing the  $\mathcal{H}_\infty$  performance when  $\lambda_0$  increases.

Table 2.2: Effects of the dwell-time parameters  $(\lambda_0, \mu)$  on optimized weighted  $\mathcal{L}_2$  performance (with fixed partition of  $\mathcal{P}$  as in Case III).

$\lambda_0$	$\mu$	$\tau_a^* = \frac{\ln(\mu)}{\lambda_0} sec$	$\gamma$	
			Full-Order	Reduced-Order
0.1	1.2	1.8232	2.6817	2.6814
0.1	1.5	4.0547	2.4624	2.4619
0.1	1.8	5.8779	2.3494	2.3493
0.11	1.8	5.3435	6.4762	2.3529
0.12	1.8	4.8982	infeasible	2.3562
0.2	1.8	2.9389	infeasible	2.3828

In controller synthesis, in order to overcome the numerical issue caused by ill-conditioning matrices, we have constrained the closed-loop poles within the same circle  $|c + 300| \leq 300$ . This pole location constraint was formulated in terms of LMIs by using the method of [11] and incorporated into the proposed control synthesis process. Selecting a pair of dwell-time parameters  $(\lambda_0, \mu) = (0.1, 1.1)$  with a partitioning of  $\mathcal{P}$  as in Case I of Fig. 2.3 will yield a switched LFT missile model with 2 subsystems, and an ADT constraint  $\tau_a^* = 0.9531 \text{ sec}$ . With this setting, we obtain the optimal weighted  $\mathcal{L}_2$  performance level  $\gamma = 5.0933$  for full-order control and  $\gamma = 5.0927$  for reduced-order control. The associated controller gain matrices can be further obtained by using the algorithm in Theorems 2 and 3.

To implement the switched gain-scheduling autopilots, we will specify the Mach number  $M(t)$  in the following form [64].

$$\begin{aligned} \dot{M}(t) &= \frac{1}{v_s} [-|\eta(t)| \sin(|\alpha(t)|) + A_x M^2(t) \cos(\alpha(t))], \\ M(0) &= 4. \end{aligned}$$

where  $v_s = 1036.4 \text{ ft/s}$  represents the speed of sound at 20000  $\text{ft}$ , and  $A_x = 0.7P_0SC_a/m$  with  $P_0 = 973.3 \text{ lbs/ft}^2$  being the static pressure at 20000  $\text{ft}$ ,  $S = 0.44 \text{ ft}^2$  being the surface area, and  $C_a = -0.3$ ,  $m = 13.98 \text{ slugs}$  being the drag coefficient and mass of the missile respectively. Another gain-scheduling parameter, the angle of attack  $\alpha(t)$ , is not measurable in real time for this missile plant. We thus must estimate  $\alpha(t)$  in terms of  $\eta(t)$ ,  $\delta(t)$  and  $M(t)$  from the output equation (2.21). To this end, we will adopt the nonlinear static estimator from [85, 87], which is a polynomial approximation of an inverse of the output equation in (2.21). Detailed analysis about its approximation accuracy can be found in [85, 87].

Based on the above system setup, nonlinear simulations will be performed to verify the performance of the designed hybrid controllers. Since the closed-loop system responses under the full-order control scheme have little difference with those obtained by using reduce-order control (which is expected from the optimized  $\gamma$  values as indicated above), only the simulation

results for reduced-order control are discussed below. With the reduced-order hybrid control scheme, the missile dynamic responses to a series of step commanded acceleration are plotted in Fig. 2.4. In particular, from Figs. 2.4(a) and (f), it is clearly verified that the performance goals are satisfied under the proposed hybrid control strategy. The angle of attack  $\alpha(t)$ , the mach number  $M(t)$  and the associated switching signals are displayed in Figs. 2.4(b)–(d), respectively. It is shown that the values of  $(\alpha(t), M(t))$  remain in the range of  $[-\frac{\pi}{6}, \frac{\pi}{6}] \times [2, 4]$  over the entire time history, which therefore validates the switched LFT model established in Section 2.3.1. Furthermore, the average dwell time over the operating time interval  $[0, 4]$  sec can be calculated by  $\tau_a = 4/3 = 1.3333 > \tau_a^* = 0.9531$ , where 3 is the number of switching instants over  $[0, 4]$  sec as can be obtained from Fig. 2.4(d). This implies satisfaction of the ADT constraint (2.10), in turn, guaranteeing switching stability.

In order to demonstrate the effectiveness of the proposed approach, the simulation results are compared with those obtained by using the parameter-dependent Lyapunov function (PDLF) method in [87]. By comparing Fig. 2.4 with the Fig. 2 of [87], it is observed that the hybrid controller is capable of rendering comparable controlled performance. On the other hand, we also conduct a similar spare simulation as in [87] to examine the robustness property of the hybrid controller by perturbing the aerodynamic coefficients  $C_n := (a_n, b_n, c_n, d_n)$  and  $C_m := (a_m, b_m, c_m, d_m)$ . We will carry out the perturbation independently between  $C_n$  and  $C_m$ . For  $C_n$ , we simultaneously change  $a_n, b_n, c_n$  from their nominal values by  $\pm 10\%$ , while separately change  $d_n$  by  $\pm 10\%$  from its nominal value. Similarly, for  $C_m$ , the perturbations are carried out with  $\pm 25\%$  over the parameters  $a_m, b_m, c_m$  and  $\pm 25\%$  over  $d_m$  independently. As such, totally 16 plots result from the combination of all of these variations, and the corresponding responses are shown in Fig. 2.5. It is observed that all cases present stable dynamic behaviors with only very slight performance degradation of missile under perturbations. Again, comparing these results with those in Fig. 4 of [87], it is interesting to note that much larger performance degradation is witnessed under the same perturbations for the PDLF-based missile autopilot in [87]. This indicates a very strong robustness property for the proposed hybrid controller,

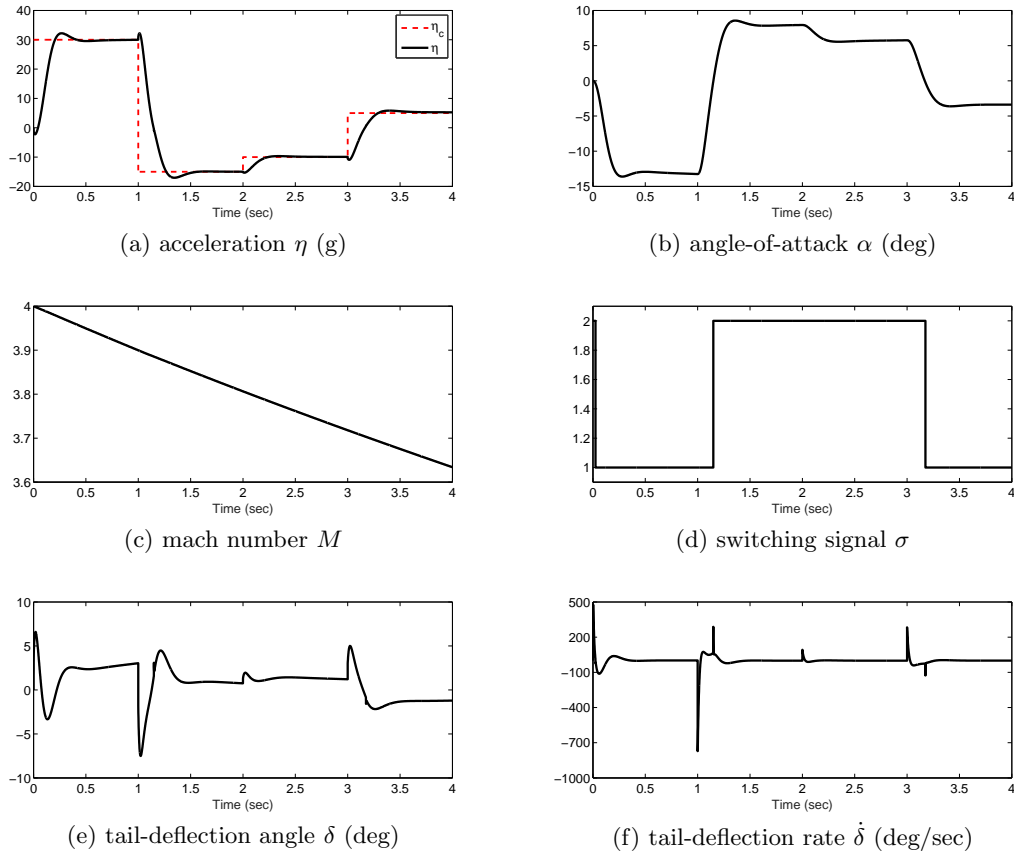


Figure 2.4: Missile dynamic response to a sequence of step acceleration commands.

due to the avoidance of utilizing parameter variation information. Apart from the robustness comparisons, we stress that the proposed hybrid gain-scheduling control scheme provides a systematic yet simple framework that overcomes deficiencies of the PDLF approaches.

## 2.4 Summary

A systematic hybrid gain-scheduling control scheme has been proposed for missile autopilot design by using the average dwell time switching technique. First, the original nonlinear missile dynamics are modeled as a switched LFT system, based on which both full-order and reduced-order hybrid LFT controllers are then synthesized by solving a finite dimensional LMI

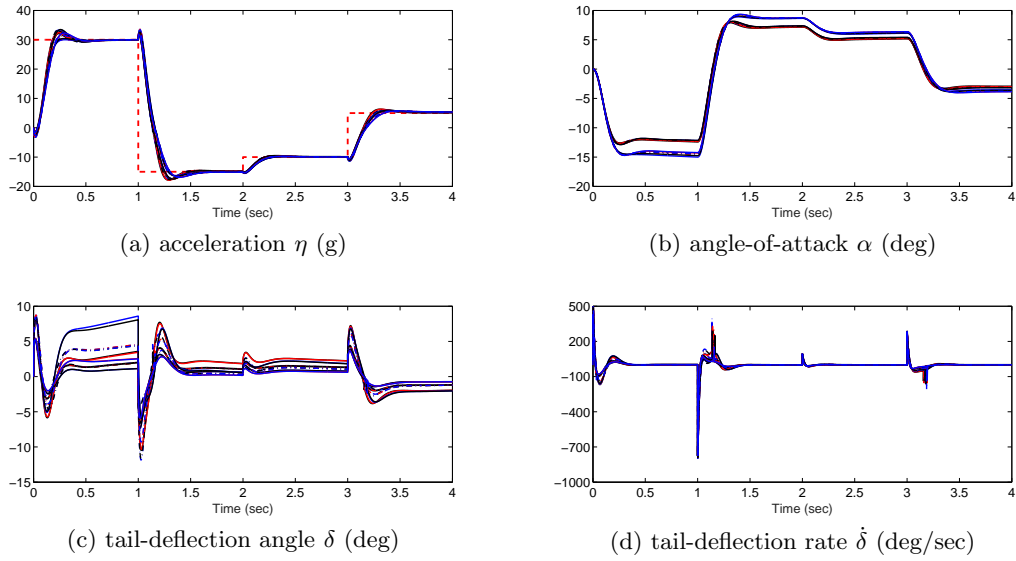


Figure 2.5: Perturbed response to a sequence of step acceleration commands.

optimization problem. This new hybrid control scheme advances existing LPV control methods for missile autopilot design in three important ways: simplified design procedure via convex optimization with reduced computational complexity by avoiding parameter-space gridding; eased controller implementation without information of scheduling parameter variations; and reduced controller state order independent of the settings of performance weighting functions employed. Promising controlled performances and strong robustness of the hybrid autopilot have been witnessed through nonlinear simulations.

## Chapter 3

# Almost Output Regulation of Switched Linear Dynamics with Switched Exosignals

For systems with switched linear dynamics and affected by persistent switched reference commands/disturbances, we propose a new hybrid control approach in order to achieve not only closed-loop stability but also tracking and/or rejection of persistent references/disturbances generated by multiple exosystems, namely, output regulation. It is assumed that both controlled plant and exosystem are described by switched linear systems. The proposed hybrid controller/output regulator is specified as a switching impulsive system, where the controller states will undergo impulsive jumps at each switching instant. Based on the average dwell-time (ADT) switching and multiple Lyapunov function techniques, it has been shown how to completely reduce the synthesis problem of the hybrid controller to a set of linear matrix equations and linear matrix inequalities (LMIs). To demonstrate its usefulness, the proposed hybrid control method has been applied to solve the output regulation problem for a mechanical system.

### 3.1 Introduction

Output regulation of dynamical systems is an important problem and has been extensively studied in control community since 1970's. This problem specifies the control task of achieving not only the overall closed-loop stability, but also the tracking and/or rejection of persistent references/disturbances generated by an exosystem [74]. Many interesting results on this topic can be found in the literature (see [24, 74, 41, 40, 55] and the reference therein). Several pioneering works are in particular worth to be mentioned. In [24], necessary and sufficient conditions to solve the output regulation problem for linear time-invariant (LTI) systems were firstly established as a set of linear algebraic equations. It is not until the nineties that the output regulation of nonlinear systems was addressed by Isidori and Byrnes [41] and Huang and Rugh [40], where the solvability conditions were given in terms of mixed partial differential and nonlinear algebraic equations. Recent years have witnessed a shift of research interests on the output regulation problem to hybrid dynamical systems that combine continuous dynamics and discrete event behaviors [59, 44, 27, 12, 93].

Despite a rich literature on switched systems, the output regulation of switched systems is a challenging problem. Most previous results for output regulation of nonlinear systems are not directly applicable to switched systems since the vector fields of switched systems are discontinuous and non-smooth. Different techniques have been proposed to tackle the output regulation problem for switched systems, virtually all of which, however, have their own limitations that restrict their applicability to practical problems. For instance, stability analysis conditions for switched systems with the output regulation requirement were derived in [56, 89] using the common Lyapunov function (CLF) approach [8], which could be very conservative or even render the control synthesis problem infeasible. On the other hand, the switching output regulation problem was tackled in [90] under the multiple Lyapunov functions (MLFs) framework [8]. However, the derived control synthesis conditions are essentially bilinear matrix inequalities (BMIs) and computationally expensive to solve. Based on a zero-error manifold switching strategy, [27] also applied the MLFs technique to analyze the output regulation problem for switched linear

systems with switched exosignals. The resulting condition for switching stability is restrictive and difficult to check, especially when full plant state information is not available. Therefore, it is highly desirable to develop a new and effective framework for the output regulation of switched systems by using MLFs.

Several technical difficulties arise in this area that are not encountered in the case of linear time-invariant (LTI) systems, two of which are worth to be mentioned. The first difficulty is related to the switching nature of the controlled plant itself. For LTI systems, the output regulation problem would usually boil down to asymptotic stabilization of a transformed system after decoupling the references/disturbances from the original system states through a coordinate transformation. However, since each subsystem of switched linear systems has different dynamics, it is difficult to find a common state transformation that is suitable for all subsystems [18]. Thus, the questions of how to establish stability analysis and efficient synthesis conditions for switched linear systems have to be answered first. Another difficulty lies in the use of MLFs and the resulting boundary condition [57], that is non-trivial to handle in the switching controller synthesis, especially for the case of output-feedback control. As opposed to LTI systems, the separation principle is in general not valid for switched linear systems. So the switching output feedback control problem cannot be addressed by designing a state-feedback controller and an observer separately. In addition, the boundary condition that constrains the difference between two adjacent Lyapunov functions usually leads to undesirable results under switching control frameworks. For state-dependent switching [29], a special structure has to be imposed on the MLFs; and for time-dependent switching [57], the boundary condition could result in a non-convex synthesis condition. Although some progress has been made using ADT switching technique [103], the output regulation problem for switched linear systems remains to be solved.

To overcome these difficulties arising in the output regulation of switched linear systems, we propose a new hybrid control approach for switched linear systems with ADT switching. It is assumed that both controlled plant and the exosystem are described by switched linear systems. Different from classical output regulation where the reference/disturbance signals are

generated by a precisely known exosystem, we extend the concept of exact output regulation to almost output regulation by allowing some unknown perturbations to affect the plant and exosystem dynamics. From this aspect, our control objectives are in twofold: output regulation to regulate the error outputs to zero in the absence of perturbations, and weighted  $\mathcal{L}_2$ -gain minimization (from [108]) to suppress the effect of perturbations on the error outputs. The proposed hybrid controller/output regulator is specified as a switched linear dynamic output-feedback controller that undergoes impulsive state jumps at each switching instant. Using the ADT technique incorporated with multiple quadratic Lyapunov functions, solvability conditions for asymptotic stability with weighted  $\mathcal{L}_2$ -gain performance and almost output regulation are formulated as a set of linear matrix equations plus linear matrix inequalities (LMIs). As a result, the proposed hybrid controller including switching control gains and state reset laws can be jointly designed by solving a convex LMI-based optimization problem. More importantly, no extra restrictions except the ADT switching are required to guarantee overall stability. To the best of our knowledge, this chapter provides for the first time a systematic and effective solution to the output regulation problem for switched linear systems via dynamic output feedback under the MLFs framework.

Apart from the theoretical contribution of developing new control design approaches for output regulation of switched linear systems, the current work is also motivated from a more practical point of view: In most existing works such as [56, 18, 19, 47], external signals (including the reference to track and/or the disturbances to be rejected) are generated by a single neutrally stable exosystem. This assumption limits the exogenous signal to the class of constant and periodic signals. In contrast, by considering multiple exosystems, we will be able to obtain more sophisticated exosignals and enhance the control system capability. Moreover, our problem setup is more realistic in the sense that unknown perturbations are allowed to affect not only the controlled plant but also the exosystem dynamics as well. These considerations largely enhance the applicability of the proposed approach to practical problems. Finally, the advantages of the proposed hybrid control approach will be demonstrated through a mechanical system example.

The rest of this chapter is organized as follows: Section 3.2 provides some preliminaries for the development of new control synthesis approach. The hybrid synthesis conditions and the controller construction schemes are presented in Section 3.3 for almost output regulation of switched linear systems. Section 3.4 presents the simulation results on a mechanical system example, and Section 3.5 summaries this chapter.

## 3.2 Preliminaries

### 3.2.1 Weighted $\mathcal{L}_2$ ( $\ell_2$ ) Analysis for Switched Linear Systems with ADT

Consider the following switched linear system.

$$\begin{bmatrix} \mathcal{D}x \\ e \end{bmatrix} = \begin{bmatrix} A_\sigma & B_\sigma \\ C_\sigma & D_\sigma \end{bmatrix} \begin{bmatrix} x \\ d \end{bmatrix} \quad (3.1)$$

where  $x \in \mathbb{R}^n$  is the state with initial condition  $x(0) = x_0$ ,  $e \in \mathbb{R}^{n_e}$  is the performance output and  $d \in \mathbb{R}^{n_d}$  is the external disturbance. The symbol  $\mathcal{D}$  denotes a differentiator for continuous-time systems and a forward shift operator for discrete-time systems.  $\sigma$  is the switching rule that selects a particular sequence of subsystems among  $N$  available ones defined by  $\{A_i, B_i, C_i, D_i\}, i \in \mathbf{I}[1, N]$ . In this chapter, we focus our study of switched linear systems in the form of (3.1) on a class of switching signals with average dwell-time (ADT) switching (see Definition 1.6).

By combing the ADT technique with multiple quadratic Lyapunov functions, the following lemma establishes the conditions for the stability and  $\mathcal{L}_2$  ( $\ell_2$ )-gain performance of the switched linear system (3.1).

**Lemma 1.** *Given two tunable scalars  $\lambda_0 \in \mathbb{R}_+$  and  $\mu > 1$ , if there exist positive definite matrices  $P_i \in \mathbb{S}_+^n$  and a positive scalar  $\gamma \in \mathbb{R}_+$  such that for all  $i, j \in \mathbf{I}[1, N]$ , the following*

conditions hold.

$$\begin{bmatrix} He\{P_i A_i\} + \lambda_0 P_i & \star & \star \\ B_i^T P_i & -\gamma I & \star \\ C_i & D_i & -\gamma I \end{bmatrix} < 0, \quad (3.2)$$

$$P_j \leq \mu P_i. \quad (3.3)$$

Then, the switched linear system (3.1) is GUAS and has its weighted  $\mathcal{L}_2$  gain smaller than  $\gamma$  for any switching signal  $\sigma$  with average dwell-time  $\tau_a \geq \frac{\ln(\mu)}{\lambda_0}$ .

*Proof.* Define the Lyapunov functions with one-to-one correspondence to the subsystems in (3.1) as  $V_i := x^T P_i x$ ,  $i \in \mathbf{I}[1, N]$ . Then, the following results can be obtained from condition (3.2) by Schur complement for all  $i \in \mathbf{I}[1, N]$ ,

$$\begin{bmatrix} He\{P_i A_i\} + \lambda_0 P_i & P_i B_i \\ B_i^T P_i & -\gamma I \end{bmatrix} + \frac{1}{\gamma} \begin{bmatrix} C_i^T \\ D_i^T \end{bmatrix} \begin{bmatrix} C_i & D_i \end{bmatrix} < 0$$

which together with condition (3.3) yields

$$\begin{aligned} \dot{V}_i &= \frac{\partial V_i}{\partial x} (A_i x + B_i d) \\ &= x^T P_i (A_i x + B_i d) + (A_i x + B_i d)^T P_i x \\ &= x^T (P_i A_i + A_i^T P_i) x + x^T P_i B_i d + d^T B_i^T P_i x \\ &< -\lambda_0 V_i - \frac{1}{\gamma} e^T e + \gamma d^T d, \end{aligned}$$

$$V_j(x) \leq \mu V_i(x)$$

for all  $x \in \mathbb{R}^n$  and any  $i, j \in \mathbf{I}[1, N]$ . Consequently, the proof can be completed by following that of Theorem 1 presented in [108].  $\square$

### 3.2.2 Dilated LMI Representations of the BRL

The following lemma provides the equivalent LMI representations (i.e., the so-called dilated LMI conditions) of the Bounded Real Lemma (BRL). These results will be very useful to derive new hybrid synthesis conditions for the output regulation of switched linear systems. Detailed proof of Lemma 2 has been provided in [21], thus will be omitted here.

**Lemma 2.** *Consider a continuous-time LTI system with  $(A, B, C, D)$ . Given a positive scalar  $\gamma \in \mathbb{R}_+$ , there exist a positive definite matrix  $P > 0$  satisfying*

$$\begin{bmatrix} PA + A^T P & \star & \star \\ B^T P & -\gamma I & \star \\ C & D & -\gamma I \end{bmatrix} < 0,$$

*if and only if for the same  $P$  there exists a square matrix  $F$  such that*

$$\begin{bmatrix} -F^T - F & \star & \star & \star \\ P - F^T + A^T F & F^T A + A^T F & \star & \star \\ B^T F & B^T F & -\gamma I & \star \\ 0 & C & D & -\gamma I \end{bmatrix} < 0. \quad (3.4)$$

### 3.3 Main Results

In classical output regulation problem, the exogenous signals are usually required to be constant or perfect sinusoid. The associated design objective is to regulate the output precisely, which in many cases is too ambitious. Following the work in [73, 17, 102], we will relax the classical output regulation requirements by allowing some unknown perturbations affecting the exogenous signals and achieving almost output regulation. More detailed descriptions of this concept will be given in the sequel.

Now, we consider a continuous-time switched linear plant with switched exogenous inputs

$$\begin{bmatrix} \dot{x}_p(t) \\ \dot{w}(t) \\ e(t) \\ y(t) \end{bmatrix} = \begin{bmatrix} A_{p,\sigma} & A_{w,\sigma} & B_{p1,\sigma} & B_{p2,\sigma} \\ 0 & A_{e,\sigma} & Q_\sigma & 0 \\ C_{p1,\sigma} & C_{w1,\sigma} & D_{p11,\sigma} & D_{p12,\sigma} \\ C_{p2,\sigma} & C_{w2,\sigma} & D_{p21,\sigma} & 0 \end{bmatrix} \begin{bmatrix} x_p(t) \\ w(t) \\ d(t) \\ u(t) \end{bmatrix}, \quad t \geq 0 \quad (3.5)$$

where  $x_p(t) \in \mathbb{R}^n$  is the plant state,  $w(t) \in \mathbb{R}^{n_w}$  is the exogenous signal governed by the switched “exosystem”  $\dot{w}(t) = A_{e,\sigma}w(t) + Q_\sigma d(t)$ ,  $d(t) \in \mathbb{R}^{n_d}$  is the unknown disturbance input affecting both controlled plant and exosystem dynamics,  $u(t) \in \mathbb{R}^{n_u}$  is the control input and  $e(t) \in \mathbb{R}^{n_e}$  is the error (performance) output,  $y(t) \in \mathbb{R}^{n_y}$  is the measurement output available for feedback control use. All of the subsystem matrices are constant with compatible dimensions.  $\sigma(t)$ , a piecewise constant function of time, takes its values in the finite set  $\mathbf{I}[1, N_p]$  with  $N_p > 1$  as the number of the subsystems. It is assumed that  $\sigma(t)$  is continuous from the right everywhere and obeys an ADT switching logic. We further assume that for any  $i \in \mathbf{I}[1, N_p]$ ,

**A1.**  $A_{e,i}$  is anti-Hurwitz (i.e., all of its eigenvalues are in the closed right half-plane);

**A2.** The pair  $(A_{p,i}, B_{p2,i})$  is stabilizable;

**A3.** The pair  $\left( \begin{bmatrix} A_{p,i} & A_{w,i} \\ 0 & A_{e,i} \end{bmatrix}, \begin{bmatrix} C_{p2,i} & C_{w2,i} \end{bmatrix} \right)$  is detectable.

The above three assumptions are general enough and follow similar discussions as presented in [55, 73] and [24] for LTI systems. Assumption **A1** is made without loss of generality because asymptotically stable modes in the exosystem would not affect the output regulation under the ADT switching. The second assumption is necessary for asymptotic stabilization of the switched closed-loop system with ADT via either state or output feedback. Although assumption **A3** is stronger than the detectability assumption of the pair  $(A_{p,i}, C_{p2,i})$  for all  $i \in \mathbf{I}[1, N_p]$ , it is necessary for the output regulability of individual subsystem as discussed by Francis in [24] for LTI systems.

**Remark 5.** Note that in (3.5), we have assumed a synchronized switching between the switched plant and the exosystem. Without loss of generality, one can always arrive at an equivalent switched plant in the form of (3.5) with synchronous switching by considering all possible combinations of the plant subsystem with each exogenous subsystem at all switching time instants. Compared with an asynchronous switching case, the synchronized plant would only differ in the number of subsystems  $N_p$ . For instance, the number of equivalent switched subsystems is  $N_p = N_1 \times N_2$  if original numbers of the asynchronous controlled plant and the exosystem are  $N_1$  and  $N_2$ , respectively.

The hybrid dynamic output-feedback control law will be in the form of

$$\begin{bmatrix} \dot{x}_c(t) \\ u(t) \end{bmatrix} = \begin{bmatrix} A_{c,\sigma} & B_{c,\sigma} \\ C_{c,\sigma} & D_{c,\sigma} \end{bmatrix} \begin{bmatrix} x_c(t) \\ y(t) \end{bmatrix} \quad (3.6)$$

$$x_c(t^+) = J_{c,ij}x_c(t), \quad \text{when switching occurs}$$

where  $x_c(t) \in \mathbb{R}^{n_c}$  ( $n_c > n_w$ ) is the controller state, the two subscripts of the matrix  $J_{c,ij}$  ( $i, j \in \mathbf{I}[1, N_p]$  with  $i \neq j$ ) denote respectively the indices of the pre-switching subsystem  $i$  and the post-switching subsystem  $j$ , i.e., at the switching instant, we have  $\sigma(t) = i$  and  $\sigma(t^+) = j$ . We assume synchronized switching both in the controlled plant (as well as the exosystem) and in the controller. Matrices  $A_{c,i}, B_{c,i}, C_{c,i}, D_{c,i}$  and  $J_{c,ij}$  for all  $i, j \in \mathbf{I}[1, N_p]$  and  $i \neq j$  are controller coefficients to be designed.

Our objective is to design a hybrid output-feedback controller (3.6) that stabilizes the switched plant (3.5) with minimal weighted  $\mathcal{L}_2$ -gain performance from the disturbance  $d(t)$  to the error output  $e(t)$ , i.e. almost output regulation. For almost output regulation, it means that for any initial conditions of the closed-loop system, there exists a function  $\beta \in \mathcal{KL}$  such that the error output  $e(t)$  satisfies  $\|e(t)\| \leq \beta(\|\varphi(0), t\|) + \epsilon\|d(t)\|$  with  $\varphi(0) := \begin{bmatrix} x_p^T(0) & x_c^T(0) & w^T(0) \end{bmatrix}$  for all  $t \geq 0$  and some  $\epsilon > 0$ . In particular,  $e(t)$  is said to be asymptotically regulated if the above condition holds for  $d(t) \equiv 0$ .

To this end, motivated by the results in Theorem 3 of [75] for output regulation of LTI systems and in [103] for hybrid stabilization of switched linear systems, we partition the hybrid controller state  $x_c$  in (3.6) as  $x_c = \begin{bmatrix} x_{c1} \\ x_{c2} \end{bmatrix}$  with  $x_{c1} \in \mathbb{R}^{n_w}$ ,  $x_{c2} \in \mathbb{R}^{n_c - n_w}$ , and parameterize the controller coefficient matrices for all  $i, j \in \mathbf{I}[1, N_p]$  and  $i \neq j$  as

$$\begin{bmatrix} A_{c,i} & B_{c,i} \\ C_{c,i} & D_{c,i} \end{bmatrix} = \begin{bmatrix} A_{e,i} - \bar{D}_{c2,i}(C_{w2,i} + C_{p2,i}\Pi_{p,i}) & \bar{C}_{c2,i} & \bar{D}_{c2,i} \\ -\bar{B}_{c,i}(C_{w2,i} + C_{p2,i}\Pi_{p,i}) & \bar{A}_{c,i} & \bar{B}_{c,i} \\ \Gamma_i - \bar{D}_{c1,i}(C_{w2,i} + C_{p2,i}\Pi_{p,i}) & \bar{C}_{c1,i} & \bar{D}_{c1,i} \end{bmatrix}, \quad J_{c,ij} = \begin{bmatrix} I & J_{c12,ij} \\ 0 & J_{c22,ij} \end{bmatrix} \quad (3.7)$$

where  $\bar{A}_{c,i} \in \mathbb{R}^{(n_c - n_w) \times (n_c - n_w)}$ ,  $\bar{B}_{c,i} \in \mathbb{R}^{(n_c - n_w) \times n_y}$ ,  $\bar{C}_{c1,i} \in \mathbb{R}^{n_u \times (n_c - n_w)}$ ,  $\bar{C}_{c2,i} \in \mathbb{R}^{n_w \times (n_c - n_w)}$ ,  $\bar{D}_{c1,i} \in \mathbb{R}^{n_u \times n_y}$ ,  $\bar{D}_{c2,i} \in \mathbb{R}^{n_w \times n_y}$ ,  $J_{c12,ij} \in \mathbb{R}^{n_w \times (n_c - n_w)}$ ,  $J_{c22,ij} \in \mathbb{R}^{(n_c - n_w) \times (n_c - n_w)}$ , and  $\Pi_{p,i} \in \mathbb{R}^{n \times n_w}$ ,  $\Gamma_i \in \mathbb{R}^{n_u \times n_w}$  are free variables subject to design. Needless to say, such a pre-specified controller parametrization would impose a structural constraint on the hybrid controller gains with reduced number of design variables. However, it is clearly necessary for the output regulation of each subsystem (see, e.g., [24, 25, 75]). Moreover, it will be shown in the sequel that output regulability of the switched linear system (3.5) can be readily achieved under the parametrization (3.7).

Consequently, the hybrid closed-loop system is formed by interconnecting the switched plant (3.5) and the hybrid controller (3.6) with the parametrization (3.7) as

$$\begin{bmatrix} \dot{x}_{cl}(t) \\ \dot{w}(t) \\ e(t) \end{bmatrix} = \begin{bmatrix} A_{cl,\sigma} & A_{clw,\sigma} & B_{cl,\sigma} \\ 0 & A_{e,\sigma} & Q_\sigma \\ C_{cl,\sigma} & C_{clw,\sigma} & D_{cl,\sigma} \end{bmatrix} \begin{bmatrix} x_{cl}(t) \\ w(t) \\ d(t) \end{bmatrix} \quad (3.8)$$

$$x_{cl}(t^+) = J_{cl,ij}x_{cl}(t), \quad \text{when switching occurs}$$

where  $x_{cl} := \begin{bmatrix} x_p^T & x_{c1}^T & x_{c2}^T \end{bmatrix}^T$ , and

$$\begin{aligned}
A_{cl,\sigma} &= \begin{bmatrix} A_{p,\sigma} + B_{p2,\sigma}\bar{D}_{c1,\sigma}C_{p2,\sigma} & B_{p2,\sigma}(\Gamma_\sigma - \bar{D}_{c1,\sigma}(C_{w2,\sigma} + C_{p2,\sigma}\Pi_{p,\sigma})) & B_{p2,\sigma}\bar{C}_{c1,\sigma} \\ \bar{D}_{c2,\sigma}C_{p2,\sigma} & A_{e,\sigma} - \bar{D}_{c2,\sigma}(C_{w2,\sigma} + C_{p2,\sigma}\Pi_{p,\sigma}) & \bar{C}_{c2,\sigma} \\ \bar{B}_{c,\sigma}C_{p2,\sigma} & -\bar{B}_{c,\sigma}(C_{w2,\sigma} + C_{p2,\sigma}\Pi_{p,\sigma}) & \bar{A}_{c,\sigma} \end{bmatrix}, \\
A_{clw,\sigma} &= \begin{bmatrix} A_{w,\sigma} + B_{p2,\sigma}\bar{D}_{c1,\sigma}C_{w2,\sigma} \\ \bar{D}_{c2,\sigma}C_{w2,\sigma} \\ \bar{B}_{c,\sigma}C_{w2,\sigma} \end{bmatrix}, \quad B_{cl,\sigma} = \begin{bmatrix} B_{p1,\sigma} + B_{p2,\sigma}\bar{D}_{c1,\sigma}D_{p21,\sigma} \\ \bar{D}_{c2,\sigma}D_{p21,\sigma} \\ \bar{B}_{c,\sigma}D_{p21,\sigma} \end{bmatrix}, \\
C_{cl,\sigma} &= \begin{bmatrix} C_{p1,\sigma} + D_{p12,\sigma}\bar{D}_{c1,\sigma}C_{p2,\sigma} & D_{p12,\sigma}(\Gamma_\sigma - \bar{D}_{c1,\sigma}(C_{w2,\sigma} + C_{p2,\sigma}\Pi_{p,\sigma})) & D_{p12,\sigma}\bar{C}_{c1,\sigma} \end{bmatrix}, \\
C_{clw,\sigma} &= C_{w1,\sigma} + D_{p12,\sigma}\bar{D}_{c1,\sigma}C_{w2,\sigma}, \quad D_{cl,\sigma} = D_{p11,\sigma} + D_{p12,\sigma}\bar{D}_{c1,\sigma}D_{p21,\sigma}, \\
J_{cl,ij} &= \begin{bmatrix} I & 0 & 0 \\ 0 & I & J_{c12,ij} \\ 0 & 0 & J_{c22,ij} \end{bmatrix}.
\end{aligned} \tag{3.9}$$

Employing multiple quadratic Lyapunov functions, the following theorem provides the synthesis conditions of the hybrid controllers that possess the special architecture and achieve almost output regulation for the closed-loop switched system (3.8). The hybrid controller construction scheme is also provided.

**Theorem 4** (Continuous-time). *Given two tunable scalars  $\lambda_0 \in \mathbb{R}_+$  and  $\mu > 1$ , if there exist positive definite matrices  $\hat{P}_i \in \mathbb{S}_+^{2(n+n_w)}$ , rectangular matrices  $X, Y, W \in \mathbb{R}^{(n+n_w) \times (n+n_w)}$ ,  $\hat{A}_{c,i} \in \mathbb{R}^{(n+n_w) \times (n+n_w)}$ ,  $\hat{B}_{c,i} \in \mathbb{R}^{(n+n_w) \times n_y}$ ,  $\hat{C}_{c,i} \in \mathbb{R}^{(n_u+n_w) \times (n+n_w)}$ ,  $\hat{D}_{c,i} \in \mathbb{R}^{(n_u+n_w) \times n_y}$ ,  $\hat{J}_{c12,ij} \in \mathbb{R}^{n_w \times (n+n_w)}$ ,  $\hat{J}_{c22,ij} \in \mathbb{R}^{(n+n_w) \times (n+n_w)}$ ,  $\Pi_{p,i} \in \mathbb{R}^{n \times n_w}$ ,  $\Gamma_i \in \mathbb{R}^{n_u \times n_w}$ , and a positive scalar  $\gamma \in \mathbb{R}_+$  such that*

conditions (3.10)–(3.13) hold for all  $i, j \in \mathbf{I}[1, N_p], i \neq j$ .

$$\Pi_{p,i}A_{e,i} - A_{w,i} = A_{p,i}\Pi_{p,i} + B_{p2,i}\Gamma_i \quad (3.10)$$

$$-C_{w1,i} = C_{p1,i}\Pi_{p,i} + D_{p12,i}\Gamma_i \quad (3.11)$$

$$\begin{bmatrix} - \begin{bmatrix} X + X^T & \star \\ W + I & Y + Y^T \end{bmatrix} & \star & \star & \star \\ \Psi_{21,i} & \Psi_{22,i} & \star & \star \\ \Psi_{31,i} & \Psi_{31,i} & -\gamma I & \star \\ 0 & \Psi_{42,i} & D_{p11,i} + D_{aug12,i}\hat{D}_{c,i}D_{p21,i} & -\gamma I \end{bmatrix} < 0, \quad (3.12)$$

$$\begin{bmatrix} \mu\hat{P}_i & \star \\ \Phi_{ij} \begin{bmatrix} X + X^T & \star \\ W + I & Y + Y^T \end{bmatrix} - \hat{P}_j \end{bmatrix} \geq 0, \quad (3.13)$$

where

$$\begin{aligned} \Psi_{21,i} &= \begin{bmatrix} A_{aug,i}X + B_{aug2,i}\hat{C}_{c,i} & A_{aug,i} + B_{aug2,i}\hat{D}_{c,i}C_{aug2,i} \\ \hat{A}_{c,i} & Y A_{aug,i} + \hat{B}_{c,i}C_{aug2,i} \end{bmatrix}^T - \begin{bmatrix} X & I \\ W & Y \end{bmatrix} + \frac{\lambda_0}{2} \begin{bmatrix} X & I \\ W & Y \end{bmatrix}^T + \hat{P}_i, \\ \Psi_{22,i} &= \begin{bmatrix} He \left\{ A_{aug,i}X + B_{aug2,i}\hat{C}_{c,i} + \frac{\lambda_0}{2}X \right\} & \star \\ \hat{A}_{c,i} + A_{aug,i}^T + C_{aug2,i}^T\hat{D}_{c,i}^T B_{aug2,i}^T + \frac{\lambda_0}{2}(W + I) & He \left\{ Y A_{aug,i} + \hat{B}_{c,i}C_{aug2,i} + \frac{\lambda_0}{2}Y \right\} \end{bmatrix}, \\ \Psi_{31,i} &= \begin{bmatrix} B_{aug1,i}^T + D_{p21,i}^T\hat{D}_{c,i}^T B_{aug2,i}^T & B_{aug1,i}^T Y^T + D_{p21,i}^T\hat{B}_{c,i}^T \end{bmatrix}, \\ \Psi_{42,i} &= \begin{bmatrix} C_{aug1,i}X + D_{aug12,i}\hat{C}_{c,i} & C_{aug1,i} + D_{aug12,i}\hat{D}_{c,i}C_{aug2,i} \end{bmatrix}, \end{aligned}$$

$$\begin{aligned}
\Phi_{ij} &= \begin{bmatrix} \begin{bmatrix} I & \Pi_{p,i} - \Pi_{p,j} \\ 0 & I \end{bmatrix} X + \begin{bmatrix} -\Pi_{p,j} \\ I \end{bmatrix} \hat{J}_{c12,ij} & \begin{bmatrix} I & \Pi_{p,i} - \Pi_{p,j} \\ 0 & I \end{bmatrix} \\ & \hat{J}_{c22,ij} & Y \begin{bmatrix} I & \Pi_{p,i} - \Pi_{p,j} \\ 0 & I \end{bmatrix} \end{bmatrix}, \\
A_{aug,i} &= \begin{bmatrix} A_{p,i} & -A_{w,i} \\ 0 & A_{e,i} \end{bmatrix}, \quad B_{aug1,i} = \begin{bmatrix} B_{p1,i} \\ -Q_i \end{bmatrix}, \quad C_{aug1,i} = \begin{bmatrix} C_{p1,i} & -C_{w1,i} \end{bmatrix}, \\
B_{aug2,i} &= \begin{bmatrix} B_{p2,i} & -\Pi_{p,i} \\ 0 & I \end{bmatrix}, \quad C_{aug2,i} = \begin{bmatrix} C_{p2,i} & -C_{w2,i} \end{bmatrix}, \quad D_{aug12,i} = \begin{bmatrix} D_{p12,i} & 0 \end{bmatrix}.
\end{aligned}$$

Then, there exists a hybrid controller in the form of (3.6) with order  $n_c = n + 2n_w$  that renders the closed-loop system (3.8) GUAS with its weighted  $\mathcal{L}_2$  gain less than  $\gamma$  for every switching signal  $\sigma$  with average dwell-time  $\tau_a \geq \frac{\ln(\mu)}{\lambda_0}$ .

Moreover, the hybrid controller gain matrices are readily obtained through the following scheme:

- Solve  $M, N \in \mathbb{R}^{(n+n_w) \times (n+n_w)}$  from the factorization problem  $MN^T = W^T - XY$ .
- Compute the controller coefficient matrices for  $i, j \in \mathbf{I}[1, N_p], i \neq j$  by

$$\begin{aligned}
\begin{bmatrix} \bar{A}_{c,i} & \bar{B}_{c,i} \\ \begin{bmatrix} \bar{C}_{c1,i} \\ \bar{C}_{c2,i} \end{bmatrix} & \begin{bmatrix} \bar{D}_{c1,i} \\ \bar{D}_{c2,i} \end{bmatrix} \end{bmatrix} &= \begin{bmatrix} N & YB_{aug2,i} \\ 0 & I \end{bmatrix}^{-1} \begin{bmatrix} \hat{A}_{c,i} - YA_{aug,i}X & \hat{B}_{c,i} \\ \hat{C}_{c,i} & \hat{D}_{c,i} \end{bmatrix} \begin{bmatrix} M^T & 0 \\ C_{aug2,i}X & I \end{bmatrix}^{-1}, \\
\begin{bmatrix} J_{c22,ij} \\ J_{c12,ij} \end{bmatrix} &= \begin{bmatrix} N & Y \begin{bmatrix} -\Pi_{p,j} \\ I \end{bmatrix} \\ 0 & I \end{bmatrix}^{-1} \begin{bmatrix} \hat{J}_{c22,ij} - Y \begin{bmatrix} I & \Pi_{p,i} - \Pi_{p,j} \\ 0 & I \end{bmatrix} X \\ \hat{J}_{c12,ij} \end{bmatrix} M^{-T}.
\end{aligned} \tag{3.14}$$

- Obtain the realization of the hybrid controller in the form of (3.6) via relation (3.7).

*Proof.* Consider the hybrid closed-loop system (3.8). For simplicity of presentation and without loss of generality, we assume that  $\sigma(t) = i$  and  $\sigma(t^+) = j$  for some  $i, j \in \mathbf{I}[1, N_p]$  and  $i \neq j$ . Then, by applying the following state transformation

$$\underbrace{\begin{bmatrix} \tilde{x}_p(t) \\ \tilde{x}_{c1}(t) \\ \tilde{x}_{c2}(t) \end{bmatrix}}_{\tilde{x}_{cl,i}(t)} = \underbrace{\begin{bmatrix} I & -\Pi_{p,i} & 0 \\ 0 & I & 0 \\ 0 & 0 & I \end{bmatrix}}_{T_i} \begin{bmatrix} x_p(t) \\ x_{c1}(t) \\ x_{c2}(t) \end{bmatrix} - \underbrace{\begin{bmatrix} 0 \\ I \\ 0 \end{bmatrix}}_{B_I} w(t) \quad (3.15)$$

to the system state, we obtain the following hybrid system

$$\begin{bmatrix} \dot{\tilde{x}}_{cl,i}(t) \\ \dot{w}(t) \\ e(t) \end{bmatrix} = \begin{bmatrix} \tilde{A}_{cl,i} & \tilde{A}_{clw,i} & \tilde{B}_{cl,i} \\ 0 & A_{e,i} & Q_i \\ \tilde{C}_{cl,i} & \tilde{C}_{clw,i} & \tilde{D}_{cl,i} \end{bmatrix} \begin{bmatrix} \tilde{x}_{cl,i}(t) \\ w(t) \\ d(t) \end{bmatrix} \quad (3.16)$$

$$\tilde{x}_{cl,j}(t^+) = T_j J_{cl,ij} T_i^{-1} \tilde{x}_{cl,i}(t) + (T_j J_{cl,ij} T_i^{-1} B_I - B_I) w(t), \quad \text{when switching occurs}$$

With the controller parametrization (3.7), it can be verified that  $T_j J_{cl,ij} T_i^{-1} B_I - B_I = 0$  for any  $i, j \in \mathbf{I}[1, N_p]$  and  $i \neq j$ . Furthermore, conditions (3.10) and (3.11) lead to the system matrices of the above transformed closed-loop system as

$$\begin{aligned} \tilde{A}_{cl,i} &= \begin{bmatrix} \begin{bmatrix} A_{p,i} & -A_{w,i} \\ 0 & A_{e,i} \end{bmatrix} + \begin{bmatrix} B_{p2,i} & -\Pi_{p,i} \\ 0 & I \end{bmatrix} \begin{bmatrix} \bar{D}_{c1,i} \\ \bar{D}_{c2,i} \end{bmatrix} & \begin{bmatrix} C_{p2,i} & -C_{w2,i} \end{bmatrix} & \begin{bmatrix} B_{p2,i} & -\Pi_{p,i} \\ 0 & I \end{bmatrix} \begin{bmatrix} \bar{C}_{c1,i} \\ \bar{C}_{c2,i} \end{bmatrix} \\ & \bar{B}_{c,i} \begin{bmatrix} C_{p2,i} & -C_{w2,i} \end{bmatrix} & \bar{A}_{c,i} \end{bmatrix}, \\ \tilde{B}_{cl,i} &= \begin{bmatrix} \begin{bmatrix} B_{p1,i} \\ -Q_i \end{bmatrix} + \begin{bmatrix} B_{p2,i} & -\Pi_{p,i} \\ 0 & I \end{bmatrix} \begin{bmatrix} \bar{D}_{c1,i} \\ \bar{D}_{c2,i} \end{bmatrix} D_{p21,i} \\ \bar{B}_{c,i} D_{p21,i} \end{bmatrix}, \end{aligned} \quad (3.17)$$

$$\begin{aligned}\tilde{C}_{cl,i} &= \left[ \begin{array}{cc} [C_{p1,i} & -C_{w1,i}] + [D_{p12,i} & 0] \begin{bmatrix} \bar{D}_{c1,i} \\ \bar{D}_{c2,i} \end{bmatrix} & [C_{p2,i} & -C_{w2,i}] & [D_{p12,i} & 0] \begin{bmatrix} \bar{C}_{c1,i} \\ \bar{C}_{c2,i} \end{bmatrix} \end{array} \right], \\ \tilde{D}_{cl,i} &= D_{p11,i} + [D_{p12,i} & 0] \begin{bmatrix} \bar{D}_{c1,i} \\ \bar{D}_{c2,i} \end{bmatrix} D_{p21,i}\end{aligned}$$

and  $\tilde{A}_{clw,i} = 0$ ,  $\tilde{C}_{clw,i} = 0$ . Since the error output  $e(t)$  does not explicitly depend on the exosystem state  $w(t)$  and  $\tilde{D}_{cl,i}$  is bounded for all  $i \in \mathbf{I}[1, N_p]$ , it suffices to prove that the above transformed system (3.16) with state  $\tilde{x}_{cl,i}(t)$  is GUAS in achieving almost output regulation.

To this end, we consider the Lyapunov-like functions for the transformed closed-loop system (3.16) as

$$V_i(\tilde{x}_{cl,i}(t)) = \tilde{x}_{cl,i}^T(t) P_i \tilde{x}_{cl,i}(t), \quad i \in \mathbf{I}[1, N_p] \quad (3.18)$$

where  $P_i \in \mathbb{S}_+^{2(n+n_w)}$ . Note that each  $V_i$  has one-to-one correspondence with the subsystems in (3.16).

According to Lemma 1, to establish the ADT-based switching stability and weighted  $\mathcal{L}_2$ -gain performance for system (3.16), we need to prove the following conditions for all  $i, j \in \mathbf{I}[1, N_p]$  ( $i \neq j$ ),

$$\begin{bmatrix} He\{P_i \tilde{A}_{cl,i}\} + \lambda_0 P_i & \star & \star \\ \tilde{B}_{cl,i}^T P_i & -\gamma I & \star \\ \tilde{C}_{cl,i} & \tilde{D}_{cl,i} & -\gamma I \end{bmatrix} < 0, \quad (3.19)$$

$$V_j(\tilde{x}_{cl,j}(t^+)) \leq \mu V_i(\tilde{x}_{cl,i}(t)). \quad (3.20)$$

It is worth pointing out that the second condition (3.20), i.e., the well-known boundary condition that constrains the jump between two adjacent Lyapunov functions [103], is slightly different from that of Lemma 1 (see, condition (3.3)) for purely switching linear systems without state jumps. The boundary condition cannot be written directly in terms of the Lyapunov matrices  $P_i$  here, due to the impulsive dynamics induced by the system state jumps at each switching instant (as shown by the second equation in (3.16)). However, it is easy to verify by following

a similar proof of Lemma 1 that weighted  $\mathcal{L}_2$  stability still holds for system (3.16) under the conditions (3.19)–(3.20), provided the satisfaction of the ADT constraint  $\tau_a \geq \frac{\ln(\mu)}{\lambda_0}$ .

Note that  $He\{P_i \tilde{A}_{cl,i}\} + \lambda_0 P_i = He\{P_i(\tilde{A}_{cl,i} + \frac{\lambda_0}{2})\}$ , condition (3.19) is ascertained from the following by applying Lemma 2,

$$\begin{bmatrix} -F - F^T & \star & \star & \star \\ P_i - F^T + \tilde{A}_{cl,i}^T F + \frac{\lambda_0}{2} F & He\{F^T \tilde{A}_{cl,i} + \frac{\lambda_0}{2} F^T\} & \star & \star \\ \tilde{B}_{cl,i}^T F & \tilde{B}_{cl,i}^T F & -\gamma I & \star \\ 0 & \tilde{C}_{cl,i} & \tilde{D}_{cl,i} & -\gamma I \end{bmatrix} < 0, \quad (3.21)$$

where  $F \in \mathbb{R}^{(n+n_c) \times (n+n_c)}$  is a general non-singular matrix.

Then, we introduce two non-singular matrices

$$Z_1 = \begin{bmatrix} X & I \\ M^T & 0 \end{bmatrix}, \quad Z_2 = \begin{bmatrix} I & Y^T \\ 0 & N^T \end{bmatrix}$$

with  $MN^T = W^T - XY$  and specify  $F = Z_2 Z_1^{-1}$ . To show the first condition (3.21), multiplying matrix  $diag\{Z_1, Z_1, I, I\}$  from the right hand side and its transpose from left of (3.21), we obtain:

$$Z_1^T P_i Z_1 = \hat{P}_i,$$

$$Z_1^T F^T Z_1 = Z_2^T Z_1 = \begin{bmatrix} X & I \\ W & Y \end{bmatrix},$$

$$Z_1^T F^T \tilde{A}_{cl,i} Z_1 = Z_2^T \tilde{A}_{cl,i} Z_1$$

$$= \begin{bmatrix} \begin{bmatrix} A_{p,i} & -A_{w,i} \\ 0 & A_{e,i} \end{bmatrix} X + \begin{bmatrix} B_{p2,i} & -\Pi_{p,i} \\ 0 & I \end{bmatrix} \hat{C}_{c,i} & \begin{bmatrix} A_{p,i} & -A_{w,i} \\ 0 & A_{e,i} \end{bmatrix} + \begin{bmatrix} B_{p2,i} & -\Pi_{p,i} \\ 0 & I \end{bmatrix} \hat{D}_{c,i} \begin{bmatrix} C_{p2,i} & -C_{w2,i} \end{bmatrix} \\ \hat{A}_{c,i} & Y \begin{bmatrix} A_{p,i} & -A_{w,i} \\ 0 & A_{e,i} \end{bmatrix} + \hat{B}_{c,i} \begin{bmatrix} C_{p2,i} & -C_{w2,i} \end{bmatrix} \end{bmatrix},$$

$$\begin{aligned}
\tilde{B}_{cl,i}^T F Z_1 &= \tilde{B}_{cl,i}^T Z_2 \\
&= \left[ \begin{array}{c} \left[ B_{p1,i} \right]^T \\ -Q_i \end{array} \right]^T + D_{p21,i}^T \hat{D}_{c,i}^T \left[ \begin{array}{cc} B_{p2,i} & -\Pi_{p,i} \\ 0 & I \end{array} \right]^T \left[ \begin{array}{c} B_{p1,i} \\ -Q_i \end{array} \right]^T Y^T + D_{p21,i}^T \hat{B}_{c,i}^T \\
\tilde{C}_{cl,i} Z_1 &= \left[ \begin{array}{cc} C_{p1,i} & -C_{w1,i} \end{array} \right] X + \left[ \begin{array}{cc} D_{p12,i} & 0 \end{array} \right] \hat{C}_{c,i} \left[ \begin{array}{cc} C_{p1,i} & -C_{w1,i} \end{array} \right] + \left[ \begin{array}{cc} D_{p12,i} & 0 \end{array} \right] \hat{D}_{c,i} \left[ \begin{array}{cc} C_{p2,i} & -C_{w2,i} \end{array} \right].
\end{aligned}$$

where

$$\begin{aligned}
\hat{A}_{c,i} &= Y \left[ \begin{array}{cc} A_{p,i} & -A_{w,i} \\ 0 & A_{e,i} \end{array} \right] X + Y \left[ \begin{array}{cc} B_{p2,i} & -\Pi_{p,i} \\ 0 & I \end{array} \right] \left[ \begin{array}{c} \bar{D}_{c1,i} \\ \bar{D}_{c2,i} \end{array} \right] \left[ \begin{array}{cc} C_{p2,i} & -C_{w2,i} \end{array} \right] X \\
&\quad + N \bar{B}_{c,i} \left[ \begin{array}{cc} C_{p2,i} & -C_{w2,i} \end{array} \right] X + Y \left[ \begin{array}{cc} B_{p2,i} & -\Pi_{p,i} \\ 0 & I \end{array} \right] \left[ \begin{array}{c} \bar{C}_{c1,i} \\ \bar{C}_{c2,i} \end{array} \right] M^T + N \bar{A}_{c,i} M^T, \\
\hat{B}_{c,i} &= Y \left[ \begin{array}{cc} B_{p2,i} & -\Pi_{p,i} \\ 0 & I \end{array} \right] \left[ \begin{array}{c} \bar{D}_{c1,i} \\ \bar{D}_{c2,i} \end{array} \right] + N \bar{B}_{c,i}, \\
\hat{C}_{c,i} &= \left[ \begin{array}{c} \bar{D}_{c1,i} \\ \bar{D}_{c2,i} \end{array} \right] \left[ \begin{array}{cc} C_{p2,i} & -C_{w2,i} \end{array} \right] X + \left[ \begin{array}{c} \bar{C}_{c1,i} \\ \bar{C}_{c2,i} \end{array} \right] M^T, \quad \hat{D}_{c,i} = \left[ \begin{array}{c} \bar{D}_{c1,i} \\ \bar{D}_{c2,i} \end{array} \right].
\end{aligned} \tag{3.22}$$

Thus, we arrive at condition (3.12).

Now, we consider condition (3.20). According to the definition (3.18), we have

$$\tilde{x}_{cl,j}^T(t^+) P_j \tilde{x}_{cl,j}(t^+) \leq \mu \tilde{x}_{cl,i}^T(t) P_i \tilde{x}_{cl,i}(t) \tag{3.23}$$

for all  $x_{cl}(t) \in \mathbb{R}^{n+n_c}$ ,  $w(t) \in \mathbb{R}^{n_w}$  and  $t \geq 0$ . In order to transform such a Lyapunov boundary condition to a condition of matrix inequality, we need to decouple the indexed matrices  $T_i$  and  $J_{cl,ij}$  (for all  $i, j \in \mathbf{I}[1, N_p]$  and  $i \neq j$ ) from the state  $x_{cl}(t)$  in the second equation of (3.16). To this end, we substitute the second equation in (3.16) together with the state transformation

(3.15) into the inequality (3.23), it yields

$$\tilde{x}_{cl,i}^T(t)(T_j J_{cl,ij} T_i^{-1})^T P_j T_j J_{cl,ij} T_i^{-1} \tilde{x}_{cl,i}(t) \leq \mu \tilde{x}_{cl,i}^T(t) P_i \tilde{x}_{cl,i}(t).$$

Thus, according to Schur complement, it is equivalent to show that for all  $\tilde{x}_{cl,i}(t) \in \mathbb{R}^{n+n_c}$  and  $t \geq 0$

$$\begin{bmatrix} \mu P_i & \star \\ T_j J_{cl,ij} T_i^{-1} & P_j^{-1} \end{bmatrix} \geq 0. \quad (3.24)$$

Furthermore, since  $P_j^{-1} \geq F^{-T}(F + F^T - P_j)F^{-1}$  for any non-singular  $F$ , condition (3.24) can be reformulated after performing a congruence transformation [75] with matrix  $diag\{I, F^T\}$  on

$$\begin{bmatrix} \mu P_i & \star \\ T_j J_{cl,ij} T_i^{-1} & F^{-T}(F + F^T - P_j)F^{-1} \end{bmatrix} \geq 0,$$

which leads to

$$\begin{bmatrix} \mu P_i & \star \\ F^T T_j J_{cl,ij} T_i^{-1} & F + F^T - P_j \end{bmatrix} \geq 0. \quad (3.25)$$

Again, multiplying matrix  $diag\{Z_1, Z_1, Z_1\}$  to the right and its transpose from the left on both sides of the above inequality, we have

$$\begin{aligned} Z_1^T F^T T_j J_{cl,ij} T_i^{-1} Z_1 &= Z_2^T T_j J_{cl,ij} T_i^{-1} Z_1 \\ &= \begin{bmatrix} \begin{bmatrix} I & \Pi_{p,i} - \Pi_{p,j} \\ 0 & I \end{bmatrix} X + \begin{bmatrix} -\Pi_{p,j} \\ I \end{bmatrix} \\ \hat{J}_{c22,ij} \end{bmatrix} \hat{J}_{c12,ij} \begin{bmatrix} \begin{bmatrix} I & \Pi_{p,i} - \Pi_{p,j} \\ 0 & I \end{bmatrix} \\ Y \begin{bmatrix} I & \Pi_{p,i} - \Pi_{p,j} \\ 0 & I \end{bmatrix} \end{bmatrix}, \end{aligned}$$

where

$$\begin{aligned} \hat{J}_{c12,ij} &= J_{c12,ij} M^T, \\ \hat{J}_{c22,ij} &= Y \begin{bmatrix} I & \Pi_{p,i} - \Pi_{p,j} \\ 0 & I \end{bmatrix} X + Y \begin{bmatrix} -\Pi_{p,j} \\ I \end{bmatrix} J_{c12,ij} M^T + N J_{c22,ij} M^T. \end{aligned} \quad (3.26)$$

Consequently, condition (3.13) can be deduced. The controller formula (3.14) can be verified readily by inverting the relations (3.22) and (3.26).  $\square$

**Remark 6.** *As mentioned in the introduction, one of the technical difficulties arise in the output regulator synthesis is that different coordinate transformations are needed for different subsystems. This difficulty has been overcome in the above proof by introducing a new coordinate transformation as in (3.15). Unlike typically used in the literature [24, 27, 18]), it results in a particular switched system with independent dynamics in each subsystem as seen in (3.16). Such a coordinate transformation allows one to decouple the indexed matrices  $T_i$  from the state  $x_{cl}(t)$  in the second equation of (3.16). Based on this transformation technique and the new hybrid controller structure (3.6) with impulsive dynamics, the convex synthesis conditions in Theorem 4 are derived.*

Conditions (3.10)–(3.11) are two linear matrix equations which essentially correspond to the regulation equations (the so-called Francis conditions) for LTI systems [24]; while condition (3.13) is termed as the boundary condition that frequently arises from ADT switching control using MLFs [103]. Based on the results derived in Theorem 4, one can solve the hybrid output regulation problem by formulating the following minimization problem of the weighted  $\mathcal{L}_2$  gain  $\gamma$  with two pre-specified scalars  $\lambda_0$  and  $\mu$ :

$$\begin{aligned} & \min_{\hat{P}_i, X, Y, W, \hat{A}_{c,i}, \hat{B}_{c,i}, \hat{C}_{c,i}, \hat{D}_{c,i}, \hat{J}_{c11,ij}, \hat{J}_{c12,ij}, \hat{J}_{c21,ij}, \hat{J}_{c22,ij}, \Pi_{p,i}, \Gamma_i} \gamma, \\ & \text{s.t.} \quad (3.10)\text{--}(3.13). \end{aligned} \quad (3.27)$$

The optimization (3.27) fits into the standard form of most convex optimization problems.

Therefore it can be solved efficiently by using existing numerical softwares, such as the CVX toolbox in MATLAB [9]. Note that the two constant parameters  $\lambda_0$  and  $\mu$  are fixed when solving the optimization problem (3.27). To determine suitable values of these two pre-specified parameters, we suggest two rules: 1). based on the switching properties of the controlled plant, one can determine desired ADT value  $\tau_a$ .  $\lambda_0, \mu$  must then satisfy the ADT constraint  $\tau_a \geq \frac{\ln(\mu)}{\lambda_0}$ ; 2). by gridding the parameter space of  $(\lambda_0, \mu)$  as in [103], one can obtain an optimal or sub-optimal weighted  $\mathcal{L}_2$  gain  $\gamma$ .

### 3.4 Application to A Mechanical System

In this section, the proposed control scheme will be applied to a mechanical system developed in [89, 90] to achieve hybrid output regulation. As shown in Fig. 3.1, the mechanical system

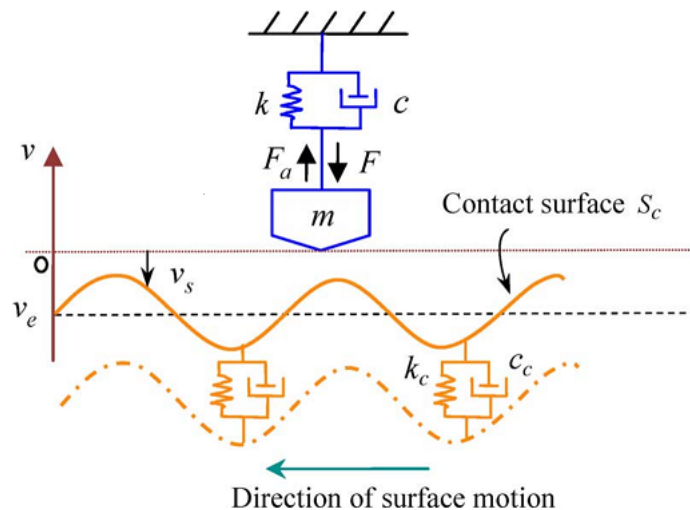


Figure 3.1: Diagram of a mechanical system with switched dynamics [90].

consists of a mass  $m$ , a spring with stiffness  $k$  and a damper with damping coefficient  $c$ , and is subject to a disturbance force  $F_a$  and a control force  $F$ . When in contact with the surface  $S_c$ , the mass experiences an additional force generated by a spring with stiffness  $k_c$  and a damper

with damping coefficient  $c_c$ . The control objective is to design an output regulator such that the mass  $m$  follows the contact surface  $S_c$  as close as possible.

The equations of motion of such a mechanical system can be described by the following switched linear system with two modes (subsystems):

$$\begin{aligned} m\ddot{q} + c\dot{q} + kq &= -F + F_a + F_c, & \text{when } q \leq q_s \text{ (contact mode)} \\ m\ddot{q} + c\dot{q} + kq &= -F + F_a, & \text{when } q > q_s \text{ (non-contact mode)} \end{aligned} \quad (3.28)$$

where the variable  $q$  is the deviation of the mass  $m$  from its equilibrium position.  $F_c$  is the contact force expressed by

$$F_c = c_c(\dot{q}_s - \dot{q}) + k_c(q_s - q)$$

with  $q_s$  being the displacement of the contact surface. According to our control goal, we define the error output  $e$  to be regulated as

$$e = q - q_s$$

where  $q - q_s$  indicates the distances between the mass  $m$  and the contact surface  $S_c$ . Furthermore, we assume that the measurement output  $y$  for the controller is the same as the error output  $e$ .

Let  $x_{p1} = q$ ,  $x_{p2} = \dot{q}$  and  $w_1 = q_s$ ,  $w_2 = \dot{q}_s$ , and define the control input  $u = F$ , the external unknown perturbation  $d = F_a$ , the switched mechanical system can be written in the following

standard form

$$\left\{ \begin{array}{l} \begin{bmatrix} \dot{x}_{p1}(t) \\ \dot{x}_{p2}(t) \end{bmatrix} = A_{p,\sigma} \begin{bmatrix} x_{p1}(t) \\ x_{p2}(t) \end{bmatrix} + A_{w,\sigma} \begin{bmatrix} w_1(t) \\ w_2(t) \end{bmatrix} + B_{p1,\sigma}d(t) + B_{p2,\sigma}u(t) \\ e(t) = C_{p1,\sigma} \begin{bmatrix} x_{p1}(t) \\ x_{p2}(t) \end{bmatrix} + C_{w1,\sigma} \begin{bmatrix} w_1(t) \\ w_2(t) \end{bmatrix} \\ y(t) = e(t) = x_{p1}(t) - w_1(t) \\ \sigma(t) = \begin{cases} 1, & \text{if } x_{p1}(t) \leq w_1(t) \\ 2, & \text{if } x_{p1}(t) > w_1(t) \end{cases} \end{array} \right. \quad (3.29)$$

where

$$\begin{aligned} A_{p,1} &= \begin{bmatrix} 0 & 1 \\ -\frac{k+k_c}{m} & -\frac{c+c_c}{m} \end{bmatrix}, & A_{w,1} &= \begin{bmatrix} 0 & 0 \\ \frac{k_c}{m} & \frac{c_c}{m} \end{bmatrix}, \\ A_{p,2} &= \begin{bmatrix} 0 & 1 \\ -\frac{k}{m} & -\frac{c}{m} \end{bmatrix}, & A_{w,2} &= \begin{bmatrix} 0 & 0 \\ 0 & 0 \end{bmatrix}, \\ B_{p1,1} = B_{p1,2} &= \begin{bmatrix} 0 \\ \frac{1}{m} \end{bmatrix}, & B_{p2,1} = B_{p2,2} &= \begin{bmatrix} 0 \\ -\frac{1}{m} \end{bmatrix}, \\ C_{p1,1} = C_{p1,2} &= \begin{bmatrix} 1 & 0 \end{bmatrix}, & C_{w1,1} = C_{w1,2} &= \begin{bmatrix} -1 & 0 \end{bmatrix}. \end{aligned}$$

For simulation purpose, we have the following parameter setup:  $m = 2kg, k = k_c = 2N/m$  and  $c = c_c = 1N \cdot s/m$ . Moreover, we adopt the following switched exosystem to generate the reference trajectories that simulate the changing contact surface profile:

$$\begin{bmatrix} \dot{w}_1(t) \\ \dot{w}_2(t) \end{bmatrix} = A_{e,\sigma} \begin{bmatrix} w_1(t) \\ w_2(t) \end{bmatrix} + Q_\sigma d(t), \quad (3.30)$$

where the switching signal  $\sigma(t)$  obeys the same switching rule for the switched plant (3.29),

and the state-space matrices in (3.30) are

$$A_{e,1} = \begin{bmatrix} 0 & 1 \\ -0.01 & 0 \end{bmatrix}, \quad Q_1 = \begin{bmatrix} 0 \\ 0 \end{bmatrix},$$

$$A_{e,2} = \begin{bmatrix} 0 & 1 \\ -0.5 & 0 \end{bmatrix}, \quad Q_2 = \begin{bmatrix} 0.5 \\ 0 \end{bmatrix}.$$

Since the two tunable parameters  $\lambda_0$  and  $\mu$  are involved in the hybrid control synthesis process, it is desirable to elucidate their effects on the optimized weighted  $\mathcal{L}_2$  gain  $\gamma$  and determine suitable values for controller synthesis. To this end, we solve the optimization problem (3.27) by gridding the parameter space of  $(\lambda_0, \mu)$  within the region  $[0.2 : 0.02 : 2] \times [5 : 0.1 : 10]$ . The relations between  $(\lambda_0, \mu)$  and the optimized  $\gamma$  and the associated ADT constant  $\tau_a^* = \frac{\ln \mu}{\lambda_0}$  are shown in Fig. 3.2. It is observed from Fig. 3.2(a) that larger  $\mu$  would in general yield better  $\gamma$ ; while the optimal  $\gamma$  is located between  $\lambda_0 = 0.4$  and  $0.8$ . The effects of  $(\lambda_0, \mu)$  on the ADT constant  $\tau_a^*$  is more explicit, as seen in Fig. 3.2(b), increasing  $\mu$  and/or decreasing  $\lambda_0$  will result in larger  $\tau_a^*$ . This can also be reflected from the equation  $\tau_a^* = \frac{\ln \mu}{\lambda_0}$ .

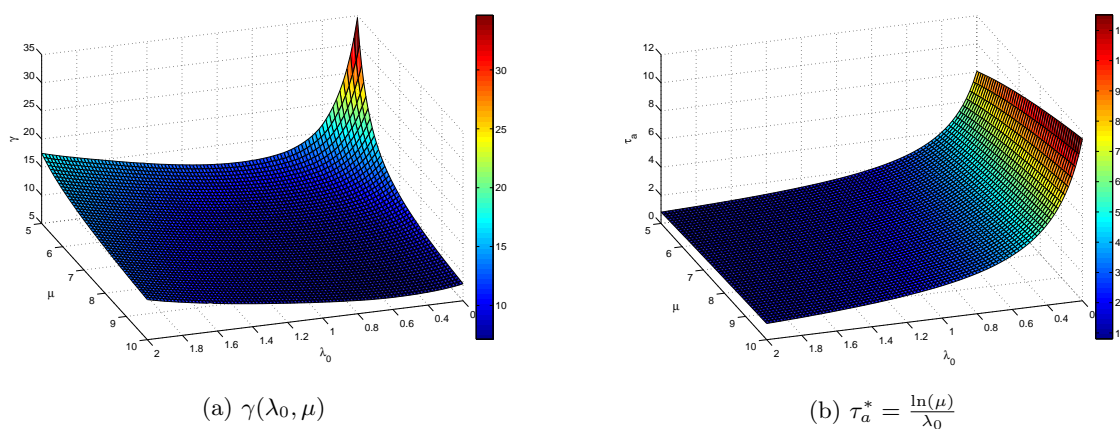


Figure 3.2: Relations between  $(\lambda_0, \mu)$  and optimized  $\gamma$  as well as  $\tau_a^*$ .

Based on these results, to balance the weighted  $\mathcal{L}_2$ -gain performance and the ADT constraint, we select  $\lambda_0 = 0.6$  and  $\mu = 10$  for the hybrid output regulator synthesis. Solving the optimization problem (3.27), it yields

$$\Pi_{p,1} = \Pi_{p,2} = \begin{bmatrix} 1 & 0 \\ 0 & 1 \end{bmatrix}, \quad \Gamma_1 = \begin{bmatrix} -1.98 & -1 \end{bmatrix}, \quad \Gamma_2 = \begin{bmatrix} -1 & -1 \end{bmatrix}.$$

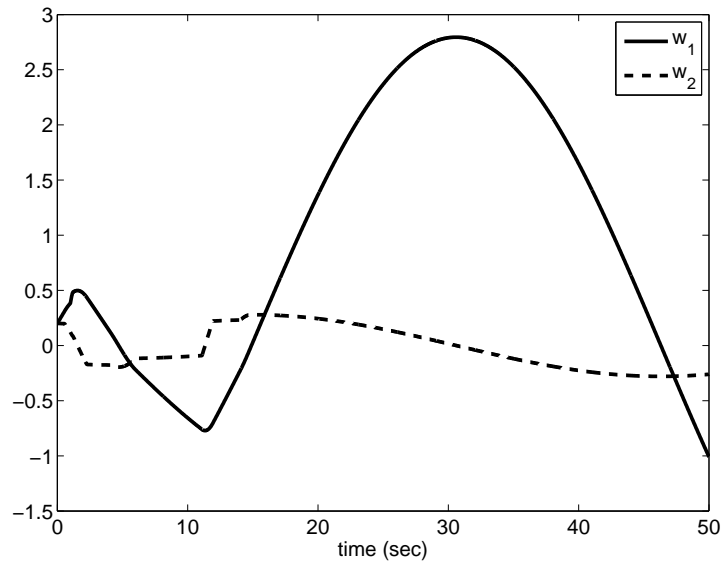
In order to avoid getting ill-conditioning matrices, we have also constrained the closed-loop poles within the circle  $|r + 10| \leq 10$ . The pole location constraint can be written as LMI conditions [11] and easily incorporated into the proposed hybrid synthesis process. The optimized weighted  $\mathcal{L}_2$  gain  $\gamma$  is  $\gamma = 2.7551$ . Finally, following the controller construction scheme in Theorem 4, we obtain hybrid controller gains as

$$\begin{aligned} A_{c,1} &= \begin{bmatrix} 0 & 1 & -1.2450 & -3.5261 & -10.2613 & 61.5338 \\ -0.01 & 0 & -1.4736 & -1.6176 & -13.1714 & 48.2543 \\ 0 & 0 & -9.2322 & -3.7521 & -12.9688 & 201.2147 \\ 0 & 0 & 0.3604 & -2.1797 & 0.1052 & -12.6183 \\ 0 & 0 & 0.0219 & -0.0072 & -2.0866 & -0.6709 \\ 0 & 0 & -0.0110 & 0.0031 & -0.0200 & -0.1666 \end{bmatrix}, & B_{c,1} &= \begin{bmatrix} -15.7401 \\ -16.9478 \\ -98.2614 \\ 5.3450 \\ 0.2943 \\ -0.2069 \end{bmatrix}, \\ C_{c,1} &= \begin{bmatrix} -1.9800 & -1 & 4.8462 & 5.1394 & 16.3808 & -157.8450 \end{bmatrix}, & D_{c,1} &= 56.8117, \\ J_{c,12} &= \begin{bmatrix} 1 & 0 & 0.0032 & -1.1167 & -1.0692 & 5.3265 \\ 0 & 1 & -0.0219 & -0.3831 & -5.2692 & -4.1407 \\ 0 & 0 & 0.9898 & 0.6723 & 1.8958 & -2.7775 \\ 0 & 0 & -0.0317 & -0.0190 & -0.0594 & 0.7010 \\ 0 & 0 & -0.0022 & -0.0018 & -0.0043 & -0.0307 \\ 0 & 0 & 0.0043 & 0.0053 & 0.0093 & 0.4392 \end{bmatrix}, \end{aligned}$$

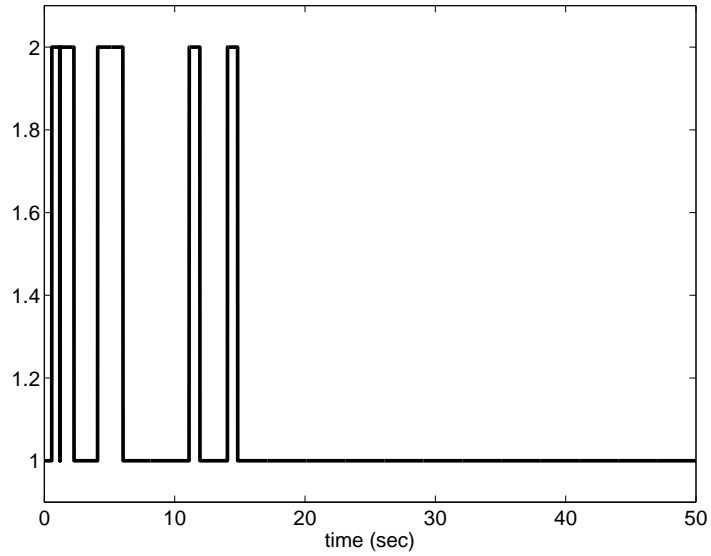
$$\begin{aligned}
A_{c,2} &= \begin{bmatrix} 0 & 1 & -1.2299 & -3.7208 & -10.8157 & 60.0411 \\ -0.5 & 0 & -1.2728 & -0.8475 & -14.5426 & 53.0860 \\ 0 & 0 & -9.1977 & -3.7732 & -15.2596 & 213.9712 \\ 0 & 0 & 0.3443 & -2.3529 & 0.7030 & -16.6330 \\ 0 & 0 & 0.0216 & 0.0119 & -2.4357 & -0.8818 \\ 0 & 0 & -0.0108 & 0.0032 & -0.0301 & -0.1286 \end{bmatrix}, \quad B_{c,2} = \begin{bmatrix} -15.2552 \\ -13.9506 \\ -97.3590 \\ 5.1535 \\ 0.3170 \\ -0.2023 \end{bmatrix}, \\
C_{c,2} &= \begin{bmatrix} -1 & -1 & 4.8370 & 4.1052 & 17.2548 & -166.8534 \end{bmatrix}, \quad D_{c,2} = 56.1634, \\
J_{c,21} &= \begin{bmatrix} 1 & 0 & -0.0173 & -1.1729 & -1.1401 & 3.0543 \\ 0 & 1 & 0.0688 & -0.2054 & -5.3365 & 14.3572 \\ 0 & 0 & 0.9624 & 0.6190 & 2.0741 & -11.9925 \\ 0 & 0 & -0.0215 & 0.0122 & -0.0639 & 5.5237 \\ 0 & 0 & 0.0090 & 0.0081 & 0.0192 & 0.1576 \\ 0 & 0 & 0.0043 & 0.0052 & 0.0078 & 0.3962 \end{bmatrix}.
\end{aligned}$$

For time-domain simulations, we choose perturbation  $d(t)$  as a periodic impulse starting from  $t = 1$  sec with 10 sec period, 0.1 sec pulse width and amplitude 1N. Then, with initial conditions  $x_p(0) = 0, x_c(0) = 0, w(0) = \begin{bmatrix} 0.2 & 0.2 \end{bmatrix}^T$ , we carry out the time-domain simulation using the synthesized hybrid output regulator. The simulation results are plotted in Fig. 3.3 through Fig. 3.4. Fig. 3.3(a) displays the reference trajectories generated by the switched linear exosystem (3.30), which cannot be obtained via a single model with a purely LTI configuration. The switching signal is also displayed in Fig. 3.3(b), which has 10 switches occurred during the entire time interval. Since the system operating duration is 50 sec, the actual average dwell-time is  $\tau_a = 50/10 = 5$  sec  $>$   $\tau_a^* = \frac{\ln(\mu)}{\lambda_0} = \frac{\ln(10)}{0.6} = 3.8376$  sec. Therefore, overall stability of the switched closed-loop system is guaranteed.

The system responses in Fig. 3.4 illustrate the performance of the proposed hybrid controller in maintaining the desired system output despite the presence of switching and perturbation  $d$ . As can be seen, the hybrid output regulator is indeed capable of rendering the overall switched



(a) exosystem states  $w(t)$



(b) switching signal  $\sigma(t)$

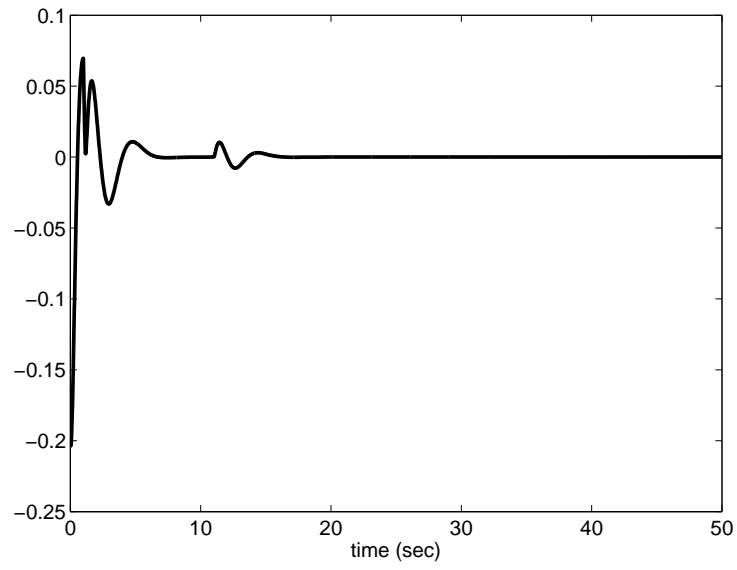
Figure 3.3: Exosystem states and switching signal.

system stable and suppress the effects of the persistent exosignal  $w$  and the unknown perturbation  $d$  on the error output  $e$ . Furthermore, the error output is regulated asymptotically to zero

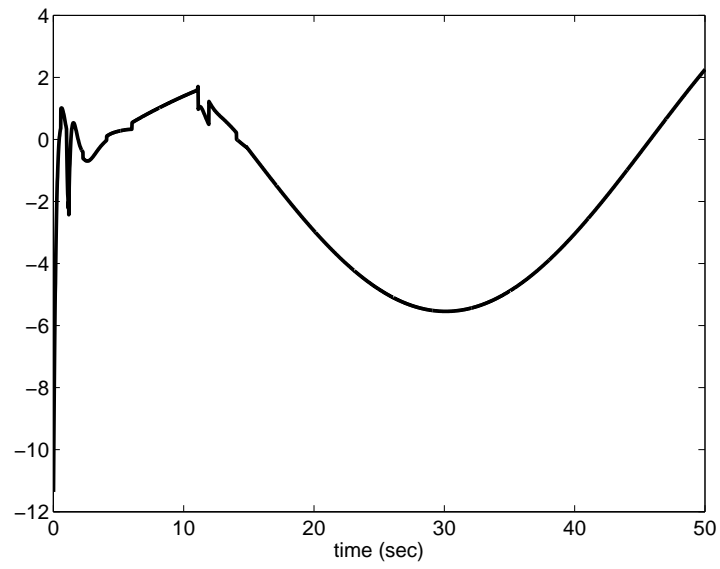
if the perturbation  $d(t) = 0$ , thus exact output regulation is achieved. On the other hand, the switched closed loop has smooth responses in both controlled output and control input (see Fig. 3.4) owing to the impulsive dynamics induced by the controller state jumps. This exemplifies the importance of controller reset in coping with switching events.

### 3.5 Summary

In this chapter, we have developed a new hybrid control approach for almost output regulation of switched linear systems. The proposed output feedback controller has a hybrid nature in the sense that the switching controller state undergoes an impulsive jump at each switching instant. Using the average dwell-time technique incorporated with multiple quadratic Lyapunov functions, the hybrid synthesis conditions are formulated as linear matrix equations plus a set of LMIs. This new hybrid control scheme provides an unified and more flexible framework for the output regulation of switched linear systems with switched exosystems. Its effectiveness has been illustrated through a mechanical system example.



(a) error output  $e(t)$



(b) control input  $u(t)$

Figure 3.4: Simulation results for the hybrid output regulation of the mechanical system (3.28).

## Chapter 4

# Robust Switched Feedforward Control of Uncertain LFT Systems

This chapter presents a new robust switched feedforward control scheme for a class of uncertain systems described in a standard linear fractional transformation (LFT) form. Firstly, the analysis conditions for switching stability are derived by using a piecewise Lyapunov function incorporated with the min-switching control technique. Based on the analysis results, the synthesis conditions are then formulated as a special type of bilinear matrix inequalities (BMIs), which can be solved by means of linear matrix inequalities (LMIs) and line search. Both robust  $\mathcal{H}_2$  and  $\mathcal{H}_\infty$  feedforward control problems are considered. The proposed robust switched control scheme outperforms existing robust feedforward control approaches for uncertain systems based on single quadratic Lyapunov function, and leads to less conservative control design. Numerical examples will be used to illustrate the effectiveness and advantages of the proposed results.

### 4.1 Introduction

In the two-degree-of-freedom control framework [92, 34, 53, 32], the control design tasks are in twofold: feedback control design and feedforward filter design. The main roles played by such

two control components are quite different. Specifically, the feedback control component, which is the only part affecting the overall closed-loop stability, is designed to (robustly) stabilize the open-loop system and to attenuate the influence of external disturbances, while the feedforward controller is usually introduced to reshape the time- or frequency-domain responses of the feedback closed loop to a reference input, such that improved tracking performance or enhanced disturbance rejection capability can be achieved. The validity and usefulness of such a two-degree-of-freedom control design approach has been demonstrated theoretically [53, 32, 43, 5], and through numerical simulations and practical applications [34, 22, 69]. In this paper, we will focus on feedforward controller design with a pre-specified feedback control part for a class of linear uncertain systems. For systems with perfectly known dynamics, the feedforward control problem is quite trivial as one can always find a feedforward controller through model-based inversion [16]. However, in the more realistic case when the controlled system is actually uncertain, such an inverse-based feedforward controller could result in a large degradation of performance [16]. This motivates the problem of designing robust feedforward controllers for various dynamical systems with uncertainties. Considerable interesting results on this topic have been reported in the literature, see for instance, [32, 69, 22, 79, 43]. In particular, [32] considered the robust feedforward control synthesis problem for a class of linear systems with time-invariant and time-varying structured uncertainties. In [69], the feedforward control problem was treated under a full-information control framework for a class of linear parameter-varying (LPV) systems with online measurable time-varying parameters. Further ramifications along this line mainly focus on the construction of different types of scalings/multipliers in the robust control problem. For instance, as an extension of [32, 22] and [79], Kose and Scherer [43] proposed a direct synthesis of robust feedforward filters by convex optimization for uncertainties described through dynamic integral quadratic constraints (IQCs) [60]. In spite of the rich literature, we observe that virtually all of the published results are obtained by using a single quadratic Lyapunov function, which could be conservative for systems with large uncertainties.

To overcome the limitations and potential conservatism encountered by the previous works

on robust feedforward control, we propose a new robust switched feedforward control scheme for a class of norm-bounded uncertain systems possessing a linear fractional transformation (LFT) representation by using a piecewise switched Lyapunov function [104, 67, 61, 70]. As opposed to the existing results where the robust feedforward controller is typically constructed as a linear time-invariant (LTI) system, the proposed robust switched feedforward controller composes multiple LTI controllers in a full-order dynamic form and a Lyapunov-based min-switching rule [67, 28] governing the switching among these controllers. The analysis conditions for both robust  $\mathcal{H}_2$  and  $\mathcal{H}_\infty$  performance are derived using a piecewise switched Lyapunov function incorporated with multiple scaling matrices (or multipliers) [110], respectively. In particular, it will be shown that the obtained Lyapunov-based  $\mathcal{H}_2$  analysis conditions recover those established in [30] using a single constant multiplier as a special case. Based on the analysis results, the synthesis conditions for robust switched feedforward control will be formulated in terms of a special type of matrix inequalities, which can be solved effectively by means of linear matrix inequalities (LMIs) and multi-dimensional search.

The contribution of this work lies in that a novel robust switched feedforward control scheme with minimal switching strategy is proposed for linear uncertain systems, it outperforms the robust control methods based on single quadratic Lyapunov function and leads to less conservative control design. Numerical examples will be used to demonstrate the effectiveness and advantages of the proposed design scheme.

The rest of this chapter is organized as follows. The problem statement and the structure of robust switched feedforward controller are presented in Section 4.2. Section 4.3 and Section 4.4 contain the main results of this chapter including the robust  $\mathcal{H}_2$  and  $\mathcal{H}_\infty$  analysis and control synthesis conditions, respectively. Simulation results on a ship steering control problem are provided in Section 4.5, and Section 4.6 summarizes the chapter.

## 4.2 Problem Statement

Consider a class of uncertain linear systems given in the following LFT form

$$\begin{bmatrix} \dot{x}_p \\ q \\ z \end{bmatrix} = \begin{bmatrix} A_p & B_{p0} & B_{p1} & B_{p2} \\ C_{p0} & D_{p00} & D_{p01} & D_{p02} \\ C_{p1} & D_{p10} & D_{p11} & D_{p12} \end{bmatrix} \begin{bmatrix} x_p \\ p \\ w \\ u \end{bmatrix}, \quad (4.1)$$

$$p = \Delta q$$

where  $x_p \in \mathbb{R}^n$  is the system state,  $u \in \mathbb{R}^{n_u}$  is the control input,  $z \in \mathbb{R}^{n_z}$  is the controlled (performance) output,  $w \in \mathbb{R}^{n_w}$  is the exogenous input signal which is assumed to be measurable for feed-forward control use, and  $p, q \in \mathbb{R}^{n_q}$  are internal variables (i.e., the pseudo-input and output). Throughout this chapter, we assume that the system matrix  $A_p$  is Hurwitz, which is a typical assumption of all works in feed-forward control area. Furthermore, it is also assumed that all the state-space matrices but  $\Delta \in \mathbb{R}^{n_q \times n_q}$  are known, and the LFT representation (4.1) is well-posed, i.e., the matrix  $I - D_{p00}\Delta$  is invertible for any bounded allowable parameter values of  $\Delta$ . Matrix  $\Delta$  represents the parametric norm-bounded time-varying uncertainty satisfying  $\|\Delta\| \leq 1$  and of the following spatial structure:

$$\Delta = \{diag\{\delta_1 I_{m_1}, \dots, \delta_s I_{m_s}, \Delta_{s+1}, \dots, \Delta_{s+f}\} : \delta_i \in \mathbb{R}, |\delta_i| \leq 1, i \in \mathbf{I}[1, s]; \Delta_{s+j} \in \mathbb{R}^{r_j \times r_j}, \|\Delta_{s+j}\| \leq 1, j \in \mathbf{I}[1, f]\}, \quad (4.2)$$

where  $\sum_{i=1}^s m_i + \sum_{j=1}^f r_j = n_q$ .

This LFT representation of uncertainty is widely used in robust control theory (for instance, in [8, 110] and the references cited therein). To handle robust stabilization and performance control problems, associated with the time-varying uncertainty  $\Delta$  in (4.2), we will introduce

the following scaling matrix set,

$$\begin{aligned} \mathbf{\Lambda} = \{ & \text{diag} \{ \Lambda_1, \dots, \Lambda_s, \lambda_{s+1} I_{r_1}, \dots, \lambda_{s+f} I_{r_f} \} : \\ & \Lambda_i \in \mathbb{S}_+^{m_i}, i \in \mathbf{I}[1, s]; \lambda_{s+j} \in \mathbb{R}_+, j \in \mathbf{I}[1, f] \}. \end{aligned} \quad (4.3)$$

Clearly, any  $\Lambda \in \mathbf{\Lambda}$  is commutable with  $\Delta$ , i.e.,  $\Lambda\Delta = \Delta\Lambda, \forall \Lambda \in \mathbf{\Lambda}$ .

In this chapter, our objective is to design a feed-forward controller robustly against the time-varying uncertainty  $\Delta$  so as to minimize the effects of the exogenous input signal  $w$  to the performance output signal  $z$ . We will construct a robust switched feed-forward (RSFF) controller in the following form:

$$\begin{aligned} \begin{bmatrix} \dot{x}_c \\ u \end{bmatrix} &= \begin{bmatrix} A_{c,\sigma} & B_{c,\sigma} \\ C_{c,\sigma} & D_{c,\sigma} \end{bmatrix} \begin{bmatrix} x_c \\ w \end{bmatrix} \\ \sigma &= \arg \min_{i \in \mathbf{I}[1, N_c]} x_c^T \bar{X}_i x_c \end{aligned} \quad (4.4)$$

where  $x_c \in \mathbb{R}^n$  is the switched controller state.  $\sigma$  is a switching rule depending on  $x_c$  in real time, it selects a particular sequence of sub-controllers among  $N_c$  available ones defined by  $\{A_{c,i}, B_{c,i}, C_{c,i}, D_{c,i}\}, i \in \mathbf{I}[1, N_c]$ . The switched controller gain matrices  $(A_{c,i}, B_{c,i}, C_{c,i}, D_{c,i})$  and Lyapunov matrices  $\bar{X}_i$  for all  $i \in \mathbf{I}[1, N_c]$  are appropriately dimensioned matrices to be determined.

The closed-loop system interconnecting the LFT plant (4.1) and the switched controller (4.4) can be written as follows.

$$\begin{aligned} \begin{bmatrix} \dot{x}_{cl} \\ q \\ z \end{bmatrix} &= \begin{bmatrix} A_{cl,\sigma} & B_{cl0,\sigma} & B_{cl1,\sigma} \\ C_{cl0,\sigma} & D_{cl00,\sigma} & D_{cl01,\sigma} \\ C_{cl1,\sigma} & D_{cl10,\sigma} & D_{cl11,\sigma} \end{bmatrix} \begin{bmatrix} x_{cl} \\ p \\ w \end{bmatrix}, \\ p &= \Delta q \end{aligned} \quad (4.5)$$

where  $x_{cl} = [x_p^T \ x_c^T]^T$ , the switching signal  $\sigma$  obeys the same rule as defined in (4.4), and for

any  $i \in \mathbf{I}[1, N_c]$ ,

$$\left[ \begin{array}{c|cc} A_{cl,i} & B_{cl0,i} & B_{cl1,i} \\ \hline C_{cl0,i} & D_{cl00,i} & D_{cl01,i} \\ C_{cl1,i} & D_{cl10,i} & D_{cl11,i} \end{array} \right] = \left[ \begin{array}{cc|cc} A_p & B_{p2}C_{c,i} & B_{p0} & B_{p1} + B_{p2}D_{c,i} \\ 0 & A_{c,i} & 0 & B_{c,i} \\ \hline C_{p0} & D_{p02}C_{c,i} & D_{p00} & D_{p01} + D_{p02}D_{c,i} \\ C_{p1} & D_{p12}C_{c,i} & D_{p10} & D_{p11} + D_{p12}D_{c,i} \end{array} \right]$$

In this chapter, two problems will be considered: the robust  $\mathcal{H}_2$  control; and the robust  $\mathcal{H}_\infty$  control. More precise descriptions about these two problems are given as follows.

**Problem 1.** *Given the uncertain LFT system (4.1). The robust  $\mathcal{H}_2$  control design objective is to determine matrices  $(A_{c,i}, B_{c,i}, C_{c,i}, D_{c,i}, \bar{X}_i)$  subject to (4.4), such that the switched closed-loop system in (4.5) is robustly asymptotically stable and achieves a minimal worst-case  $\mathcal{H}_2$  norm  $\gamma_2$  defined by*

$$\max_{\Delta} \sum_{k=1}^{n_w} \|z_k\|_2^2 < \gamma_2^2 \quad (4.6)$$

where for each  $k \in \mathbf{I}[1, n_w]$  the trajectory  $z_k$  is the outcome of the closed-loop system associated with the input  $w(t) = \eta_k \delta(t)$  with  $\eta_k \in \mathbb{R}^{n_w}$  being the  $k$ -th column of the  $n_w \times n_w$  identity matrix, and  $\delta(t)$  being the Dirac Delta function.

**Problem 2.** *Given the uncertain LFT system (4.1). The robust  $\mathcal{H}_\infty$  control design objective is to determine matrices  $(A_{c,i}, B_{c,i}, C_{c,i}, D_{c,i}, \bar{X}_i)$  subject to (4.4), such that the switched closed-loop system in (4.5) is robustly asymptotically stable and achieves a minimal worst-case  $\mathcal{H}_\infty$  norm  $\gamma_\infty$  defined by*

$$\max_{\Delta} \sup_{\|w\|_2 \neq 0} \frac{\|z\|_2}{\|w\|_2} < \gamma_\infty. \quad (4.7)$$

### 4.3 Robust $\mathcal{H}_2$ Control

In the section, we will consider the robust  $\mathcal{H}_2$  control design problem. Throughout this section, we assume that  $D_{p01} = 0, D_{p02} = 0, D_{p11} = 0$  and  $D_{p12} = 0$ . With this assumption, it renders the corresponding closed-loop matrices  $D_{cl01,i} = 0$  and  $D_{cl11,i} = 0$  in (4.5) for all  $i \in \mathbf{I}[1, N_c]$ . This is a typical assumption of all work in the area of  $\mathcal{H}_2$  control to ensure a meaningful and bounded  $\mathcal{H}_2$  norm.

#### 4.3.1 Robust $\mathcal{H}_2$ Analysis

Before proceeding to the study of the controller synthesis, we first present a sufficient condition for robust  $\mathcal{H}_2$  performance of the closed-loop system (4.5) in terms of a set of Riccati-Metzler inequalities by using a piecewise switched Lyapunov function.

**Theorem 5.** *Given a positive integer  $N_c$ , if there exist positive definite matrices  $P_i \in \mathbb{S}_+^{2n}$  and  $W_i \in \mathbb{S}_+^{n_w}$ , scaling matrix  $\Lambda_i \in \mathbf{\Lambda}$ , positive scalar  $\gamma_2 \in \mathbb{R}_+$ , and a Metzler matrix  $\Pi \in \mathcal{M}$  such that for all  $i \in \mathbf{I}[1, N_c]$  the following conditions hold.*

$$\begin{bmatrix} He\{P_i A_{cl,i}\} + \sum_{j=1}^{N_c} \pi_{ji} P_j & \star & \star & \star \\ B_{cl0,i}^T P_i & -\Lambda_i^{-1} & \star & \star \\ C_{cl0,i} & D_{cl00,i} & -\Lambda_i & \star \\ C_{cl1,i} & D_{cl10,i} & 0 & -I \end{bmatrix} < 0 \quad (4.8)$$

$$\begin{bmatrix} W_i & \star \\ P_i B_{cl1,i} & P_i \end{bmatrix} > 0 \quad (4.9)$$

$$tr(W_i) < \gamma_2^2 \quad (4.10)$$

Then, under the switching rule

$$\sigma = \arg \min_{i \in \mathbf{I}[1, N_c]} x_{cl}^T P_i x_{cl}, \quad (4.11)$$

the uncertain switched LFT system (4.5) is robustly stable and has its robust  $\mathcal{H}_2$  norm less than  $\gamma_2$  for all  $\Delta$  satisfying (4.2).

*Proof.* To prove asymptotic stability, we first consider the switched closed-loop system (4.5) with  $w = 0$ . Define the Lyapunov function  $V(x_{cl}) = \min_{i \in \mathbf{I}[1, N_c]} x_{cl}^T P_i x_{cl}$ , and assume without loss of generality that the index of currently active subsystem is  $i \in \mathbf{I}[1, N_c]$ . Then, we have

$$\begin{aligned} \dot{V} &= (A_{cl,i}x_{cl} + B_{cl0,i}p)^T P_i x_{cl} + x_{cl}^T P_i (A_{cl,i}x_{cl} + B_{cl0,i}p) \\ &= x_{cl}^T (A_{cl,i}^T P_i + P_i A_{cl,i}) x_{cl} + 2p^T B_{cl0,i}^T P_i x_{cl}. \end{aligned}$$

On the other hand, the feasibility of condition (4.8) implies via Schur complement that

$$\begin{aligned} &\begin{bmatrix} He\{P_i A_{cl,i}\} + \sum_{j=1}^{N_c} \pi_{ji} P_j & P_i B_{cl0,i} \\ B_{cl0,i}^T P_i & -\Lambda_{ji}^{-1} \end{bmatrix} + \begin{bmatrix} C_{cl0,i}^T \\ D_{cl00,i}^T \end{bmatrix} \Lambda_i^{-1} \begin{bmatrix} C_{cl0,i} & D_{cl00,i} \end{bmatrix} \\ &+ \begin{bmatrix} C_{cl1,i}^T \\ D_{cl10,i}^T \end{bmatrix} \begin{bmatrix} C_{cl1,i} & D_{cl10,i} \end{bmatrix} < 0, \quad \forall i \in \mathbf{I}[1, N_c]. \end{aligned}$$

Multiplying vector  $[x_{cl}^T \ p^T]^T$  from the right of the above matrices and its transpose to the left, we obtain

$$\begin{aligned} &x_{cl}^T (A_{cl,i}^T P_i + P_i A_{cl,i} + \sum_{j=1}^{N_c} \pi_{ji} P_j) x_{cl} + 2p^T B_{cl0,i}^T P_i x_{cl} \\ &+ q^T \Lambda_i^{-1} q - p^T \Lambda_i^{-1} p + z^T z < 0, \quad \forall i \in \mathbf{I}[1, N_c]. \end{aligned}$$

Substituting  $p = \Delta q$  into the above condition, and since  $\Lambda_i \in \mathbf{\Lambda}, \forall i \in \mathbf{I}[1, N_c]$  which implies

$\Lambda_i^{-1} \in \mathbf{\Lambda}, \forall i \in \mathbf{I}[1, N_c]$ , it yields for all  $\Delta$  that

$$\begin{aligned}
\dot{V} &< -x_{cl}^T \sum_{j=1}^{N_c} \pi_{ji} P_j x_{cl} - z^T z \\
&= -x_{cl}^T \sum_{j=1, j \neq i}^{N_c} \pi_{ji} (P_j - P_i) x_{cl} - z^T z \\
&\leq -z^T z \leq 0.
\end{aligned} \tag{4.12}$$

where the second inequality is obtained in light of the min-switching logic (4.11).

Now, we examine the value of  $V(x_{cl})$  at the switching instants. Suppose that a switching occurs at time instant  $t_s$  with  $t_s^-$  and  $t_s^+$  representing the time instants of pre- and post-switching, respectively. Then based on the min-switching strategy, switching occurs if and only if the following condition is satisfied,

$$\begin{aligned}
V(x_{cl}(t_s^+)) &= \min_{i \in \mathbf{I}[1, N_c]} x_{cl}^T(t_s^+) P_i x_{cl}(t_s^+) \\
&< \min_{i \in \mathbf{I}[1, N_c]} x_{cl}^T(t_s^-) P_i x_{cl}(t_s^-) = V(x_{cl}(t_s^-)).
\end{aligned}$$

This implies that the piecewise switched Lyapunov function  $V(x_{cl})$  is monotonically decreasing, which according to the Theorem 2.3 in [10] concludes the asymptotically stability of the switched system (4.5).

Furthermore, from (4.12), we have  $z^T z < -\dot{V}$ . Integrating both sides of this inequality from  $t = 0$  to  $\infty$  and taking into account that  $V(x_{cl}(\infty)) = 0$  from asymptotic stability of the switched system and the system evolves from the initial condition  $x_{cl}(0)$ , we obtain

$$\max_{\Delta} \int_0^{\infty} z^T(t) z(t) dt < \min_{i \in \mathbf{I}[1, N_c]} x_{cl}^T(0) P_i x_{cl}(0). \tag{4.13}$$

On the other hand, as we notice that the output  $z_k$  of the system (4.5) with zero initial condition and input  $w = \eta_k \delta$  can be alternatively determined from the response of the same system with zero input and initial condition  $x_{cl}(0) = B_{cl1,i} \eta_k$  for all  $k \in \mathbf{I}[1, n_w]$ , using the result in (4.13),

we have

$$\begin{aligned}
\max_{\Delta} \sum_{k=1}^{n_w} \|z_k\|_2^2 &= \max_{\Delta} \int_0^{\infty} z^T(t)z(t)dt \\
&\leq \sum_{k=1}^{n_w} \max_{\Delta} \|z_k\|_2^2 \\
&< \sum_{k=1}^{n_w} \min_{i \in \mathbf{I}[1, N_c]} (B_{cl1, i} \eta_k)^T P_i (B_{cl1, i} \eta_k) \\
&\leq \min_{i \in \mathbf{I}[1, N_c]} \sum_{k=1}^{n_w} (B_{cl1, i} \eta_k)^T P_i (B_{cl1, i} \eta_k) \\
&= \min_{i \in \mathbf{I}[1, N_c]} \text{tr}(B_{cl1, i}^T P_i B_{cl1, i}) \\
&< \min_{i \in \mathbf{I}[1, N_c]} \text{tr}(W_i) \\
&< \gamma_2^2.
\end{aligned}$$

The last two inequalities are deduced from conditions (4.9) and (4.10), respectively. This ends the proof.  $\square$

**Remark 7.** Note that the robust  $\mathcal{H}_2$  analysis condition (4.8) in Theorem 5 generalizes the corresponding analysis results in [30]. When all the scaling matrices  $\Lambda_i \in \mathbf{\Lambda}$ ,  $i \in \mathbf{I}[1, N_c]$  are specified as an identity, it will recover the analysis condition (18) of Lemma 1 in [30]. Furthermore, by enforcing  $N_c = 1$  and  $P_i = P$ ,  $W_i = W$ ,  $\Lambda_i = \Lambda$ , the results in Theorem 5 will specialize to a solution for robust  $\mathcal{H}_2$  feed-forward control of the uncertain system (4.1) based on a single quadratic Lyapunov function. The associated robust feed-forward controller can be constructed in the following LTI form

$$\begin{bmatrix} \dot{x}_c \\ u \end{bmatrix} = \begin{bmatrix} A_c & B_c \\ C_c & D_c \end{bmatrix} \begin{bmatrix} x_c \\ w \end{bmatrix} \quad (4.14)$$

Similar arguments concerning the generalization of the proposed results in this chapter also applies to the case of robust  $\mathcal{H}_\infty$  control that will be discussed in Section 4.4.

### 4.3.2 Robust $\mathcal{H}_2$ Controller Synthesis

Based on the analysis results in subsection 4.3.1, the synthesis problem of the switched feed-forward controller (4.4) with robust  $\mathcal{H}_2$  performance will be addressed in the subsection. The synthesis conditions will be formulated in terms of a special type of BMIs through variable transformation [75, 103], which can be solved by using the existing LMI solvers [8] coupled with a line search over scalar variables.

**Theorem 6.** *Given a positive integer  $N_c$ , if there exist positive definite matrices  $Y, S_i \in \mathbb{S}_+^n$  and  $W_i \in \mathbb{S}_+^{n_w}$ , scaling matrix  $\Lambda_i \in \mathbf{\Lambda}$ , rectangular matrices  $\hat{A}_{c,i} \in \mathbb{R}^{n \times n}$ ,  $\hat{B}_{c,i} \in \mathbb{R}^{n \times n_w}$ ,  $\hat{C}_{c,i} \in \mathbb{R}^{n_u \times n}$ ,  $\hat{D}_{c,i} \in \mathbb{R}^{n_u \times n_w}$ , positive scalar  $\gamma_2 \in \mathbb{R}_+$ , and a Metzler matrix  $\Pi \in \mathcal{M}$  such that for all  $i \in \mathbf{I}[1, N_c]$  the following conditions hold.*

$$\begin{bmatrix} He\{A_p Y\} & \star & \star & \star & \star & \star \\ \hat{A}_{c,i}^T + A_p Y & He\{A_p S_i + B_{p2} \hat{C}_{c,i}\} + \pi_{ii}(S_i - Y) & \star & \star & \star & \star \\ \Lambda_i B_{p0}^T & \Lambda_i B_{p0}^T & -\Lambda_i & \star & \star & \star \\ C_{p0} Y & C_{p0} S_i & D_{p00} \Lambda_i & -\Lambda_i & \star & \star \\ C_{p1} Y & C_{p1} S_i & D_{p10} \Lambda_i & 0 & -I & \star \\ 0 & S_{ji} & 0 & 0 & 0 & \Phi_{ji} \end{bmatrix} < 0 \quad (4.15)$$

$$\begin{bmatrix} W_i & \star & \star \\ B_{p1} + \hat{B}_{c,i} & Y & \star \\ B_{p1} + B_{p2} \hat{D}_{c,i} & Y & S_i \end{bmatrix} > 0 \quad (4.16)$$

$$tr(W_i) < \gamma_2^2 \quad (4.17)$$

where

$$\mathcal{S}_{ji} = \left[ \begin{array}{c} \vdots \\ \pi_{ji}(S_i - Y) \\ \vdots \end{array} \right] \Bigg\} N_c - 1, \quad \Phi_{ji} = \text{diag} \left\{ \overbrace{\cdots, \pi_{ji}(Y - S_j), \cdots}^{N_c - 1} \right\}, \quad \forall j \in \mathbf{I}[1, N_c] \text{ and } j \neq i \quad (4.18)$$

Then, the switched LFT system (4.5) is robustly stabilized by the switched feed-forward controller (4.4) and has its robust  $\mathcal{H}_2$  norm less than  $\gamma_2$  for all  $\Delta$  satisfying (4.2). Moreover, the coefficient matrices of the controller and the min-switching rule are given by

$$\begin{bmatrix} A_{c,i} & B_{c,i} \\ C_{c,i} & D_{c,i} \end{bmatrix} = \begin{bmatrix} M^T & -M^T B_{p2} \\ 0 & I \end{bmatrix} \begin{bmatrix} \hat{A}_{c,i} - A_p S_i & \hat{B}_{c,i} \\ \hat{C}_{c,i} & \hat{D}_{c,i} \end{bmatrix} \begin{bmatrix} (Y_i - S_i)^{-1} M^{-T} & 0 \\ 0 & I \end{bmatrix}, \quad (4.19)$$

$$\sigma = \arg \min_{i \in \mathbf{I}[1, N_c]} x_c^T \hat{X}_i x_c.$$

where  $M \in \mathbb{R}^{n \times n}$  is a nonsingular matrix and  $\bar{X}_i = M^{-1} Y^{-1} S_i (S_i - Y)^{-1} M^{-T}$ .

*Proof.* Based on Theorem 5, let  $Q_i = P_i^{-1}$  for all  $i \in \mathbf{I}[1, N_c]$ , then condition (4.8) is equivalent to the following via congruence transformation,

$$\begin{bmatrix} He\{A_{cl,i} Q_i\} + \sum_{j=1}^{N_c} \pi_{ji} Q_i P_j Q_i & \star & \star & \star \\ \Lambda_i B_{cl0,i}^T & -\Lambda_i & \star & \star \\ C_{cl0,i} Q_i & D_{cl00,i} \Lambda_i & -\Lambda_i & \star \\ C_{cl1,i} Q_i & D_{cl10,i} \Lambda_i & 0 & -I \end{bmatrix} < 0, \quad (4.20)$$

We specify

$$Q_i = \begin{bmatrix} S_i & N_i \\ N_i^T & N_i^T (S_i - Y)^{-1} N_i \end{bmatrix}, \quad Z_{1,i} = \begin{bmatrix} I & I \\ N_i^{-1} (Y - S_i) & 0 \end{bmatrix}, \quad Z_{2,i} = \begin{bmatrix} Y & S_i \\ 0 & N_i^T \end{bmatrix} \quad (4.21)$$

such that  $Q_i Z_{1,i} = Z_{2,i}$ , and let without loss of generality  $N_i = (Y - S_i) M$  with  $M \in \mathbb{R}^{n \times n}$

nonsingular. Then, we have

$$\begin{aligned}
Z_{1,i}^T Q_i Z_{1,i} &= Z_{1,i}^T Z_{2,i} = \begin{bmatrix} Y & Y \\ Y & S_i \end{bmatrix}, \\
Z_{1,i}^T Q_i P_j Q_i Z_{1,i} &= Z_{2,i}^T Z_{1,j} Z_{2,j}^{-1} Z_{2,i} = \begin{bmatrix} Y & Y \\ Y & Y + (S_i - Y)(S_j - Y)^{-1}(S_i - Y) \end{bmatrix}, \\
Z_{1,i}^T A_{cl,i} Q_i Z_{1,i} &= Z_{1,i}^T A_{cl,i} Z_{2,i} = \begin{bmatrix} A_p Y & \hat{A}_{c,i} \\ A_p Y & A_p S_i + B_{p2} \hat{C}_{c,i} \end{bmatrix}, \\
\Lambda_i B_{cl0,i}^T Z_{1,i} &= \begin{bmatrix} \Lambda_i B_{p0}^T & \Lambda_i B_{p0}^T \end{bmatrix}, \\
B_{cl1,i}^T Z_{1,i} &= \begin{bmatrix} B_{p1}^T + \hat{B}_{c,i}^T & B_{p1}^T + \hat{D}_{c,i}^T B_{p2}^T \end{bmatrix}, \\
C_{cl0,i} Q_i Z_{1,i} &= C_{cl0,i} Z_{2,i} = \begin{bmatrix} C_{p0} Y & C_{p0} S_i \end{bmatrix}, \\
C_{cl1,i} Q_i Z_{1,i} &= C_{cl1,i} Z_{2,i} = \begin{bmatrix} C_{p1} Y & C_{p1} S_i \end{bmatrix}
\end{aligned}$$

where

$$\begin{aligned}
\hat{A}_{c,i} &= A_p S_i + B_{p2} C_{c,i} M^T (Y - S_i) + M^{-T} A_{c,i} M^T (Y - S_i), \\
\hat{B}_{c,i} &= M^{-T} B_{c,i} + B_{p2} D_{c,i}, \\
\hat{C}_{c,i} &= C_{c,i} M^T (Y - S_i), \\
\hat{D}_{c,i} &= D_{c,i}.
\end{aligned} \tag{4.22}$$

Consequently, perform congruence transformation to condition (4.9) with matrices  $\text{diag}\{I, Z_{2,i}\}$ , we arrive at conditions (4.16). Again, perform congruence transformation to condition (4.20)



the LMI optimization techniques [8] plus multi-dimensional search over the scalar variables  $\pi_{ji}$  for all  $i, j \in \mathbf{I}[1, N_c]$ . Alternatively, it can be solved using the well-known path following method [35]. After obtaining the suboptimal solution in (4.24), the robust switched feed-forward controller can be subsequently constructed using (4.19).

## 4.4 Robust $\mathcal{H}_\infty$ Control

All the results for robust  $\mathcal{H}_2$  feed-forward control have counterparts for robust  $\mathcal{H}_\infty$  control. For  $\mathcal{H}_\infty$  control, we will consider the uncertain LFT plant (4.1), the switched controller (4.4), and the corresponding closed-loop system (4.5), all in their general form. Similar to the case of robust  $\mathcal{H}_2$  control, the robust  $\mathcal{H}_\infty$  analysis results will be first derived based on the Lyapunov Metzler inequality technique, upon which the associated synthesis conditions for robust  $\mathcal{H}_\infty$  control problem will be established.

### 4.4.1 Robust $\mathcal{H}_\infty$ Analysis

**Theorem 7.** *Given a positive integer  $N_c$ , if there exist positive definite matrices  $P_i \in \mathbb{S}_+^{2n}$ , scaling matrix  $\Lambda_i \in \mathbf{\Lambda}$ , positive scalar  $\gamma_\infty \in \mathbb{R}_+$ , and a Metzler matrix  $\Pi \in \mathcal{M}$  such that for all  $i \in \mathbf{I}[1, N_c]$  the following conditions hold.*

$$\begin{bmatrix} \text{He}\{P_i A_{cl,i}\} + \sum_{j=1}^{N_c} \pi_{ji} P_j & \star & \star & \star & \star \\ B_{cl0,i}^T P_i & -\Lambda_i^{-1} & \star & \star & \star \\ B_{cl1,i}^T P_i & 0 & -\gamma_\infty I & \star & \star \\ C_{cl0,i} & D_{cl00,i} & D_{cl01,i} & -\Lambda_i & \star \\ C_{cl1,i} & D_{cl10,i} & D_{cl11,i} & 0 & -\gamma_\infty I \end{bmatrix} < 0 \quad (4.25)$$

*Then, under the switching rule (4.11), the uncertain switched LFT system (4.5) is robustly stable and has its robust  $\mathcal{H}_\infty$  norm less than  $\gamma_\infty$  for all  $\Delta$  satisfying (4.2).*

*Proof.* Similar to the proof of Theorem 5, consider the switched closed-loop system (4.5). Define

the Lyapunov function  $V(x_{cl}) = \min_{i \in \mathbf{I}[1, N_c]} x_{cl}^T P_i x_{cl}$ , and assume without loss of generality that the index of currently active subsystem is  $i \in \mathbf{I}[1, N_c]$ . Then, we have

$$\begin{aligned} \dot{V} &= (A_{cl,i}x_{cl} + B_{cl0,i}p + B_{cl1,i}w)^T P_i x_{cl} + x_{cl}^T P_i (A_{cl,i}x_{cl} + B_{cl0,i}p + B_{cl1,i}w) \\ &= x_{cl}^T (A_{cl,i}^T P_i + P_i A_{cl,i}) x_{cl} + 2p^T B_{cl0,i}^T P_i x_{cl} + 2w^T B_{cl1,i}^T P_i x_{cl}. \end{aligned}$$

Feasibility of condition (4.25) implies via Schur complement that

$$\begin{aligned} &\begin{bmatrix} He\{P_i A_{cl,i}\} + \sum_{j=1}^{N_c} \pi_{j_i} P_j & P_i B_{cl0,i} & P_i B_{cl1,i} \\ B_{cl0,i}^T P_i & -\Lambda_i^{-1} & 0 \\ B_{cl1,i}^T P_i & 0 & -\gamma_\infty I \end{bmatrix} + \begin{bmatrix} C_{cl0,i}^T \\ D_{cl00,i}^T \\ D_{cl01,i}^T \end{bmatrix} \Lambda_i^{-1} \begin{bmatrix} C_{cl0,i} & D_{cl00,i} & D_{cl01,i} \end{bmatrix} \\ &+ \frac{1}{\gamma_\infty} \begin{bmatrix} C_{cl1,i}^T \\ D_{cl10,i}^T \\ D_{cl11,i}^T \end{bmatrix} \begin{bmatrix} C_{cl1,i} & D_{cl10,i} & D_{cl11,i} \end{bmatrix} < 0, \quad \forall i \in \mathbf{I}[1, N_c]. \end{aligned}$$

Multiplying vector  $[x_{cl}^T \ p^T \ w^T]^T$  from the right of the above matrices and its transpose to the left, we obtain

$$\begin{aligned} &x_{cl}^T (A_{cl,i}^T P_i + P_i A_{cl,i} + \sum_{j=1}^{N_c} \pi_{j_i} P_j) x_{cl} + 2p^T B_{cl0,i}^T P_i x_{cl} + 2w^T B_{cl1,i}^T P_i x_{cl} \\ &+ q^T \Lambda_i^{-1} q - p^T \Lambda_i^{-1} p + \frac{1}{\gamma_\infty} z^T z - \gamma_\infty w^T w < 0, \quad \forall i \in \mathbf{I}[1, N_c]. \end{aligned}$$

Substituting  $p = \Delta q$  into the above condition, and since  $\Lambda_i \in \mathbf{\Lambda}, \forall i \in \mathbf{I}[1, N_c]$  which implies

$\Lambda_i^{-1} \in \mathbf{\Lambda}, \forall i \in \mathbf{I}[1, N_c]$ , it yields for all  $\Delta$ ,

$$\begin{aligned}
\dot{V} &< -x_{cl}^T \sum_{j=1}^{N_c} \pi_{ji} P_j x_{cl} - \frac{1}{\gamma_\infty} z^T z + \gamma_\infty w^T w \\
&= -x_{cl}^T \sum_{j=1, j \neq i}^{N_c} \pi_{ji} (P_j - P_i) x_{cl} - \frac{1}{\gamma_\infty} z^T z + \gamma_\infty w^T w \\
&\leq -\frac{1}{\gamma_\infty} z^T z + \gamma_\infty w^T w.
\end{aligned} \tag{4.26}$$

When  $w = 0$ , we have  $\dot{V} < 0$ , and similar arguments as given in the proof for Theorem 5 can be applied here to conclude the monotonically decreasing property of the Lyapunov function  $V(x_{cl})$ , which proves the asymptotic stability of the closed-loop system.

On the other hand, integrating both sides of (4.26) from  $t = 0$  to  $\infty$  and taking into account that  $V(x_{cl}(0)) = 0$  under zero initial condition, and  $V(x_{cl}(\infty)) \geq 0$ , we conclude that  $\|z\|_2 < \gamma_\infty \|w\|_2$ .  $\square$

#### 4.4.2 Robust $\mathcal{H}_\infty$ Controller Synthesis

Based on the analysis results derived in subsection 4.4.1, the synthesis problem of the switched disturbance feed-forward controller (4.4) with robust  $\mathcal{H}_\infty$  performance will be addressed in the subsection.

**Theorem 8.** *Given a positive integer  $N_c$ , if there exist positive definite matrices  $Y, S_i \in \mathbb{S}_+^n$ , scaling matrix  $\Lambda_i \in \mathbf{\Lambda}$ , rectangular matrices  $\hat{A}_{c,i} \in \mathbb{R}^{n \times n}, \hat{B}_{c,i} \in \mathbb{R}^{n \times n_w}, \hat{C}_{c,i} \in \mathbb{R}^{n_u \times n}, \hat{D}_{c,i} \in \mathbb{R}^{n_u \times n_w}$ , positive scalar  $\gamma_\infty \in \mathbb{R}_+$ , and a Metzler matrix  $\Pi \in \mathcal{M}$  such that for all  $i \in \mathbf{I}[1, N_c]$*

the following conditions hold.

$$\begin{bmatrix}
He\{A_p Y\} & * & * & * & * & * & * \\
\hat{A}_{c,i}^T + A_p Y & \left\{ \begin{array}{l} He\{A_p S_i + B_{p2} \hat{C}_{c,i}\} \\ + \pi_{ii}(S_i - Y) \end{array} \right\} & * & * & * & * & * \\
\Lambda_i B_{p0}^T & \Lambda_i B_{p0}^T & -\Lambda_i & * & * & * & * \\
B_{p1}^T + \hat{B}_{c,i}^T & B_{p1}^T + \hat{D}_{c,i}^T B_{p2}^T & 0 & -\gamma_\infty I & * & * & * \\
C_{p0} Y & C_{p0} S_i + D_{p02} \hat{C}_{c,i} & D_{p00} \Lambda_i & D_{p01} + D_{p02} \hat{D}_{c,i} & -\Lambda_i & * & * \\
C_{p1} Y & C_{p1} S_i + D_{p12} \hat{C}_{c,i} & D_{p10} \Lambda_i & D_{p11} + D_{p21} \hat{D}_{c,i} & 0 & -\gamma_\infty I & * \\
0 & S_{ji} & 0 & 0 & 0 & 0 & \Phi_{ji}
\end{bmatrix} < 0, \tag{4.27}$$

$$\begin{bmatrix}
Y & * \\
Y & S_i
\end{bmatrix} > 0, \tag{4.28}$$

where  $S_{ji}$  and  $\Phi_{ji}$  are defined by (4.18) for all  $i, j \in \mathbf{I}[1, N_c]$  and  $j \neq i$ . Then, the switched LFT system (4.5) is robustly stabilized by the switched feed-forward controller (4.4) and has its robust  $\mathcal{H}_\infty$  norm less than  $\gamma_\infty$  for all  $\Delta$  satisfying (4.2). Moreover, the coefficient matrices of the controller and the min-switching rule are given by (4.19).

*Proof.* The proof can be immediately completed by following a similar line as the proof for robust  $\mathcal{H}_2$  control in Theorem 6 (based on the variable transformation method).  $\square$

Similar to the case of robust  $\mathcal{H}_2$  control, Theorem 8 provides sufficient conditions for robust  $\mathcal{H}_\infty$  switched control. The suboptimal control solution to the robust  $\mathcal{H}_\infty$  control problem can be obtained by solving the following BMI optimization problem:

$$\begin{aligned}
& \min_{Y, S_i, \Lambda_i, \hat{A}_{c,i}, \hat{B}_{c,i}, \hat{C}_{c,i}, \hat{D}_{c,i}, \Pi, \forall i \in \mathbf{I}[1, N_c]} \gamma_\infty \\
& \text{s.t.} \quad (4.27)-(4.28)
\end{aligned} \tag{4.29}$$

Again, the LMI-based optimization techniques in [8] with multi-dimensional search, or the path-following method in [35] can be applied to solve such a special type of BMI optimization problem. Afterwards, the robust switched feed-forward controller gains will be constructed from (4.19).

**Remark 8.** *It is worth pointing out that due to the products of the variables  $\Pi$  and  $\{Y, S_i\}$  for all  $i \in \mathbf{I}[1, N_c]$ , the optimization problems (4.24) for  $\mathcal{H}_2$  control and (4.29) for  $\mathcal{H}_\infty$  control are by nature non-convex, solving this type of non-convex optimization problems may be computationally expensive. One way to obtain a simpler, although certainly more conservative, version of optimization with LMI constraints is to consider a special Metzler matrix  $\Pi$  with the same diagonal elements [28], i.e.,  $\pi_{ii} = \pi$ ,  $i \in \mathbf{I}[1, N_c]$ . The simplified optimization problem could be relatively easier to solve using LMIs plus a line search. Interested readers are referred to [28] for more detailed discussions along this line.*

## 4.5 Examples

In this section, two examples will be used to demonstrate the effectiveness and usefulness of the theoretical results. Specifically, the first example is concerned about the robust  $\mathcal{H}_2$  control problem, while the proposed robust switched feed-forward control scheme will be applied to solve the robust  $\mathcal{H}_\infty$  feed-forward control problem for a ship steering system in the second example.

### 4.5.1 A Numerical Example

Consider an uncertain LFT system in the form of (4.1) with the nominal system matrices given by

$$\begin{aligned}
 A_p &= \begin{bmatrix} -5 & 2 & -1 \\ -2 & -10 & -1 \\ -13 & 11 & -7 \end{bmatrix}, & B_{p0} &= \begin{bmatrix} 1 & -1 \\ 3 & 0.5 \\ -2 & -2 \end{bmatrix}, & B_{p1} &= \begin{bmatrix} -1 \\ 0.5 \\ 1 \end{bmatrix}, & B_{p2} &= \begin{bmatrix} 0 \\ 0.5 \\ 0 \end{bmatrix}, \\
 C_{p0} &= \begin{bmatrix} 1 & -0.2 & 0.5 \\ 0.2 & 0 & 1 \end{bmatrix}, & D_{p00} &= \begin{bmatrix} -0.1 & 0.5 \\ 0.5 & 0.1 \end{bmatrix}, & D_{p01} &= D_{p02} = \begin{bmatrix} 0 \\ 0 \end{bmatrix}, \\
 C_{p1} &= \begin{bmatrix} 1 & 1 & 1 \end{bmatrix}, & D_{p10} &= \begin{bmatrix} 0.1 & 0 \end{bmatrix}, & D_{p11} &= D_{p12} = 0.
 \end{aligned} \tag{4.30}$$

The parametric uncertainty  $\Delta \in \mathbb{R}^{2 \times 2}$  is assumed to be in the form of  $\delta I_2$  satisfying  $|\delta| \leq 1$ .

In this example, we will consider the robust  $\mathcal{H}_2$  control problem. The synthesis results using the proposed RSFF control design scheme with different values of  $N_c$  are listed in Table 4.1. All the results are obtained through a two-step procedure: First solve the optimization problem (4.24) via multi-dimensional search to yield a suboptimal control solution; Then conduct a post-design analysis on the resulting closed loop using the analysis conditions in Theorem 5. Note that when  $N_c = 0$ , it stands for the case of pure feedback control (without using feed-forward controller); and  $N_c = 1$  represents the case of using a single LTI feed-forward controller (as discussed in Remark 7). As expected, it is observed that using single LTI feedforward controller in the case of  $N_c = 1$  provides better performance than that obtained in the case of  $N_c = 0$  without using feedforward control. Furthermore, compared to both cases of  $N_c = 0$  and  $N_c = 1$ , the newly proposed RSFF control approach with  $N_c = 2$  through  $N_c = 4$  is capable to provide better performance measured by the  $\mathcal{H}_2$  norm  $\gamma_2$ , although it consumes more computational power because more decision variables involved in the optimization process. On the other hand, as the number of  $N_c$  increases from 2 to 4, the respective optimized  $\mathcal{H}_2$  norms are essentially the same. The small difference between their calculated performance values is mainly due to

numerical accuracy.

Table 4.1: Optimized robust  $\mathcal{H}_2$  norms (Example 1).

$N_c$	0	1	2	3	4
$\gamma_2^2$	1.2148	0.2475	0.0376	0.0376	0.0375
# of decision variables	10	32	62	101	150

We also compare the control performance via time domain simulation of three different control strategies: (i) “FB Control” using pure feedback control; (ii) “Single FF + FB” combining single feedforward controller with feedback control; and (iii) “Switched FF + FB” applying the proposed switched feedforward control with feedback control. The time-domain simulation is

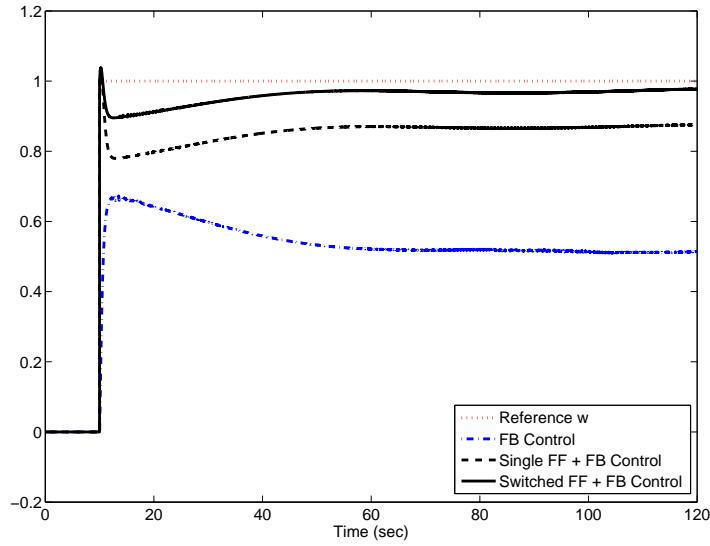


Figure 4.1: Tracking performance comparison (Example 1).

conducted under zero initial conditions with  $\delta = \cos(2t)$ . The resulting tracking responses to a unit step input are plotted in Fig. 4.1. It is clearly seen that the proposed RSFF control indeed

outperforms the other two control strategies. Moreover, only one switching event from value 1 to 2 for the switching signal of the RSFF controller occurred at time  $t = 10$  sec.

#### 4.5.2 Application to A Ship Steering Problem

In the second example, to demonstrate the usefulness of the proposed feed-forward control scheme, we focus on the ship steering problem as discussed in [86, 42]. The open-loop dynamics of the ship steering system can be approximated by the following model

$$\ddot{\psi}(t) = av(t)\dot{\psi}(t) + bv^2(t)\delta(t)$$

where  $\psi$  denotes the heading of the ship,  $\delta$  denotes the rudder angle as control input, and  $v$  is the speed of the ship satisfying  $v(t) = v_0 + \mathcal{V}\cos(w_0t)$ . Define  $x_1 = \psi$  and  $x_2 = \dot{\psi}$ , this open-loop model can be written as an uncertain system in LFT form

$$\mathcal{P} : \begin{bmatrix} \dot{x}_1 \\ \dot{x}_2 \\ q \\ y \end{bmatrix} = \begin{bmatrix} 0 & 1 & 0 & 0 & 0 \\ 0 & av_0 & 1 & 0 & bv_0^2 \\ \hline 0 & a\mathcal{V} & 0 & 1 & 2bv_0\mathcal{V} \\ 0 & 0 & 0 & 0 & b\mathcal{V}^2 \\ \hline 1 & 0 & 0 & 0 & 0 \end{bmatrix} \begin{bmatrix} x_1 \\ x_2 \\ p \\ \delta \end{bmatrix}$$

$$p = \Delta q$$

where  $\Delta := \cos(w_0t)I_2$  denotes the uncertain parameter.

The ship steering control design problem will be treated under a standard two-degree of freedom control structure for servo systems [15] as shown in Fig. 4.2, where  $K$  represents a feedback controller acts on the error signal  $z := \psi_{ref} - \psi$ . For numerical purpose, we assume a simple stabilizing PID feedback controller  $K$  with the following approximation

$$K(s) = k_p + k_i \frac{1}{s} + k_d \frac{s}{0.01s + 1}.$$

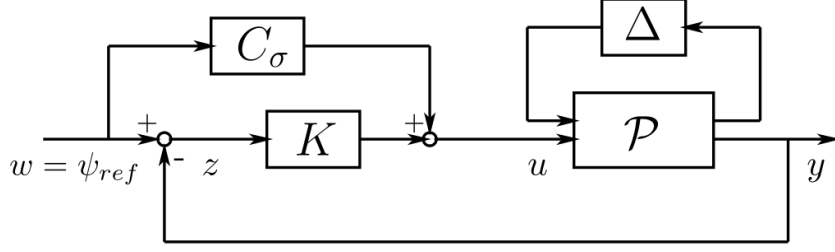


Figure 4.2: Control diagram for the ship steering problem (Example 2).

Our objective is to design an additional feed-forward controller  $C_\sigma$  by using the proposed RSFF design scheme so as to minimize the  $\mathcal{H}_\infty$  norm from  $w$  to  $z$ . To fit into the proposed RSFF control framework, the uncertain LFT system in the form of (4.1) used for feed-forward control synthesis can be obtained by absorbing the feedback controller  $K$  into the open-loop plant, which results in an augmented uncertain plant with

$$\begin{aligned}
 A_p &= \begin{bmatrix} 0 & 1 & 0 & 0 \\ -bv_0^2(k_p + 100k_d) & av_0 & bv_0^2(k_i - 10000k_d) & 100bv_0^2k_i \\ -1 & 0 & -100 & 0 \\ 0 & 0 & 1 & 0 \end{bmatrix}, \\
 \left[ \begin{array}{ccc|cc} B_{p0} & B_{p1} & B_{p2} \end{array} \right] &= \left[ \begin{array}{ccc|cc} 0 & 0 & 0 & 0 \\ 1 & 0 & bv_0^2(k_p + 100k_d) & bv_0^2 \\ 0 & 0 & 1 & 0 \\ 0 & 0 & 0 & 0 \end{array} \right], \\
 \left[ \begin{array}{c} C_{p0} \\ C_{p1} \end{array} \right] &= \left[ \begin{array}{cccc} -2bv_0\mathcal{V}(k_p + 100k_d) & a\mathcal{V} & 2bv_0\mathcal{V}(k_i - 10000k_d) & 200bv_0\mathcal{V}k_i \\ -b\mathcal{V}^2(k_p + 100k_d) & 0 & b\mathcal{V}^2(k_i - 10000k_d) & 100b\mathcal{V}^2k_i \\ \hline -1 & 0 & 0 & 0 \end{array} \right],
 \end{aligned}$$

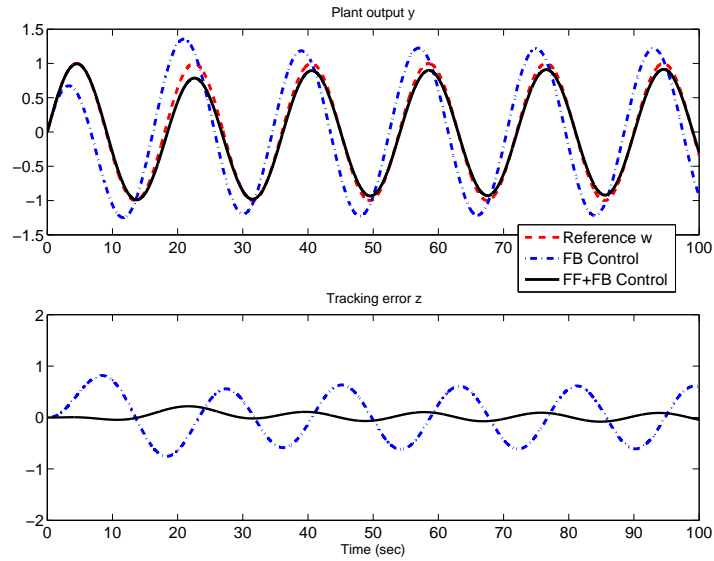
$$\begin{bmatrix} D_{p00} & D_{p01} & D_{p02} \\ D_{p10} & D_{p11} & D_{p12} \end{bmatrix} = \left[ \begin{array}{cc|cc} 0 & 1 & 2bv_0\mathcal{V}(k_p + 100k_d) & 2bv_0\mathcal{V} \\ 0 & 0 & b\mathcal{V}^2(k_p + 100k_d) & b\mathcal{V}^2 \\ \hline 0 & 0 & 1 & 0 \end{array} \right].$$

With the parameter selections  $a = -1, b = 0.8, v_0 = 3, \mathcal{V} = 0.85$  and  $k_p = 0.05, k_i = 0.01, k_d = 0$ , the achievable  $\mathcal{L}_2$  gains for changing number of sub-controllers  $N_c$  that we obtain via a similar two-step procedure as in Example 1 with correspondence to the optimization problem (4.29) and Theorem 7 are listed in Table 4.2. Similar to the first example, due to the extra degrees of freedom provided by more free variables in the proposed RSFF design framework, including the Metzler matrix variables  $\pi_{ji}$ , the multiple Lyapunov function matrix variables  $S_i$  and the multiple scaling matrix variables  $\Lambda_i$  for all  $i \in \mathbf{I}[1, N_c]$ , the proposed robust switched synthesis approach provides less conservative results than those obtained in both cases of without using feed-forward control and using a single LTI feed-forward control. Furthermore, as  $N_c$  increases, the performance bounds are further improved.

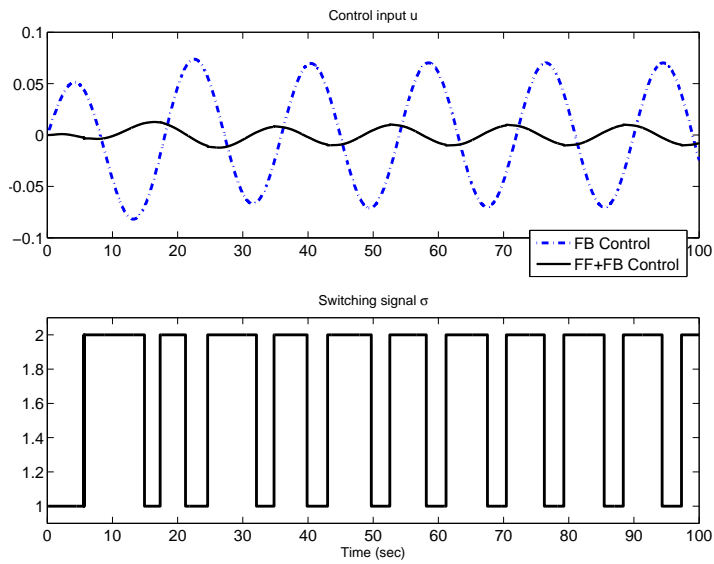
Table 4.2: Optimized robust  $\mathcal{H}_\infty$  norms (Example 2).

$N_c$	0	1	2	3	4	5
$\gamma_\infty$	2.8915	1.4382	1.1568	1.0947	1.0807	1.0459
# of decision variables	14	49	91	134	179	226

For time-domain simulation, we select  $N_c = 2$  for the proposed  $\mathcal{H}_\infty$  RSFF control synthesis. The simulation results with zero initial conditions and  $w(0) = 0.2$  are shown in Fig. 4.3, where the reference input signal is chosen as a sinusoid input satisfying  $w = \sin(20t)$ . As can be seen, compared to the case of pure feedback control, the proposed RSFF controller provides much better tracking control performance (see Fig. 4.3(a)) with largely reduced control efforts (see Fig. 4.3(b)). The switching signal involved is also plotted in Fig. 4.3(b) to show the control effectiveness.



(a) Tracking performance



(b) Control force and switching signal

Figure 4.3: Time-domain simulation of robust feed-forward control (Example 2).

## 4.6 Summary

A new robust switched feedforward control scheme has been presented for a class of uncertain LFT systems. The proposed robust switched feedforward controller consists of multiple LTI

feedforward controllers and a min-switching rule that governs the switching among them. The synthesis conditions that guarantee robust  $\mathcal{H}_2$  and  $\mathcal{H}_\infty$  performance are derived and formulated in terms of BMIs, respectively, which can be solved effectively using LMI-based optimization coupled with multi-dimensional search over the scalar variables. The proposed approach utilizes a piecewise Lyapunov function with multiple multipliers to reduce the conservatism of robust feedforward filtering methods based on single Lyapunov function and/or single constant multiplier. It has been demonstrated through numerical examples that performance improvements have been gained with a price of solving a computationally more-expensive non-convex BMI problem with more optimization variables. The proposed switching control design scheme can be easily extended to more general uncertain systems with IQCs using dynamic scalings/multipliers [77].

# Chapter 5

## Conclusion

### 5.1 Dissertation Contributions and Concluding Remarks

In this dissertation, our general goal is to develop systematic and unified design schemes for output-feedback control synthesis of hybrid switched control systems. To be more specific, we have developed new hybrid impulsive switching controller structures that simultaneously yield optimal controlled performance and computationally tractable synthesis conditions for three important control problems, directed at different engineering applications.

1. In the first part, we considered the gain-scheduling  $\mathcal{H}_\infty$  output-feedback control problem for a pitch-axis missile dynamic systems. In order to pursue stringent controlled performance with easy-to-implement control algorithms, the original nonlinear missile dynamics is formulated as a switched LFT parameter-dependent system such that advanced gain-scheduling switching techniques can be applied under the multiple quadratic Lyapunov functions framework. Based on this system setup, a new hybrid gain-scheduling missile autopilot is proposed, which consists of a standard switching output-feedback LFT controller and a supervisor monitoring the switching behavior of the plant and enforcing a reset/jump dynamics to the controller states once switching occurs. Both full-order and reduced-order hybrid output-feedback control problems are addressed under a unified

framework. Under this novel hybrid missile autopilot structure, it has been shown that the proposed design method advances existing missile control methods in three important ways:

- The associated control synthesis conditions that guarantee weighted  $\mathcal{L}_2$  stability performance are formulated in terms of a finite number of LMIs. As a result, the optimal control solution can be readily obtained by solving a convex optimization problem without taking the involved gridding and post-analysis procedures that are typically required in most existing LPV design techniques.
  - Stringent controlled performance are achieved without utilizing scheduling parameter variations in both controller synthesis and implementation processes.
  - For reduced-order hybrid control, the controller state order is always equal to that of the missile plant state regardless what type and how many performance weighting functions are employed. This would largely simplify the implementation of missile autopilot in practice, especially when more complicated weighting functions are employed for more stringent performance goals.
2. The second part of the dissertation considers a more complicated control design problem, i.e., mixed  $\mathcal{H}_\infty$  and output regulation control of switched linear dynamics subject to switched exosignals. Specifically, both controlled plant and exosystem are described by switched linear models. The control objective specifies not only closed-loop stability, but also tracking/rejection of persistent references/disturbances generated by multiple linear exosystems. A new impulsive switching control approach has been proposed to address this problem. The proposed hybrid output regulator is constructed as an impulsive switching system, where the controller states will undergo impulsive jumps at each switching instant. Based on the ADT switching technique and MLFs design framework, the hybrid synthesis conditions are formulated in terms of LMIs plus linear matrix equations, which can be solve effectively via convex optimization. Furthermore, the proposed hybrid control

method has been applied to solve the hybrid output regulation problem for a mechanical system. Compared to existing results, the novelties of the proposed hybrid output regulation design scheme include:

- *Technical Novelty:* A new hybrid controller structure and a new coordinate transformation technique, i.e., the multiple coordinate transformation (MCT), are proposed to overcome several technical difficulties encountered in existing hybrid output regulation literatures.
  - *Practical Novelty:* First, the exosignals (containing the reference trajectories to track) are generated by a switched linear system consisting of multiple linear models, which would render more sophisticated exosignals and enhance the control system capability. Second, we consider a more realistic system setup, i.e., unknown perturbations are allowed to affect both controlled plant and the exosystem, and almost output regulation can be achieved under the proposed design framework.
3. The last part of this dissertation research has focused on the two-degree-of-freedom robust control problem for a class of uncertain systems described in a standard LFT form. A new robust switched feedforward control scheme has been proposed. Firstly, analysis conditions for switching stability are derived by using a piecewise Lyapunov function incorporated with the min-switching control technique. Based on the analysis results, the control synthesis conditions are then formulated as a special type of BMIs involving multiplications between scalar and matrix variables, which can be solved by means of LMIs coupled with a line search. Both robust  $\mathcal{H}_2$  and  $\mathcal{H}_\infty$  feedforward control problems are considered under a unified framework. Numerical examples have been used to demonstrate the effectiveness and advantages of the proposed robust switched control design approach. In particular, its usefulness has also been demonstrated through a real-world application of the tracking control problem for a ship steering system. As opposed to the existing methods where the robust feedforward controller is typically constructed as an LTI system, the proposed

robust switched feedforward controller composes multiple LTI controllers in a full-order dynamic form and a Lyapunov-based min-switching rule governing the switching among there controllers. The novel contributions of these results are:

- A new robust switched control scheme is proposed to handle robust feedforward stabilization and performance optimization problems for uncertain LFT systems by using a piecewise Lyapunov function and multiple scalings/multipliers, such that both robust  $\mathcal{H}_2$  and  $\mathcal{H}_\infty$  control problems are addressed under a systematic and unified design framework. It has been demonstrated both theoretically and through numerical simulations that the proposed robust switched control scheme outperforms the existing robust control methods based on single quadratic Lyapunov function and/or single constant multiplier, and leads to less conservative control design.

## 5.2 Future Work

Besides the results presented in this dissertation, the following discussion provides some remaining issues as well as promising directions that are worth to be further pursued in the future.

1. *Robust Switching Output-Feedback Control for Systems with Large Uncertainties.*

Recent trends in modern engineering control practice, such as high-precision control systems and wide-range flight control systems, show the growing demand of effective control solutions to achieve stringent performance requirements, while at the same time maintain robustness against unavoidable large uncertainties in the systems. Conventional robust control schemes of designing a single stabilizing controller to cover the entire set of uncertainties may no longer be a feasible solution in this case. To complement the research on feedforward robust switching control in Chapter 4 of this dissertation, we plan to further investigate the robust switching output-feedback control synthesis problem for systems with large uncertainties.

Specifically, in order to overcome the limitations in conventional robust control, we plan to develop new mathematical techniques for high-performance robust switching control designs. To this end, two promising directions are worth to be pursued:

- *Lyapunov-based min-switching robust control*: The basic idea of this method is to partition the entire system state space into finite number of subregions, and assign each individual subregion with a Lyapunov function and an associated controller, then switch among these individual controllers online based on the evolution of the system trajectory [107]. Switching stability can be guaranteed by using the min-switching technique and the piecewise switching Lyapunov function from the switching control theory. Two potential technical issues of this method include: (1) The min-switching logic usually requires full information of the system states to instantaneously calculate and compare the Lyapunov function values so as to decide which controller should be active at each time instant; (2) The synthesis problem of min-switching controllers is typically a non-convex optimization problem, which could be very difficult to solve. Research along this direction should first focus on solving these two technical issues.
- *Multiple controllers via uncertainty set division*: Different from the first method to partition the system state space, this approach will divide the model uncertainty set into finite numbers of subsets. For uncertain plants in each subset, a controller is specialized to achieve robust performance. This approach aims to improve the closed-loop performance by employing multiple controllers with each robustly against a small subset of the model uncertainty, rather than using a single robust controller for the entire set. Two critical issues that would also be encountered along this direction are needed to be first addressed: (1) how to develop an effective framework to guide suitable divisions of a given uncertainty set; (2) how to develop new switching logics and/or switching controller structures to guarantee switching stability and facilitate switching control implementation.

## 2. *Hybrid Switching Control for Systems Subject to Physical Constraints.*

In this dissertation research, all of the controlled systems under consideration are assumed to be free of physical constraints, such as actuator saturations [97] and/or time-varying delays [100, 99, 106]. In order to consider a more realistic control design scenario, we plan to further investigate the hybrid output-feedback synthesis problems for systems subject to different types of physical constraints. Specifically, we will focus on control systems with actuator saturations and/or time-varying delays because of two reasons: (1) Actuator saturation is an inherent nonlinearity for all dynamic systems, the need to develop effective actuator saturation control algorithms is evident for practical control applications; (2) Moreover, time delay is also ubiquitous in various engineering systems, such as the recycle delays in a chemical reactor plant; the fueling and combustion process delay in an automobile diesel engine system; and more typically the communication delays in networked control systems. In control engineering practice, time delay is a key source leading to performance degradation and even destabilization of control systems. Thus it is necessary to take the time delay effects into account for delay tolerant control design.

One important mathematical foundation worth to be pursued along this line is to develop new integral quadratic constraints (IQCs) from robust control theory for future robustness analysis and high-performance robust saturation/delay controller design use. The IQCs have been recognized to be powerful in modeling a large variety of nonlinearities/uncertainties of various dynamical systems. The basic idea of applying IQCs in nonlinear system analysis is that instead of directly considering the nonlinear system itself for stability/performance analysis (which usually could be very difficult), we apply IQCs to model/approximate the input-output dynamic behavior of the corresponding nonlinear components, and then replace them with an LTI model induced from the employed dynamic IQCs. By doing so, many techniques, such as the passivity/dissipativity theory and semi-definite programming techniques, can be easily incorporated into the analysis and control design process.

### 3. *Hybrid Impulsive Modeling and Control in Networked Control Systems.*

Typically, a networked control system (NCS) can be described as a control system where in the control loops are closed through a communication wireless network. The defining feature of an NCS is that control and feedback signals are exchanged among the system components (like sensors/samplers; actuators/zero-order-hold (ZOH) devices; and controllers) in the form of information packages through a network medium [101]. Compared to conventional point-to-point interconnected feedback control systems, NCSs have many advantages, such as high system operatability, more efficient resource utilization and sharing, lower cost, reduced weight and power requirements, as well as simplicity for system installation and maintenance, etc. This justifies their widespread applications in modern real-world engineering problems over a broad range of areas, such as mobile sensor networks, remote surgery; automated traffic control; unmanned vehicles; and cyber-physical systems.

In spite of many distinctive features of NCSs, the insertion of the communication network in the feedback control loops makes the analysis and design of an NCS complex. Various challenging issues are encountered due to the network-induced time delays and/or possibility of data package losses. This motivates one of our future research interests to develop an effective and systematic framework for both NCS analysis and synthesis. Promising approach is to combine two different control methods, i.e., the hybrid impulsive control technique and the dynamic IQC-based robust control technique, for both modeling and design of NCSs with time-varying measurement and actuation delays.

## REFERENCES

- [1] P. Apkarian and R. Adams. Advanced gain-scheduling techniques for uncertain systems. *IEEE Trans. Control Syst. Technol.*, 6:21–31, 1998.
- [2] P. Apkarian and P. Gahinet. A convex characterization of gain-scheduled  $\mathcal{H}_\infty$  controllers. *IEEE Trans. Autom. Control*, 40:853–864, 1995.
- [3] P. Apkarian, P. Gahinet, and G. Becker. Self-scheduled  $\mathcal{H}_\infty$  control of linear parameter varying systems. In *Proc. Ameri. Control Conf.*, pages 856–860, 1994.
- [4] P. Apkarian, P. C. Pellanda, and H. D. Tuan. Mixed  $\mathcal{H}_2/\mathcal{H}_\infty$  multi-channel linear parameter-varying control in discrete time. *Syst. Control Lett.*, 41:333–346, 2000.
- [5] B. Bayon, G. Scorletti, and E. Blanco. An LMI solution for a class of robust open-loop problems. In *Proc. Ameri. Control Conf., Montreal, Canada*, pages 5234–5239, 2012.
- [6] G. Becker and A. Packard. Robust performance of linear parametrically varying systems using parametrically-dependent linear feedback. *Syst. Control Lett.*, 23:205–215, 1994.
- [7] J.-M. Biannic and P. Apkarian. Missile autopilot design via a modified LPV synthesis technique. *Aerospace Science and Technology*, 3:153–160, 1999.
- [8] S. Boyd, L. E. Ghaoui, E. Feron, and V. Balakrishnan. *Linear Matrix Inequalities in System and Control Theory (Studies in Applied and Numerical Mathematics)*. Society for Industrial and Applied Mathematics, 2004.
- [9] S. Boyd and L. Vandenberghe. *Convex Optimization*. Cambridge University Press, 2004.
- [10] M. S. Branicky. Multiple Lyapunov functions and other analysis tools for switched and hybrid systems. *IEEE Trans. Autom. Control*, 43(4):475–482, 1998.
- [11] M. Chilali and P. Gahinet.  $\mathcal{H}_\infty$  design with pole placement constraints: An LMI approach. *IEEE Trans. Autom. Control*, 41(3):358–367, 1996.
- [12] N. Cox, L. Marconi, and A. R. Teel. High-gain observers and linear output regulation for hybrid exosystems. *Int. J. Robust Nonlin. Control*, 24(6):1043–1063, 2014.
- [13] J. Daafouz, J. C. Geromel, and G. S. Deaecto. A simple approach for switched control design with control bumps limitation. *Syst. Control Lett.*, 61:1215–1220, 2012.
- [14] G. S. Deaecto, J. C. Geromel, and J. Daafouz. Switched state-feedback control for continuous time-varying polytopic systems. *Int. J. Control*, 84(9):1500–1508, 2011.
- [15] E. deGelder, M. van de Wal, C. W. Scherer, C. Hol, and O. Bosgra. Nominal and robust feedforward design with time domain constraints applied to a wafer stage. *ASME Trans. J. Dynamical Syst. Measur. Control*, 128(2):204–215, 2006.

- [16] S. Devasia. Should model-based inverse inputs be used as feedforward under plant uncertainty? *IEEE Trans. Autom. Control*, 47(11):1865–1871, 2002.
- [17] K. Dong and C. Wang. Almost output regulation for parameter-dependent linear fractional transformation systems. *IET Contr. Theory Appl.*, 2(3):200–209, 2008.
- [18] X. Dong, X. Sun, J. Zhao, and G. M. Dimirovski. Output regulation for switched linear systems with different coordinate transformations. In *Proc. UKACC Int. Conf. Control, Cardiff, UK*, pages 92–95, 2012.
- [19] X. Dong and J. Zhao. Solvability of the output regulation problem for switched nonlinear systems. *IET Control Theory Appl.*, 6(8):1130–1136, 2012.
- [20] N. H. El-Farra, A. Gani, and P. D. Christofides. A switched systems approach for the analysis and control of mode transitions in biological networks. In *Proc. Amer. Control Conf., Portland, OR*, pages 3247–3252, 2005.
- [21] M. Farhoodi and M. T. H. Beheshti. Extended  $\mathcal{H}_2$ ,  $\mathcal{H}_\infty$  and pole placement LMI characterization for continuous-time systems. In *Proc. IEEE India Conf., Kanpur, India*, pages 536–541, 2008.
- [22] G. Ferreres and C. Roos. Efficient convex design of robust feedforward controllers. In *Proc. Europ. Control Conf., Seville*, pages 6460–6465, 2005.
- [23] F. Fichera, C. Prieur, S. Tarbouriech, and Z. L. Using Luenberger observers and dwell-time logic for feedback hybrid loops in continuous-time control systems. *Int. J. Robust Nonlin. Control*, 23(10):1065–1086, 2013.
- [24] B. A. Francis. The linear multivariable regulator problem. *SIAM J. Control Optim.*, 15(3):486–505, 1977.
- [25] B. A. Francis and W. M. Wonham. The internal model principle of control theory. *Automatica*, 12:457–465, 1976.
- [26] N. R. Gans and S. A. Hutchinson. Stable visual servoing through hybrid switched-system control. *IEEE Trans. Robotics*, 23(3):530–540, 2007.
- [27] V. Gazi. Output regulation of a class of linear systems with switched exosystems. *Int. J. Control*, 80(10):1665–1675, 2007.
- [28] J. C. Geromel and P. Colaneri. Stability and stabilization of continuous-time switched linear systems. *SIAM J. Control Optim.*, 45:1915–1930, 2006.
- [29] J. C. Geromel, P. Colaneri, and P. Bolzern. Dynamic output feedback control of switched linear systems. *IEEE Trans. Autom. Control*, 53:720–733, 2008.
- [30] J. C. Geromel and G. S. Deaecto. Switched state feedback control of continuous-time uncertain systems. *Automatica*, 45:593–597, 2009.

- [31] T. Geyer, G. Papafotiou, and M. Morari. Model predictive control in power electronics: A hybrid systems approach. In *Proc. IEEE Conf. Dec. Control*, pages 5606–5611, 2005.
- [32] A. Giusto and F. Paganini. Robust synthesis of feedforward compensators. *IEEE Trans. Autom. Control*, 44(8):1578–1582, 1999.
- [33] R. Goebel, R. G. Sanfelice, and A. R. Teel. *Hybrid Dynamical Systems*. Princeton Univ. Press, Princeton, NJ, 2012.
- [34] M. J. Grimble. Two and a half degrees of freedom LQG controller and application to wind turbines. *IEEE Trans. Autom. Control*, 39:122–127, 1994.
- [35] A. Hassibi, J. How, and S. Boyd. A path-following method for solving BMI problems in control. In *Proc. Amer. Control Conf., San Diego, CA*, pages 1385–1389, 1999.
- [36] J. P. Hespanha, D. Liberzon, and A. R. Teel. Lyapunov conditions for input-to-state stability for impulsive systems. *Automatica*, 44(11):2735–2744, 2008.
- [37] J. P. Hespanha and A. S. Morse. Stability of switched systems with average dwell-time. In *Proc. IEEE Conf. Dec. Control*, pages 2655–2660, 1999.
- [38] L. Hetel, J. Daafouz, S. Tarbouriech, and C. Prieur. Stabilization of linear impulsive systems through a nearly-periodic reset. *Nonlin. Anal.: Hybrid Syst.*, 7(1):4–15, 2013.
- [39] K. Hirata and J. P. Hespanha.  $\mathcal{L}_2$ -induced gains of switched systems and classes of switching signals. In *Proc. 49th IEEE Conf. Dec. Control*, pages 438–442, 2010.
- [40] J. Huang and W. J. Rugh. On a nonlinear multivariable servomechanism problem. *Automatica*, 26:963–972, 1990.
- [41] A. Isidori and C. I. Byrnes. Output regulation of nonlinear systems. *IEEE Trans. Autom. Control*, 35(2):131–140, 1990.
- [42] I. E. Kose and C. W. Scherer. Robust feedforward control of uncertain systems using dynamic IQCs. In *Proc. IEEE Conf. Dec. Control*, pages 2181–2186, 2007.
- [43] I. E. Kose and C. W. Scherer. Robust  $\mathcal{L}_2$ -gain feedforward control of uncertain systems using dynamic IQCs. *Int. J. Robust Nonlin. Control*, 19:1224–1247, 2009.
- [44] D. A. Lawrence and E. A. Medina. Output regulation for linear systems with sampled measurements. In *Proc. Amer. Control Conf.*, pages 2044–2049, 2001.
- [45] D. A. Lawrence and W. J. Rugh. Gain scheduling dynamic linear controllers for a nonlinear plant. *Automatica*, 31(3):381–390, 1995.
- [46] L. H. Lee. *Identification and Robust Control of Linear Parameter-Varying Systems*. Ph.D. Dissertation, Dept. Mech. Eng., Univ. California, Berkeley, CA, 1997.
- [47] W. J. Lee and P. P. Khargonekar. Optimal output regulation for discrete-time switched and markovian jump linear systems. *SIAM J. Control Optim.*, 47(1):40–72, 2008.

- [48] D. Liberzon. *Switching in Systems and Control*. Birkhauser, Boston, MA, 2003.
- [49] D. Liberzon and A. S. Morse. Basic problems in stability and design of switched systems. *IEEE Control Syst. Mag.*, 19(5):59–70, 1999.
- [50] S. Lim. *Analysis and Control of Linear Parameter-Varying Systems*. Ph.D. Dissertation, Stanford University, 1999.
- [51] S. Lim and K. Chan. Stability analysis of hybrid linear parameter-varying systems. In *Proc. Amer. Control Conf.*, pages 4822–4827, 2003.
- [52] S. Lim and J. P. How. Modeling and  $\mathcal{H}_\infty$  control for switched linear parameter-varying missile autopilot. *IEEE Trans. Control Syst. Techn.*, 11(6):830–838, 2003.
- [53] D. J. N. Limebeer, E. M. Kasenally, and D. J. Perkins. On the design of robust two degree of freedom controllers. *Automatica*, 29(1):157–168, 1993.
- [54] H. Lin and P. J. Antsaklis. Stability and stabilizability of switched linear systems: A survey of recent results. *IEEE Trans. Autom. Control*, 54(1):308–322, 2009.
- [55] Z. Lin, A. A. Stoorvogel, and A. Saberi. Output regulation for linear systems subject to input saturation. *Automatica*, 32(1):29–47, 1996.
- [56] Y. Liu and J. Zhao. Output regulation of a class of switched linear systems with disturbances. In *Proc. Amer. Control Conf.*, pages 882–883, 2001.
- [57] B. Lu and F. Wu. Switching LPV control designs using multiple parameter-dependent Lyapunov functions. *Automatica*, 40:1973–1980, 2004.
- [58] B. Lu, F. Wu, and S. Kim. Switching LPV control of an F-16 aircraft via controller state reset. *IEEE Trans. Control Syst. Technol.*, 14(2):267–277, 2006.
- [59] L. Marconi and A. R. Teel. Internal model principle for linear systems with periodic state jumps. *IEEE Trans. Autom. Control*, 58(11):2788–2802, 2013.
- [60] A. Megretski and A. Rantzer. System analysis via integral quadratic constraints. *IEEE Trans. Autom. Control*, 42:819–830, 1997.
- [61] M. A. Micks, P. Peleties, and R. A. DeCarlo. Construction of piecewise Lyapunov functions for stabilizing switched systems. In *Proc. IEEE Conf. Dec. Control, Lake Buena Vista, FL*, pages 3492–3497, 1994.
- [62] A. S. Morse. *Control Using Logic-Based Switching*. Springer, Heidelberg, Germany, 1997.
- [63] D. Nesic, L. Zaccarian, and A. R. Teel. Stability properties of reset systems. *Automatica*, 44:2019–2026, 2008.
- [64] R. Nichols, R. Reichert, and W. Rugh. Gain scheduling for  $\mathcal{H}_\infty$  controllers: a flight control example. *IEEE Trans. Control Syst. Techn.*, 1(2):69–79, 1993.

- [65] M. C. Oliveira, J. Bernussou, and J. C. Geromel. A new discrete-time robust stability condition. *Syst. Control Lett.*, 37:261–265, 1999.
- [66] A. K. Packard. Gain scheduling via linear fractional transformations. *Syst. Control Lett.*, 22:79–92, 1994.
- [67] P. Peleties and R. DeCarlo. Asymptotic stability of m-switched systems using Lyapunov-like functions. In *Proc. Ameri. Control Conf., Boston, MA*, pages 1679–1684, 1991.
- [68] P. C. Pellanda, P. Apkarian, and H. D. Tuan. Missile autopilot design via a multi-channel LFT/LPV control method. *Int. J. Robust Nonlin. Control*, 12:1–20, 2002.
- [69] E. Prempain and I. Postlethwaite. A feedforward control synthesis approach for LPV systems. In *Proc. Ameri. Control Conf., Seattle, Washington*, pages 3589–3594, 2008.
- [70] A. Ranzer and M. Johansson. Piecewise linear quadratic optimal control. *IEEE Trans. Autom. Control*, 45(4):629–637, 2000.
- [71] R. T. Reichert. Dynamic scheduling of modern-robust-control autopilot designs for missiles. *IEEE Control Syst. Mag.*, 12(5):35–42, 1992.
- [72] W. J. Rugh. Analytical framework for gain scheduling. *IEEE Control Syst. Mag.*, 11(2):78–84, 1991.
- [73] A. Saberi, A. A. Stoorvogel, and Z. Lin. Generalized output regulation for linear systems. In *Proc. Amer. Control Conf.*, pages 3909–3914, 1997.
- [74] A. Saberi, A. A. Stoorvogel, and P. Sannuti. *Control of Linear Systems with Regulation and Input Constraints*. Springer, Berlin, 1999.
- [75] C. Scherer, P. Gahinet, and M. Chilali. Multiobjective output-feedback control via LMI optimization. *IEEE Trans. Autom. Control*, 42(7):896–911, 1997.
- [76] C. W. Scherer. *Robust Mixed Control and LPV Control with Full Block Scalings, in Recent Advances of LMI Methods in Control*. Philadelphia, SIAM, 1999.
- [77] C. W. Scherer and I. E. Kose. Gain-scheduled control synthesis using dynamic D-scales. *IEEE Trans. Autom. Control*, 57:2219–2234, 2012.
- [78] C. Schumacher and P. P. Khargonekar. Missile autopilot designs using  $\mathcal{H}_\infty$  control with gain scheduling and dynamic inversion. *AIAA J. Guidance, Control, and Dynamics*, 21(2):234–243, 1998.
- [79] G. Scorletti and V. Fromion. Further results on the design of robust  $\mathcal{H}_\infty$  feedforward controllers and filters. In *Proc. IEEE Conf. Dec. Control, San Diego, CA*, pages 3560–3565, 2006.
- [80] J. S. Shamma and M. Athans. Analysis of gain scheduled control for nonlinear plants. *IEEE Trans. Autom. Control*, 35(8):898–907, 1990.

- [81] J. S. Shamma and J. R. Cloutier. Gain-scheduled missile autopilot design using linear parameter varying transformations and  $\mu$ -synthesis. *AIAA J. Guidance, Control, and Dynamics*, 16(2):256–263, 1993.
- [82] Z. Sun and S. S. Ge. *Switched Linear Systems: Control and Design*. Springer, Verlag, NY, 2005.
- [83] F. Wang and K. Balakrishnan. Improved stability analysis and gain-scheduled controller synthesis for parameter-dependent systems. *IEEE Trans. Autom. Control*, 47:720–734, 2002.
- [84] R. Wang, J. Zhao, G. M. Dimirovski, and G. P. Liu. Output feedback control for uncertain linear systems with faulty actuators based on a switching method. *Int. J. Robust Nonlin. Control*, 19:1295–1312, 2009.
- [85] F. Wu. *Control of Linear Parameter Varying Systems*. Ph.D. Dissertation, University of California, Berkeley, 1995.
- [86] F. Wu and K. Dong. Gain-scheduling control of LFT systems using parameter-dependent Lyapunov functions. *Automatica*, 42:39–50, 2006.
- [87] F. Wu, A. Packard, and G. Balas. Systematic gain-scheduling control design: a missile autopilot example. *Asian J. Control*, 4(3):341–347, 2002.
- [88] F. Wu, X. H. Yang, A. Packard, and G. Becker. Induced  $\mathcal{L}_2$  norm control for LPV systems with bounded parameter variation rates. *Int. J. Robust Nonlin. Control*, 6(9):983–998, 1996.
- [89] Z. Wu and F. B. Amara. Regulation in bimodal systems. *Int. J. Robust Nonlin. Control*, 18:1115–1141, 2008.
- [90] Z. Wu and F. B. Amara. Regulator synthesis for bimodal linear systems. *IEEE Trans. Autom. Control*, 56(2):390–394, 2011.
- [91] H. Ye, A. N. Michel, and L. Hou. Stability theory for hybrid dynamical systems. *IEEE Trans. Autom. Control*, 43(4):461–474, 1998.
- [92] D. C. Youla and J. J. Bongiorno. A feedback theory of two-degree of freedom optimal Wiener-Hopf design. *IEEE Trans. Autom. Control*, 30(2):652–665, 1985.
- [93] C. Yuan, C. Duan, and F. Wu. Almost output regulation of discrete-time switched linear systems. In *Proc. Ameri. Control Conf., Chicago, IL*, pages 4042–4047, 2015.
- [94] C. Yuan and F. Wu. Robust control of switched linear systems via min of quadratics. In *Proc. ASME Conf. Dynam. Syst. Control, Palo Alto, CA*, pages Paper No. DSCC2013–3715, 2013.
- [95] C. Yuan and F. Wu. Analysis and synthesis of linear hybrid systems with state-triggered jumps. *Nonlin. Analys.: Hybrid Syst.*, 14:47–60, 2014.

- [96] C. Yuan and F. Wu. Output feedback reset control of general MIMO LTI systems. In *Proc. European Control Conf., Strasbourg, France*, pages 2334–2339, 2014.
- [97] C. Yuan and F. Wu. A switching control approach for linear systems subject to asymmetric actuator saturation. In *Proc. Chinese Control Conf., Nanjing, China*, pages 3959–3964, 2014.
- [98] C. Yuan and F. Wu. Asynchronous switching output feedback control of discrete-time switched linear systems. *Int. J. Control*, 88(9):1–9, 2015.
- [99] C. Yuan and F. Wu. Dynamic IQC-based control of uncertain LFT systems with time-varying state delay. *IEEE Trans. Cybernetics*, 2015, doi: 10.1109/TCYB.2015.2503741.
- [100] C. Yuan and F. Wu. Exact-memory and memoryless control of linear systems with time-varying input delay using dynamic IQCs. *Automatica*, 2016, accepted.
- [101] C. Yuan and F. Wu. Delay scheduled impulsive control for networked control systems. *IEEE Transactions on Control of Network Systems*, 2016, accepted.
- [102] C. Yuan and F. Wu. Hybrid almost output regulation of linear impulsive systems with average dwell time. *Nonlin. Analys.: Hybrid Syst.*, 2015, doi: <http://dx.doi.org/10.1016/j.nahs.2015.11.001>.
- [103] C. Yuan and F. Wu. Hybrid control for switched linear systems with average dwell time. *IEEE Trans. Autom. Control*, 60(1):240–245, 2015.
- [104] C. Yuan and F. Wu. Robust  $\mathcal{H}_2$  and  $\mathcal{H}_\infty$  switched feedforward control of uncertain LFT systems. *Int. J. Robust Nonlin. Control*, 2015, doi: 10.1002/rnc.3380.
- [105] C. Yuan and F. Wu. Switching control of linear systems subject to asymmetric actuator saturation. *Int. J. Control*, 88(1):204–215, 2015.
- [106] C. Yuan, F. Wu, and C. Duan. Robust gain-scheduling output feedback control of state-delayed LFT systems using dynamic IQCs. In *Proc. ASME Dynam. Syst. Control Conf., Columbus, OH*, 2015.
- [107] C. Yuan and F. Wu. Robust switching output-feedback control of time-varying polytopic uncertain systems. *Int. J. Control*, 2016, accepted.
- [108] G. Zhai, B. Hu, K. Yasuda, and A. N. Michel. Disturbance attenuation properties of time-controlled switched systems. *J. Franklin Inst.*, 338(7):765–779, 2001.
- [109] G. Zhai, B. Hu, K. Yasuda, and A. N. Michel. Qualitative analysis of discrete-time switched systems. In *Proc. Amer. Control Conf., Anchorage, AK*, pages 1880–1885, 2002.
- [110] K. Zhou, J. C. Doyle, and K. Glover. *Robust and Optimal Control*. Prentice Hall, Englewood Cliffs, NJ, 1996.